

THERMAL TRANSMITTANCE ASSESSMENT OF BUILDING WALLS BY
USING IN-SITU INFRARED THERMOGRAPHY

A THESIS SUBMITTED TO
THE GRADUATE SCHOOL OF NATURAL AND APPLIED SCIENCES
OF
MIDDLE EAST TECHNICAL UNIVERSITY

BY

MURAT SAYIN

IN PARTIAL FULFILLMENT OF THE REQUIREMENTS
FOR
THE DEGREE OF MASTER OF SCIENCE
IN
BUILDING SCIENCE IN ARCHITECTURE

SEPTEMBER 2019

Approval of the thesis:

**THERMAL TRANSMITTANCE ASSESSMENT OF BUILDING WALLS BY
USING IN-SITU INFRARED THERMOGRAPHY**

submitted by **MURAT SAYIN** in partial fulfillment of the requirements for the degree of **Master of Science in Building Science in Architecture Department, Middle East Technical University** by,

Prof. Dr. Halil Kalıpçılar
Dean, Graduate School of **Natural and Applied Sciences**

Prof. Dr. Cana Bilsel
Head of Department, **Department of Architecture**

Assoc. Prof. Dr. Ayşe Tavukçuoğlu
Supervisor, **Department of Architecture, METU**

Examining Committee Members:

Prof. Dr. Sinan Turhan Erdoğan
Department of Civil Engineering, METU

Assoc. Prof. Dr. Ayşe Tavukçuoğlu
Department of Architecture, METU

Prof. Dr. Emine N. Caner-Saltık
Department of Architecture, METU

Assist. Prof. Dr. Ozan Keysan
Department of Electrical-Electronics Engineering, METU

Assist. Prof. Dr. Erk İnger
Department of Airframe and Powerplant Maintenance, Atılım U.

Date: 05.09.2019

I hereby declare that all information in this document has been obtained and presented in accordance with academic rules and ethical conduct. I also declare that, as required by these rules and conduct, I have fully cited and referenced all material and results that are not original to this work.

Name, Surname: Murat Sayın

Signature:

ABSTRACT

THERMAL TRANSMITTANCE ASSESSMENT OF BUILDING WALLS BY USING IN-SITU INFRARED THERMOGRAPHY

Sayın, Murat

Master of Science, Building Science in Architecture

Supervisor: Assoc. Prof. Dr. Ayşe Tavukçuoğlu

September 2019, 138 pages

The main concerns of the study are the thermal transmittance (U , $Wm^{-2}K^{-1}$) assessment of building walls by quantitative analyses of surface temperature data obtained by infrared thermography (IRT) and the identification of thermal failure types in terms of measurable parameters.

Mainly six types of non-insulated and insulated wall compositions belonging to three different buildings were examined. The actual thermal performances of the walls (U_{INSITU}) determined with in-situ quantitative IRT (QIRT) was assessed in comparison with their theoretically-expected thermal transmittance values (U_{CALC}) calculated with standard methods. The progress in thermal resistance of one type wall with thermal insulation treatment was monitored with in-situ QIRT investigation and the estimation annual heating energy consumption of the building (θ , kWh). Thermal failures, which weaken the thermal resistivity of a wall, were identified in terms of temperature index, TI (unitless). Adverse impact of thermal failures was examined with the comparison of thermal transmittance values belonging to the problem area (U_{DEF}) and reference area (U_{REF}).

The actual thermal performances of the existing walls were determined to be poorer than the theoretically-expected performances. The walls designed with low thermal

resistance were observed to be highly-susceptible to thermal failures resulting in considerable heat loss.

In-situ use of QIRT allows practically-assessing and monitoring the actual thermal performance of building walls in terms of thermal transmittance and that makes this method preferable for the studies on Energy Performance Certification (EPC) of buildings. The common use of QIRT in the studies of building diagnostics and monitoring has to be encouraged.

Keywords: Quantitative Infrared Thermography, Thermal Transmittance, Temperature Index, In-Situ Assessment, Annual Energy Consumption,

ÖZ

YAPI DUVARLARININ ISIL GEÇİRGENLİĞİNİN KANTİTATİF KIZIL ÖTESİ ISIL GÖRÜNTÜLEME YÖNTEMİ İLE DEĞERLENDİRİLMESİ

Sayın, Murat
Yüksek Lisans, Yapı Bilimleri
Tez Danışmanı: Doç. Dr. Ayşe Tavukçuoğlu

Eylül 2019, 138 sayfa

Çalışmanın ana konuları, kızılötesi ısı görüntüleme (IRT) ile elde edilen yüzey sıcaklık verilerinin kantitatif analizi ile bina duvarlarının ısı geçirgenlik niteliklerinin (U , $Wm^{-2}K^{-1}$) değerlendirilmesi ve ısı sorunlarının ölçülebilir parametreler ile tanımlanmasıdır.

Başlıca üç farklı binaya ait altı çeşit yalıtımsız ve yalıtımlı duvar bileşeni incelenmiştir. Duvarların kantitatif IRT (QIRT) ile yerinde ölçülerek belirlenen gerçek ısı performansları (U_{INSITU}), standart yöntemlerle hesaplanmış olan teorik ısı performansları (U_{CALC}) ile karşılaştırmalar yapılarak değerlendirilmiştir. Bir duvar çeşidinin ısı performansı dış yüzeyleri ısı yalıtım levhalarıyla kaplanarak iyileştirilmiş; duvarın ısı direncindeki gelişme yerinde QIRT ölçümleri ile ve binanın ısıtma amacıyla tüketileceği yıllık ısıtma enerjisi (θ , kWh) hesaplanarak takip edilmiştir. Duvarların ısı direncini zayıflatan ısı sorunları, sıcaklık indeksi (TI, birimsiz) cinsinden belirlenmiştir. Isı sorunların olumsuz etkisi, sorunlu bölgenin (U_{DEF}) ve referans bölgenin (U_{REF}) ısı geçirgenlik değerleri birbirleriyle karşılaştırılarak değerlendirilmiştir.

Mevcut duvarların gerçek ısı performanslarının teorik olarak duvarlardan beklenen performanslardan daha zayıf olduğu tespit edilmiştir. Düşük ısı dirençli tasarlanmış

olan duvarların ısı sorulara karşı daha zayıf oldukları, sorunlu bölgelerde ısı kayıplarının ciddi seviyelere ulaştığı görülmüştür.

Yerinde ölçüm yapılabilen QIRT yöntemi, yapı duvarlarının mevcut durumdaki ısı geçirgenlik değeri için pratik olarak ölçülebilmeye ve duvarların ısı performanslarının yerinde değerlendirilmesi ve zaman içerisinde izlenmesine olanak sağlamaktadır. Bu türden olanaklar, IRT yöntemini binaların Enerji Performans Belgelendirme (EPC) çalışmaları için tercih edilebilir kılmaktadır. QIRT yönteminin yapılarda sorunların tespiti ve sorun takibi ile ilgili çalışmalarda yaygın olarak kullanılması teşvik edilmelidir.

Anahtar Kelimeler: Kantitatif Kızıl Ötesi Isı Görüntüleme, Isı Geçirgenlik, Sıcaklık İndeksi, Yerinde Ölçüm, Yıllık Ortalama Enerji Tüketimi

ACKNOWLEDGEMENTS

I would like to thank to my supervisor Ayşe Tavukçuoğlu for her valuable help, her deep knowledge about the subject matter, encouragement, sacrifices and patience.

I would also like to thank Board Member, Mr. Levent Tosun and General Manager, Ms. F. Hale Can of EBI AŞ (owned by METU foundation) for their encouragement and support during the study.

TABLE OF CONTENTS

| | |
|--|------|
| ABSTRACT | v |
| ÖZ | vii |
| ACKNOWLEDGEMENTS..... | ix |
| TABLE OF CONTENTS | x |
| LIST OF TABLES..... | xiii |
| LIST OF FIGURES | xiv |
| LIST OF ABBREVIATIONS..... | xx |
| CHAPTERS | |
| 1. INTRODUCTION..... | 1 |
| 1.1. Argument | 1 |
| 1.2. Objectives..... | 4 |
| 1.3. Procedure | 6 |
| 1.4. Disposition | 7 |
| 2. LITERATURE SURVEY | 9 |
| 2.1. Infrared Thermography (IRT) and Infrared Cameras | 9 |
| 2.2. Use of Heat Flow Meter for building diagnostics..... | 17 |
| 2.3. Heat Transfer; Modes and Parameters | 19 |
| 2.4. Types of Thermal Failures Observed in Buildings | 32 |
| 2.5. Using Infrared Thermography for Thermal Transmittance Estimation | 35 |
| 2.6. Physical parameters needed for Quantitative Infrared Thermography | 39 |
| 2.7. Certification of Building Energy Performance in Reference to Annual Total Energy Consumption..... | 41 |

| | |
|--|-----|
| 3. MATERIAL & METHOD..... | 45 |
| 3.1. Building Wall Configurations under Examinations | 47 |
| 3.2. In-situ IR Imaging for Thermal Failure Assessment..... | 49 |
| 3.3. Condensation Analyses by the combined use of IRT & Partial Vapour Pressure Distribution Calculations | 52 |
| 3.4. Calculation of Temperature Index..... | 54 |
| 3.5. In-situ Thermal Transmittance Estimation by Quantitative Infrared Thermography (QIRT) | 55 |
| 3.6. Thermal Transmittance Estimation with Standard Calculation Method | 60 |
| 3.7. Annual Heating Energy Consumption Estimation with Standard Calculation Method and Identification of Building Performance Certification | 63 |
| 4. RESULTS | 67 |
| 4.1. Inspection of thermal and moisture failures with qualitative analyses of IR images..... | 67 |
| 4.1.1. Failures detected in villa type house (B1) | 67 |
| 4.1.2. Failures detected in two-storey height residential unit (B2)..... | 78 |
| 4.1.3. Failures detected in Faculty of Architecture Building (B3) | 82 |
| 4.2. Identification of thermal and moisture failures in terms of TI | 86 |
| 4.3. Thermal transmittance values of wall configurations determined with in-situ QIRT ($U_{\text{INSITU-REF}}$) and standard calculation method (U_{CALC}) | 89 |
| 4.4. Actual thermal transmittance values determined for the thermal failure zones ($U_{\text{INSITU-DEF}}$)..... | 97 |
| 4.5. Actual thermal transmittance values ($U_{\text{INSITU-AVG}}$) of wall configurations to be used for Energy Performance Certification | 100 |
| 4.6. Estimation of Annual Heating Energy Consumption and identification of Energy Performance Rating: Case B1 - before and after insulation treatment | 102 |

| | |
|---|-----|
| 5. DISCUSSION | 107 |
| 5.1. Performance evaluation of in-situ QIRT method for thermal transmittance assessment..... | 107 |
| 5.2. Considerations for in-situ thermal transmittance measurements with the use of QIRT | 110 |
| 6. CONCLUSION | 117 |
| 6.1. Conclusion | 117 |
| 6.2. Expected impacts | 119 |
| 6.3. Further studies..... | 121 |
| REFERENCES | 123 |
| A. Specifications of the IR Cameras used for in-situ thermal imaging..... | 135 |
| B. Specifications of the software's used for IR analysis..... | 135 |
| C. Saturation pressure of water-vapour at various temperatures | 136 |
| D. Sample energy performance certificate (EPCs) | 137 |
| E. U Value Comparison Table | 138 |

LIST OF TABLES

TABLES

| | |
|---|----|
| Table 2.1. Brief History of Infrared Cameras (Flir Systems, 2013) | 11 |
| Table 2.2. Comparison table of estimated U_{INSITU} and U_{CALC} values in related researches | 26 |
| Table 2.3. Emissivity values of some common materials (Flir Systems, 2013) | 31 |
| Table 2.4. Maximum/Allowed annual energy consumption calculation table for different climatic regions according to standard TS825:2013. | 44 |
| Table 3.1. List of wall types under examination including their codes, configuration descriptions and the buildings where the wall components belong to. | 48 |
| Table 3.2. Surface thermal convection coefficient (BS EN ISO 10456, 2007; TS 825, 2013) | 62 |
| Table 3.3. Theoretically-calculated thermal transmittance values of the walls according the thermal conductivity data given in the standards (BS EN ISO 10456, 2007; TS 825, 2013)..... | 62 |
| Table 3.4. Theoretically-calculated thermal transmittance values (U_{CALC}) of the walls according the thermal conductivity data given in the standards | 66 |
| Table 4.1. Temperature index(TI) values of six walls with and without defect areas corresponding to the thermal failure and reference points in each IR image..... | 88 |

LIST OF FIGURES

FIGURES

| | |
|---|----|
| Figure 2.1. Electromagnetic wave spectrum..... | 10 |
| Figure 2.2. Comparison of real and thermal images..... | 14 |
| Figure 2.3. Sample temperature distribution of the thermal image at Figure 2.2, 30.4°C is the hottest part of the cat, close to ear..... | 15 |
| Figure 2.4. Schematic representation of thermographic measurement..... | 16 |
| Figure 2.5. Energy interaction at wall surface | 20 |
| Figure 2.6. Using handheld anemometer to measure wind velocity near wall surface | 24 |
| Figure 2.7. Using black electrical tape for surface emissivity measurement and aluminum foil for reflected temperature measurement. | 31 |
| Figure 2.8. Thermal bridges occurring because of non-insulated surfaces at the façade of the building. ($T_{out}= 1.9^{\circ}\text{C}$ and RH= 43%)..... | 33 |
| Figure 2.9. Thermal Bridges occurring due to the faults during fastening the thermal insulation boards to the backing wall, ($T_{out}=-3.9^{\circ}\text{C}$ and RH= 60%) | 33 |
| Figure 3.1. Villa type house (B1) under examination in the campus of METU, construction time: 1998 (Ankara, Turkey) | 46 |
| Figure 3.2. Villa type house (B1) during and after externally-insulation of reinforced concrete walls, renovation time: 2014. | 46 |
| Figure 3.3. Two-storey height residential unit (B2) under examination in the campus of METU, construction time: 2001 (Ankara, Turkey)..... | 46 |
| Figure 3.4. Faculty of Architecture Building (B3) under examination in the campus of METU, construction time: 1962 (Ankara, Turkey)..... | 47 |
| Figure 3.5. Wall configurations under examination | 48 |
| Figure 3.6. Unified Language Modeling (ULM) Diagram of in-situ IRT survey for the actual U-value assessment of exterior walls | 51 |

| | |
|---|----|
| Figure 3.7. Partial water vapour pressure distribution and temperature distribution profiles show if there is risk of condensation (a) or not (b). | 54 |
| Figure 3.8. Obtaining surface temperature value close to outside air temperature cold spot tool of the software is used and CS1 shows the coldest surface temperature of W3 which represents the reference temperature value and $U_{\text{INSITU-REF}}$ is calculated accordingly. To obtain surface temperature value away from the outside air temperature hot spot tool is used and HS1 shows the warmest surface temperature of W3 which represents the defect temperature value and $U_{\text{INSITU-DEF}}$ is calculated accordingly. Finally, to obtain average surface temperature value temperature profile passing through W3 surface is used and the average surface temperature value is gathered and this value is used for calculation of $U_{\text{INSITU-AVG}}$ value. This method is repeated for eight times and average U values represent the in-situ thermal transmittance values. | 59 |
| Figure 3.9. Villa Type Houses (B1) that IR images were taken are marked at the site plan..... | 65 |
| Figure 4.1. Surface temperatures of non-insulated shear wall (W5) and beams are about 4-5°C higher than the insulated cavity brick wall surfaces (W1). W5 surfaces are about 7-8°C higher than the outside air temperature. These temperature differences shows that there are serious heat loss through the surfaces of non-insulated reinforced concrete wall and beams (W5). ($T_{\text{out}} = -3^{\circ}\text{C}$ and $\text{RH} = 43\%$) | 69 |
| Figure 4.2. Surface temperature of W5 wall is about 7-8°C higher than the outside air temperature. This temperature difference demonstrates that there is a serious heat loss from non-insulated basement shear wall (W5). ($T_{\text{out}} = -3^{\circ}\text{C}$ and $\text{RH} = 43\%$). | 69 |
| Figure 4.3. IR image showing the warm areas where radiator is positioned behind the insulated cavity walls. Those warm areas have surface temperatures 4-5°C higher than the rest of W1 surfaces. The surface temperatures of W1 being 3-5°C higher than the outside air temperature signal the insufficient thermal resistance of its composition ($T_{\text{out}} = 0.3^{\circ}\text{C}$, $\text{RH} = 60\%$). | 70 |
| Figure 4.4. The warm edges reaching 6°C difference higher than the outside air temperature exhibit the significant heat loss through the edges where the window | |

frames come together with the structure. The warmer surfaces of the uninsulated reinforced concrete beam (W5) and the insulated cavity brick wall (W1) where the radiator is positioned behind the parapet signal the inadequate thermal resistance of those walls ($T_{out} = 0.3^{\circ}\text{C}$, $\text{RH} = 60\%$)..... 70

Figure 4.5. The warmest area with surface temperature reaching 8°C higher than the outside air temperature is the edge where roof and gable wall come together. Heat loss through the structural elements of the building (columns and beams) is also visible in IR images. ($T_{out} = -3^{\circ}\text{C}$, $\text{RH} = 43\%$). 71

Figure 4.6. The coldest zones having interior surface temperatures almost 10°C colder than indoor air temperature are observed at the corners where building wall and ceiling comes together and those coldest zones are under risk of condensation ($T_{in} = 19.5^{\circ}\text{C}$, $\text{RH} = 45\%$)..... 72

Figure 4.7. Temperature and dew point temperature profiles of non-insulated reinforced concrete surface (W5) and insulated reinforced concrete surface (W2), showing the risk of interstitial condensation (C) in W5, reaching to 5cm depth from interior surface while that risk was eliminated for the same wall after it was externally-insulated (W2) ($\text{TI}_{W5\text{-REFERENCE}} = 0.75$; $\text{TI}_{W5\text{-DEFECT}} = 0.58$; $\text{TI}_{W2\text{-REFERENCE}} = 0.94$; $\text{TI}_{W2\text{-DEFECT}} = 0.71$) ($T_{in} = 20^{\circ}\text{C}$, $\text{RH}_{in} = 45\%$ and $T_{out} = -1^{\circ}\text{C}$, $\text{RH}_{out} = 60\%$)... 73

Figure 4.8. The window frames, especially the edges where window frame and building wall come together are the coldest zones with surface temperatures 15°C colder than the indoor air temperature. That temperature difference signals the risk of condensation and air tightness problems occurring at the coldest zones ($T_{in} = 19.5^{\circ}\text{C}$, $\text{RH} = 45\%$)..... 74

Figure 4.9. Surface temperature of W2 being close to the outside air temperature shows the improvement in thermal resistance while being still $1\text{-}2^{\circ}\text{C}$ higher than the outside air temperature ($T_{out} = -3.1^{\circ}\text{C}$, $\text{RH} = 65\%$). 75

Figure 4.10. The IR image and temperature profile on Line P1 showing the exterior temperature distribution on the insulated cavity brick wall (W1) and insulated reinforced concrete wall (W2). The average surface temperature of W2 is close to the outside air with a temperature difference of $1\text{-}2^{\circ}\text{C}$. The thermal resistance of W2

| | |
|--|----|
| seems to be better than the thermal resistance of W1 that is provided by the insulation treatment ($T_{out} = -3.1^{\circ}\text{C}$, RH= 65%). | 76 |
| Figure 4.11. IR image taken from the exterior building envelope of villa house and temperature profile on Line P1 showing that thermal bridges occurs because of the discontinuity of insulation material. Thermal bridges are visible in IR images with surface temperatures about 5-6°C warmer than the insulated walls surfaces (non-problem area) as well as about 7°C warmer than outside air temperature. ($T_{out} = 5.0^{\circ}\text{C}$, RH= 65%). | 77 |
| Figure 4.12. The IR image taken from the rear side of the villa house and temperature profile on Line P1 showing that, thermal bridges occur because of the discontinuity of insulation material. Thermal bridges with surface temperatures about 4-5°C higher than the externally-insulated concrete surfaces (non-problem areas) and 6-7°C higher than the outside ambient temperature ($T_{out} = -3.1^{\circ}\text{C}$, RH= 65%). | 78 |
| Figure 4.13. Externally-insulated shear wall (W3, P2&P3 profiles) surface temperature is 3,2°C higher than the surface temperature of externally-insulated autoclaved aerated concrete wall (W4, P1&P4 profiles). Heterogeneous temperature distribution visible in the temperature profile (P3) in the form of peak temperature values shows heat source (radiator) behind the wall and this situation signals the insufficiency of the wall's thermal resistance. ($T_{out} = -3.9^{\circ}\text{C}$, RH= 60%). | 79 |
| Figure 4.14. Heterogeneous temperature distribution is visible in the IR images in the form of warm patches at the intersection of thermal insulation boards and Temperature profiles passing through these zones shows that, surface temperature at the bridge zones are up to 3-4°C higher than surface temperature without defect ($T_{out} = -3.9^{\circ}\text{C}$, RH= 60%). | 80 |
| Figure 4.15. IR image and temperature profile taken from inside of the building show the thermal performance difference between W3 and W4 ($T_{in} = 19^{\circ}\text{C}$, RH= 55%). | 81 |
| Figure 4.16. Temperature profile of B2 shows the possibility of the surface and interstitial moisture problem ($T_{in} = 19^{\circ}\text{C}$, RH= 55%). | 81 |

| | |
|---|----|
| Figure 4.17. Temperature and dew point temperature profiles of insulated reinforced concrete wall (W3) show the risk of interstitial condensation (C) reaching to 4 cm depth from interior surface ($TI_{W3-REFERENCE} = 0.92$; $TI_{W3-DEFECT} = 0.71$) ($T_{in} = 20^{\circ}C$, $RH_{in} = 45\%$ and $T_{out} = -1^{\circ}C$, $RH_{out} = 60\%$). | 82 |
| Figure 4.18. Exterior surface temperature of non-insulated shear wall (W6) is about $4^{\circ}C$ higher and surface temperature of aluminum window frame is about $8^{\circ}C$ higher than the outside air temperature. These temperature differences shows that there are serious heat loss through the wall and aluminum window frame surfaces ($T_{out} = 6.4^{\circ}C$ and $RH = 65\%$). | 83 |
| Figure 4.19. IR image shows that surface temperatures of W6 is about $4^{\circ}C$ colder than the inside ambient temperature and tie-rod holes can be seen in thermal images in the form of circular colder patches ($T_{out} = 6.4^{\circ}C$ and $RH = 45\%$). | 84 |
| Figure 4.20. Temperature and dew point temperature profiles of W6 showing that temperature gradient throughout the wall section is very close to the dew point temperatures curve, therefore, the wall is under risk of surface and interstitial condensation ($TI_{W6-REFERENCE} = 0.84$; $TI_{W6-DEFECT} = 0.72$) ($T_{in} = 20^{\circ}C$, $RH_{in} = 45\%$ and $T_{out} = -1^{\circ}C$, $RH_{out} = 60\%$). | 85 |
| Figure 4.21. Green painted area at IR image shows the surfaces colder than outside air temperature and at the lower corner of W6 there is possibility of evaporative cooling due to damp zones. ($T_{out} = 6.4^{\circ}C$ and $RH = 65\%$). | 85 |
| Figure 4.22. Temperature index values calculated for the wall surfaces without any defect and wall surfaces suffering from thermal bridges and air leakages. | 89 |
| Figure 4.23. Reference in-situ thermal transmittance ($U_{INSITU-1-REF}$ and $U_{INSITU-2-REF}$) and the theoretically calculated (U_{CALC}) thermal transmittance values of the walls . | 90 |
| Figure 4.24. In-situ U values of W6, obtained at hot and cold weather conditions .. | 93 |
| Figure 4.25. The reference value of actual thermal transmittance ($U_{INSITU-REF}$), the actual thermal transmittance at thermal bridge zones ($U_{INSITU-DEF}$) and the theoretically calculated thermal transmittance (U_{CALC}) values of the six wall components under examination. | 98 |

| | |
|---|-----|
| Figure 4.26. The increase in reference values of actual thermal transmittance at thermal bridge zones ($U_{\text{INSITU-REF}}$) in percentages | 99 |
| Figure 4.27. The plot of increase in the reference values of actual thermal transmittance values at thermal bridge zones (in percentages) versus $U_{\text{INSITU-REF}}$ values of existing building walls..... | 99 |
| Figure 4.28. The reference value of actual thermal transmittance ($U_{\text{INSITU-REF}}$), the average value of actual thermal transmittance ($U_{\text{INSITU-AVG}}$) and the theoretically calculated thermal transmittance (U_{CALC}) values of the six wall components under examination..... | 101 |
| Figure 4.29. The increase in percentages, which were observed in the reference values of actual thermal transmittance ($U_{\text{INSITU-REF}}$) due to the thermal bridges occurred in time in existing building walls | 101 |
| Figure 4.30. The plot of increase in the reference values of actual thermal transmittance values in percentages versus $U_{\text{INSITU-DEF}}$ values of existing building walls | 102 |
| Figure 4.31. Comparison of annual energy consumption for heating purposes for Villa Type Building (B1): theoretically and in-situ θ_{annual} values for both before and after renovation works..... | 105 |

LIST OF ABBREVIATIONS

ABBREVIATIONS

| | |
|--------------------------|---|
| A | Surface Area, m^2 |
| BEP | Building Energy Performance |
| d | Wall thickness, cm |
| EPC | Energy Performance Certificate |
| h | Thermal Convection Coefficient, $\text{Wm}^{-2}\text{K}^{-1}$ |
| HFM | Heat flow Meter |
| HVAC | Heating Ventilation Air Conditioning |
| IR | Infrared |
| IRT | Infrared Thermography |
| k | Thermal Conduction Coefficient, $\text{Wm}^{-1}\text{K}^{-1}$ |
| QIRT | Quantitative Infrared Thermography |
| R | Thermal Resistance, m^2KW^{-1} |
| RH | Relative Humidity, % |
| RH_{IN} | Inside Relative Humidity, % |
| RH_{OUT} | Outside Relative Humidity, % |
| SCM | Standard Calculation Method |
| t | Time, s |
| T | Temperature, K |

| | |
|------------------|--|
| T_{so} | Outside Surface Temperature, K |
| T_{SI} | Inside Surface Temperature, K |
| T_{OUT} | Outside Ambient Temperature, K |
| T_{IN} | Inside Ambient Temperature, K |
| T_{REF} | Reflected Temperature, K |
| TI | Temperature Index, unitless |
| TI_{DEF} | Temperature Index value for defect zones, unitless |
| TI_{AVG} | Temperature Index value for average zones, unitless |
| TI_{REF} | Temperature Index value for reference zones, unitless |
| U | Thermal Transmittance, $Wm^{-2}K^{-1}$ |
| U_{CALC} | Theoretical Thermal Transmittance, $Wm^{-2}K^{-1}$ |
| U_{INSITU} | In-situ Thermal Transmittance, $Wm^{-2}K^{-1}$ |
| $U_{INSITU-DEF}$ | Defect in-situ Thermal Transmittance, $Wm^{-2}K^{-1}$ |
| $U_{INSITU-AVG}$ | Average in-situ Thermal Transmittance, $Wm^{-2}K^{-1}$ |
| $U_{INSITU-REF}$ | Reference in-situ Thermal Transmittance, $Wm^{-2}K^{-1}$ |
| ULM | Unified language modelling |
| v | Velocity, ms^{-1} |
| W | Radiation Power, W |
| θ | Energy, W |
| ε | Emissivity, unitless |
| σ | Stefan Boltzmann Constant, $Wm^{-2} T^{-4}$ |

| | |
|---------------|---|
| ΔT | Temperature Difference, K |
| τ | Atmosphere Radiation Transfer Coefficient, unitless |
| θ_{nd} | Needed Energy Requirement, Wm^{-2} |
| θ_{ht} | Total Heat Loss Energy, Wm^{-2} |
| θ_{gn} | Total Heat Gain, Wm^{-2} |

CHAPTER 1

INTRODUCTION

The argument and objectives of the study on which this thesis was based is presented under the respective sections. It continues with a section titled “Procedure” where the basic steps of the study are outlined and ends with one titled “Disposition” which gives a preview of what is embodied in the rest of the study.

1.1. Argument

Energy efficiency in buildings is one of the most important research and development topics in the world. Reducing energy consumption for heating and cooling purposes in the built environment is one of the essential criteria which contribute to the energy sustainability.

Buildings are responsible from consuming about 35% of total energy usage, which is a very huge amount that should be taken under control. Most of this energy is used for heating, ventilation and air-conditioning (HVAC) purposes in buildings. Therefore, several directives or regulations (BEP, 2008; European Council, 2010; TS 825, 2013) were set by national and international organizations and some of them were put into the force in Turkey since 2002 (BEP, 2008; TS 825, 2013). The certification of building envelopes, namely Energy Performance Certification (EPC) of buildings was started to control energy consumption in relation to the climatic zones in Turkey, to encourage energy save and minimize the energy consumption costs. That certification also requires the monitoring the changes in the initial thermal resistance performance of building envelope in 10 years intervals (BEP, 2008). From this point of view, monitoring actual thermal transmittance performance

of newly-constructed and existing building envelopes in time, without doubt with a practical, non-destructive and remote sensing investigation method, has vital importance. Use of InfRared Thermography (IRT) for quantitative assessment of thermal resistance performance of building envelope is very promising in this regard (Albatici & Tonelli, 2010; Albatici, Tonelli, & Chiogna, 2015; Fokaides & Kalogirou, 2011; Kylili, Fokaides, Christou, & Kalogirou, 2014; Nardi, Sfarra, & Ambrosini, 2014).

The recent studies dealing with the actual thermal performance assessment of existing building walls revealed that the as-is thermal transmittance value of existing building walls is ~~about 20%~~ higher than the thermal transmittance values theoretically-calculated in design stage (Albatici & Tonelli, 2010; Albatici et al., 2015; Fokaides & Kalogirou, 2011; Kylili et al., 2014; Nardi et al., 2014). The certification of energy efficiency is based on Standard Calculation Method (SCM) involving theoretical energy consumption calculations which is defined in TS825:2013 standards and Building Energy Performance regulations (BEP, 2008). For those calculations, the overall thermal transmittance values (U value, $\text{Wm}^{-2}\text{K}^{-1}$) of the single and multi-layered wall configurations should be determined by taken into consideration the thickness of materials layers and their thermal conductivity values (k , $\text{Wm}^{-1}\text{K}^{-1}$) listed in the standards (TS 825, 2013). Since it is known that the theoretically-calculated U values (U_{CALC}) do not represent the actual thermal transmittance of wall configurations, any energy performance certification based on the theoretical calculations is expected to be misleading. Considering all, the reliability to the theoretically-calculated U values and Energy Efficiency Ratings based on those U values are under discussion (Albatici & Tonelli, 2010; Albatici et al., 2015; Fokaides & Kalogirou, 2011; Kylili et al., 2014; Nardi et al., 2014). Therefore, there is necessity for using IRT on quantitative basis for the correct estimation of the actual thermal transmittance values of existing building walls, and

for the development of practical methods for in-situ use of quantitative IRT when the exterior walls are exposed to outside climatic conditions.

There are some studies in which IRT is used for the in-situ U value estimation and some methods are developed in which equations require either exterior or interior surface temperature data achieved by IR scanning of exterior or interior wall surfaces are used (Albatici & Tonelli, 2010; Albatici et al., 2015; Fokaides & Kalogirou, 2011). However, those studies are still under development and comprehensive researches are needed in this regard. For instance, the method using the interior surface temperature data necessitates the thermal imaging study inside the building (Fokaides & Kalogirou, 2011) which may be disturbing for the occupants. Therefore, its widespread use is not expected for U-value estimation and energy performance certification studies in the future. On the other hand, the approach in which thermal imaging is applied externally appears to be more preferable (Albatici & Tonelli, 2010; Albatici et al., 2015). However, the relevant studies are limited in number and the use of in-situ QIRT method needs to be improved for the thermal failure and thermal performance assessment in terms of U-value. Considering all, this research is shaped:

- to estimate U-value of various types of wall configurations having different thermal failures by using QIRT methods,
- to compare their actual thermal resistance performances with their theoretically-calculated ones.
- to better-understand advantages and limitations of those QIRT methods
- to describe the in-situ QIRT testing method that will allow its common and effective use in the fields of building diagnostics with a focus on energy efficiency studies.

In short the main arguments and reasons for selecting Quantitative Infrared Thermography (QIRT) for Thermal Transmittance Assessment of the building walls are summarized below:

- Infrared thermography is a non-destructive and practical investigation method. Its quantitative use is promising for in-situ thermal performance assessment in terms of measurable thermal parameters, such as U-value that is the determinative parameter for energy consumption analysis and energy performance rating in buildings.
- The complaints about thermal and moisture failures, even in properly-insulated buildings, aroused the necessity of the as-is thermal performance examination both for new and existing buildings and development of in-situ QIRT survey in this regard.
- The advances in this field have crucial importance to identify the types of thermal/moisture failures and their reasons in buildings on quantitative basis, to assess the as-is thermal resistance performance of building components, and their monitoring.
- The common-use of QIRT for actual thermal performance assessment is expected to improve consciousness in design and construction of energy efficient buildings and enhance thermal performance quality of buildings in Turkey.
- Increase in QIRT use for diagnostic and monitoring studies in Turkey necessitates the training of experts and researchers in this field; such a demand, therefore, encourages the formation of such a profession which can be charged in relevant ministries, private and academic institutions.

1.2. Objectives

The main aim of the study is to develop and define practical in-situ assessment methods by using quantitative IRT for the actual thermal transmittance estimation of

existing building walls. The horizon targeted by the study is the providing common and effective use of in-situ QIRT methods by the governmental institutes and private sector for the building research and practice studies related with energy efficiency in buildings and sustainable energy development in Turkey. In this regard, the achievements of the study, specifically, is expected to be involved in the energy performance certification or rating (EPC) studies of the buildings and be useful for the training of the prospective specialists/researchers interested in quantitative infrared thermography.

By the end of this research, the study intends to achieve the following objectives:

- to examine as-is thermal performance of various building wall compositions, insulated and non-insulated ones, in terms of thermal transmittance value by using QIRT method,
- to develop techniques for the estimation of as-is thermal transmittance values (U_{INSITU}) of building walls, specifically to determine: the actual thermal resistance performance of the wall composition and thermal transmittance through the failure areas
- to compare the “as-is thermal performance of existing building walls” with the “theoretically-calculated thermal performances” which are used for energy performance certification.
- to discuss the impact of thermal and moisture failures occurred in time on “as-is thermal performance of walls” and on “annual energy consumption of buildings”.
- to achieve reference values of temperature index (TI) for the identification of thermal and moisture failure types observed in building walls.
- to discuss the experience achieved during the in-situ studies in terms of potentials and restrictions of QIRT method.

Two types of residential building and one faculty building in the campus of Middle East Technical University (Ankara, Turkey) were examined to achieve the knowledge based on these objectives.

1.3. Procedure

The study was carried out in three steps. As a first phase, introductory information about the studied buildings and wall compositions were gathered; the present condition of the buildings was observed, a survey about the structures was carried out and architectural drawings about the examined buildings were. The literature review was done to cover methodology to estimate in-situ thermal transmittance value of the building walls.

Then, in-situ IRT method was done by single IR imaging from both inner and outer surfaces of the exterior walls of the buildings. Those studies were performed for several times: winter 2013, 2015, 2016, 2017 and summer 2017. The data of ambient temperature and relative humidity were also collected throughout the study by handled anemometers in both interiors and exteriors.

Finally, the data collected in-situ was analyzed to obtain the results. For IRT analyses, professional programs were used and the data was interpreted together with the graphs. All results were evaluated together to determine the condition of structure.

1.4. Disposition

This thesis study is presented in six main chapters. This introductory chapter is the first one and it provides a brief information about the aim of the research and expectations from it.

After this introductory chapter summary of literature on this topic is given: U value estimation with Quantitative Infrared Thermography method, overview of the parameters affecting the thermal performance of building materials, the heat transfer mechanisms of building components and the physical properties. The third chapter is about the material and method of the study. The aim of this chapter is, to show what is examined and the method how the materials are studied. The fourth chapter is where the results obtained from the various analyses of QIRT and heat transfer calculations are presented in the form of tables and figures. In the fifth and last chapter are presented a discussion on the study and a conclusion regarding the study as a whole. Some suggestions for in-situ thermal transmittance measurements with the use of IRT on site as well as some guidelines those for future studies are also given here.

CHAPTER 2

LITERATURE SURVEY

This chapter explores the studies of building diagnostics via qualitative infrared thermography, assessment of thermal transmittance value with theoretical calculation and quantitative infrared thermography methods and estimation of annual heating energy consumption, in the literature. These studies compiled under nine subchapters.

2.1. Infrared Thermography (IRT) and Infrared Cameras

Infrared segment of electromagnetic spectrum was discovered by astronomer Sir Frederick William Herschell, who is the discoverer of the planet Uranus, at the beginning of the 19th century. While William Hershel was searching a new optical parameter to reduce the brightness of the sun's image taken with telescope, he accidentally made this discovery(Flir Systems, 2013). Of course, this discovery is not only his achievement, before him, many other scientists worked on similar subjects. He measured that, temperature of the light at the electromagnetic spectrum beyond red colors reaches to maximum value. Therefore, at the electromagnetic spectrum beyond red colors is termed as Infrared.

Infrared radiation is between visible and microwaves sections of Electromagnetic spectrum (Figure 2.1), and heat is the primary source of infrared radiation (Çengel & Ghajar, 2015; Flir Systems, 2013; Kylili et al., 2014; Lucchi, 2018; Modest, 2003; Rao P., 2008).

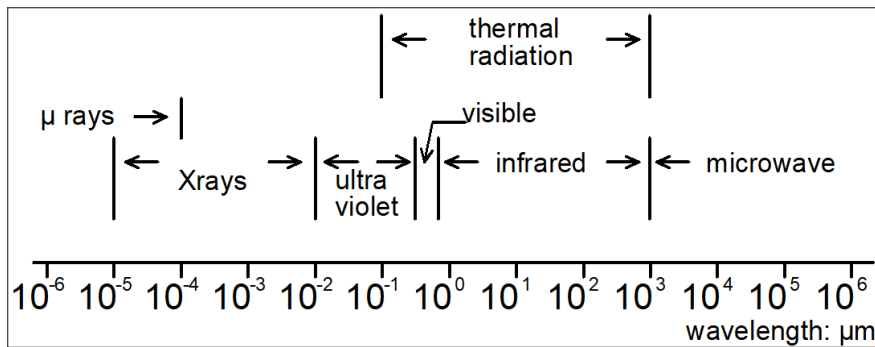


Figure 2.1. Electromagnetic wave spectrum

Heat transfer caused because of electromagnetic waves is called as thermal radiation. Some daily life examples of radiative heat transfer are: (i) heating effect of sun, (ii) the body's side facing the radiator/heater feels hotter than the other side and (iii) during a cold night in a room with closed curtains thermal comfort is higher than another room with same temperature with open curtains, radiative heat transfer from inside to outside through windows is the reason of this difference (Modest, 2003).

The sensitivity of the infrared cameras significantly increased by the invention of bolometer, which is used for measuring power of radiation, by Langley in late 19th century. The first infrared camera was invented for military purposes like many other technological developments, in 1929 in Britain and spectacular developments were done on these cameras during between World Wars. Finally, at late 1960s commercialization of infrared cameras began (Table 2.1) (Grinzato, 2012; Rao P., 2008; Rinaldi, 2012; Tattersall, 2016).

Table 2.1. *Brief History of Infrared Cameras (Flir Systems, 2013)*

| year | Main Technological Development |
|---|--------------------------------|
| 1835 | thermopile IR detector |
| 1840 | first IR image |
| 1880 | bolometer |
| 1929 | IR sensitive camera |
| 1930 | IR detectors |
| MILITARY SECTOR | |
| 1966 | Thermovision IR camera |
| MEDICINE- VETERINARY - ASTRONOMY | |
| 1985 | IR camera with computer |
| 1987 | Single IR camera |
| BUILDING DIAGNOSTICS | |
| 1997 | Uncooled micro bolometer |
| 2000 | Portable IR camera |
| BUILDING ENERGY AUDIT | |
| 2015 | Little IR camera |
| AUTOMOTIVE - SMART BUILDING - ENVIRONMENTAL CONTROL | |

Parallel to development of the infrared cameras, using IRT method for many kind of civil applications has become widespread (Grinzato, 2012; Rao P., 2008; Rinaldi, 2012; Tattersall, 2016), such as:

- Military purposes; first systems of cameras began to developed during between World War 1 and 2, for several purposes, for example night vision provides tactical advantages, enemy soldiers and aircraft detection by remote temperature measuring (Flir Systems, 2013).
- Manufacturing industries; thermoelastic stress analysis, investigation of tensile deformation and fatigue action of metals or composites, maintenance of the machines, materials testing, efficiency estimation of manufacturing machines, temperature measurements into an automobile cabin, food production industry (Chen, Zhang, Zhao, & Ouyang, 2013; Gowen, Tiwari, Cullen, McDonnell, & O'Donnell, 2010; Korukcu & Kilic, 2009; Rinaldi, 2012).

- Biological researches; level of biological activity, animal research (Alastair Fothergill, 2006; Berry, Kennedy, Scott, Kyle, & Schaefer, 2003; Cilulko, Janiszewski, Bogdaszewski, & Szczygieska, 2013; Knížková, Kunc, Gürdil, Pinar, & Selvi, 2007; Mccafferty, 2007).
- Environmental studies; investigation of soil moisture content, meteorological studies, volcano activities, environmental pollution determination (Costa, Grant, & Chaves, 2013; Doulos, Santamouris, & Livada, 2004).
- Fire detection; for both in urban and rural areas as well as forests (Amon, Hamins, Bryner, & Rowe, 2008; Brogi & Pietranera, 1995; Owrutsky et al., 2006).
- Psychological studies and medical science; body temperature is a sign for illness and checking body temperature may be very useful for estimating illness: skin temperature mapping, depression, breast cancer, situation of heart, brain imaging, etc. and also it is possible to collect data about the abnormalities of body (Esposito et al., 2015; Hazenberg, van Netten, van Baal, & Bus, 2014; Nakanishi & Imai-Matsumura, 2008; Rinaldi, 2012; Seeley, Abramson, Perry, Rothblatt, & Seeley, 1980; Stewart et al., 2007).
- Observation of functional/service systems of buildings; monitoring microclimate, thermal comfort, performance of HVAC systems and electrical systems, maintenance of buildings, corrosion detection on pipes, leakage and blockage determination at ventilation ducts and plumbing and domestic water pipes (Balaras & Argiriou, 2002; Barreira & de Freitas, 2007; Djupkep, Maldague, Bendada, & Bison, 2013; Grinzato, 2012; Kylili et al., 2014; Rinaldi, 2012)
- Diagnostic studies on problems in buildings, their sources and monitoring before and after maintenance and repair works, in this context; delamination and crack determination, positioning the masonry structure under plaster without rasping especially for historical buildings, investigation of moisture problems near surface region, evaluation of thermal characteristics of the building envelope, estimation of the thermal bridges, air leakage areas, moisture problems and

estimation of performance of the building materials, with the increase of using new materials and new systems without knowing their performance, this evaluation is much more important than before, non-destructive control of structural system of the buildings, moisture and crack detection (Albatici & Tonelli, 2010; Albatici et al., 2015; Fokaides & Kalogirou, 2011; Tavukçuoğlu, Akevren, & Grinzato, 2010; Tavukçuoğlu, Düzgüneş, Caner-Saltık, & Demirci, 2005; Tavukçuoğlu, A., Caner-Saltık, E.N., Akoğlu, K.G., Işıkoğlu, M., & Caner, E., 2011).

There are two main approaches for IRT method: (i) Active thermography and (ii) Passive thermography. Active thermography is used for the condition where temperature difference between matters does not naturally exist, and an external source is needed. Therefore active thermography is usually used for laboratory researches. Active thermography is beneficial especially for detection of internal defects, because, thermal defects are effectively seen by active thermography. Passive thermography is used while test materials are naturally at different temperatures, which means heat flux between matters is produced naturally, so, there is no need to have an external heat source. Therefore, passive thermography is usually used for site/in-situ researches. Because, the aim of this study is assess the natural heat transfer between building envelope and atmosphere, passive IRT method is used for site measurements (Asdrubali, Baldinelli, & Bianchi, 2012; Barreira & de Freitas, 2007; Grinzato, 2012; Kylili et al., 2014; Lucchi, 2018; Maldague, 2002).

IRT analyses can be done by single or sequential. Former one is done by taking single infrared images of the target area and latter one is done by taking sequential images 5-10 second intervals for a period of 5-10 minutes of the target area. The differential IR images can be produced by taking the temperature differences as a

function of time, therefore sequential method mainly very helpful when hidden structures and crack mapping are studied (Hoyano, Asano, & Kanamaru, 1999; Bortolin et al., 2013; Titman, 2001).

Thermal radiation theory is base of the infrared camera technology. Infrared cameras, which are used at infrared thermography method (IRT), measure the infrared radiation emitted from the target area (bodies above absolute zero temperature ($0^{\circ}\text{K}=-273^{\circ}\text{C}$) emits electromagnetic radiation) with its special lenses in the form of digital signals, then, convert this radiative energy to temperature values and prepare the images of the temperature distribution of the target area (Flir Systems; 2013) (Figure 2.2, Figure 2.3).

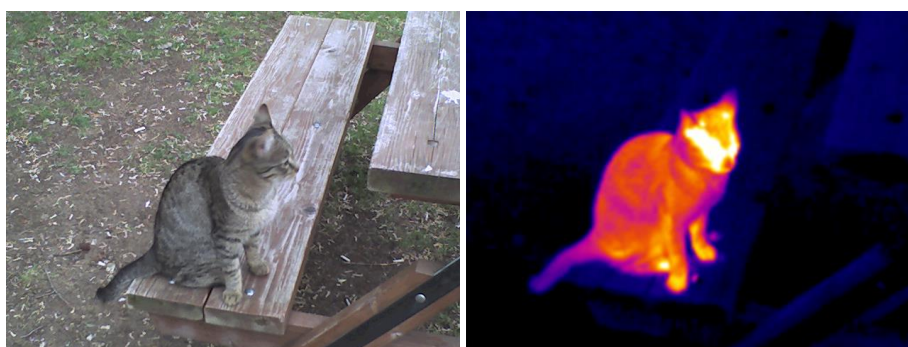


Figure 2.2. Comparison of real and thermal images

Different colors at the infrared images represent the temperature pattern of the target area. These thermal maps can be defined as the matrix of the surface which shows temperature distribution of each pixels of the image and number of pixels is depended on the camera properties. In other words, these cameras detect the infrared waves that cannot be seen with naked human eyes (Balaras & Argiriou, 2002; Modest, 2003; Rao P., 2008).

| | | | | | | | | | | | | | |
|------|------|------|------|------|------|------|------|------|------|------|------|------|------|
| 3.5 | 3.3 | 3.4 | 3.2 | 3.3 | 2.9 | 3.2 | 2.0 | 2.0 | 3.2 | 3.8 | 4.7 | 6.7 | 10.0 |
| 3.5 | 3.4 | 3.3 | 3.3 | 3.3 | 3.2 | 3.2 | 3.4 | 3.9 | 4.9 | 6.5 | 8.7 | 11.0 | 12.6 |
| 4.1 | 3.6 | 3.5 | 3.3 | 3.7 | 3.5 | 3.9 | 5.0 | 6.9 | 9.9 | 11.7 | 12.5 | 13.3 | 14.3 |
| 5.9 | 4.8 | 4.4 | 4.9 | 5.1 | 5.6 | 7.3 | 9.9 | 12.5 | 14.1 | 15.2 | 15.2 | 15.5 | 16.0 |
| 8.5 | 7.3 | 6.5 | 8.3 | 9.9 | 10.9 | 13.0 | 13.7 | 14.0 | 14.8 | 15.6 | 16.4 | 16.8 | 18.2 |
| 10.3 | 10.9 | 8.5 | 8.7 | 11.7 | 12.5 | 14.7 | 15.0 | 14.5 | 14.9 | 16.2 | 16.3 | 16.9 | 18.1 |
| 11.9 | 13.2 | 12.1 | 9.0 | 11.1 | 13.8 | 16.3 | 16.2 | 15.6 | 15.7 | 16.7 | 17.1 | 17.6 | 17.5 |
| 13.1 | 14.5 | 13.7 | 11.3 | 11.1 | 15.7 | 19.4 | 17.2 | 16.1 | 15.9 | 16.8 | 17.5 | 17.2 | 17.5 |
| 13.6 | 15.3 | 14.0 | 13.5 | 13.9 | 15.6 | 20.7 | 19.4 | 15.7 | 16.2 | 16.7 | 16.2 | 17.1 | 17.2 |
| 14.5 | 16.4 | 15.9 | 17.2 | 19.4 | 18.1 | 17.8 | 16.9 | 15.1 | 15.5 | 15.7 | 15.5 | 16.6 | 16.5 |
| 16.1 | 21.3 | 21.4 | 24.2 | 24.7 | 22.0 | 21.7 | 20.0 | 16.2 | 15.3 | 15.6 | 15.8 | 15.8 | 17.0 |
| 16.8 | 24.4 | 26.3 | 27.2 | 26.8 | 21.0 | 21.3 | 23.2 | 19.4 | 16.4 | 16.9 | 16.6 | 16.0 | 17.4 |
| 14.0 | 19.8 | 24.1 | 25.1 | 23.4 | 21.1 | 22.2 | 22.2 | 20.6 | 18.7 | 18.1 | 17.3 | 16.5 | 16.9 |
| 12.3 | 14.4 | 17.6 | 20.0 | 22.8 | 22.9 | 23.4 | 24.2 | 23.3 | 22.6 | 20.8 | 19.4 | 17.8 | 16.6 |
| 11.1 | 12.5 | 14.7 | 18.3 | 22.3 | 23.9 | 25.9 | 26.2 | 25.6 | 24.9 | 24.6 | 23.1 | 20.0 | 17.1 |
| 10.1 | 11.4 | 13.9 | 16.2 | 19.1 | 22.8 | 24.7 | 25.4 | 24.4 | 23.3 | 24.1 | 24.1 | 21.9 | 17.7 |
| 10.5 | 11.6 | 12.6 | 13.5 | 15.4 | 18.0 | 21.8 | 23.3 | 21.8 | 21.2 | 23.7 | 24.1 | 23.6 | 19.8 |
| 10.2 | 11.3 | 12.2 | 12.6 | 13.2 | 15.3 | 18.7 | 20.8 | 20.7 | 22.0 | 25.6 | 28.4 | 27.1 | 24.2 |
| 10.5 | 11.0 | 12.3 | 13.0 | 14.0 | 15.1 | 17.3 | 20.9 | 26.4 | 28.8 | 29.6 | 30.4 | 28.7 | 25.9 |
| 10.0 | 10.8 | 11.7 | 12.2 | 13.2 | 14.4 | 15.7 | 18.5 | 22.7 | 26.7 | 28.5 | 28.5 | 27.1 | 24.2 |
| 10.3 | 10.5 | 11.4 | 11.9 | 12.7 | 13.2 | 14.8 | 16.5 | 18.7 | 21.2 | 23.7 | 25.4 | 24.6 | 21.2 |
| 11.0 | 10.8 | 11.2 | 11.9 | 12.4 | 13.0 | 14.3 | 15.3 | 16.7 | 18.6 | 20.0 | 21.8 | 22.0 | 19.5 |
| 12.8 | 11.3 | 11.0 | 11.6 | 12.9 | 13.8 | 15.2 | 16.7 | 17.4 | 18.6 | 20.7 | 21.6 | 21.2 | 18.4 |
| 13.9 | 13.6 | 12.2 | 11.3 | 11.9 | 12.6 | 13.2 | 14.0 | 15.6 | 17.5 | 19.7 | 21.0 | 20.6 | 17.8 |
| 14.1 | 14.9 | 14.0 | 13.4 | 12.5 | 12.2 | 11.9 | 11.9 | 12.3 | 13.7 | 16.9 | 19.1 | 19.5 | 18.0 |
| 13.9 | 14.8 | 14.9 | 15.0 | 13.7 | 13.4 | 12.1 | 12.2 | 12.0 | 11.9 | 12.6 | 13.8 | 14.5 | 14.0 |
| 13.2 | 14.3 | 14.9 | 14.8 | 14.4 | 13.3 | 12.9 | 12.1 | 11.9 | 11.4 | 10.9 | 10.6 | 10.1 | 10.3 |
| 12.9 | 14.0 | 14.1 | 14.4 | 14.4 | 13.7 | 12.7 | 12.2 | 11.6 | 11.6 | 10.7 | 10.7 | 10.7 | 10.3 |
| 12.4 | 13.1 | 13.5 | 14.2 | 13.6 | 13.1 | 13.1 | 12.0 | 11.3 | 11.2 | 11.2 | 11.2 | 10.5 | 9.4 |
| 12.4 | 12.4 | 12.9 | 13.1 | 13.6 | 13.1 | 13.5 | 12.7 | 11.0 | 10.9 | 11.2 | 11.1 | 9.9 | 8.7 |
| 12.3 | 12.4 | 12.5 | 12.4 | 13.2 | 12.9 | 13.2 | 12.2 | 10.6 | 10.5 | 10.5 | 10.6 | 9.4 | 8.4 |
| 12.1 | 11.9 | 12.2 | 12.6 | 12.6 | 12.3 | 12.2 | 11.5 | 10.6 | 9.9 | 9.7 | 9.7 | 9.5 | 8.0 |
| 12.2 | 11.8 | 12.1 | 12.3 | 12.3 | 11.9 | 11.3 | 10.6 | 9.9 | 9.4 | 8.9 | 8.6 | 7.8 | 7.1 |
| 12.6 | 12.4 | 12.2 | 11.9 | 12.1 | 11.7 | 10.7 | 10.2 | 9.6 | 8.9 | 8.0 | 7.5 | 7.1 | 6.0 |
| 12.9 | 12.6 | 12.9 | 11.9 | 11.9 | 11.1 | 10.2 | 9.6 | 9.1 | 8.1 | 7.2 | 7.2 | 6.7 | 4.9 |
| 12.8 | 12.6 | 12.4 | 12.0 | 11.7 | 10.7 | 10.2 | 9.2 | 8.2 | 7.6 | 7.5 | 6.7 | 5.2 | 3.9 |
| 12.8 | 12.6 | 12.2 | 11.7 | 11.0 | 10.1 | 9.4 | 8.3 | 7.8 | 7.1 | 6.9 | 5.1 | 4.0 | 3.6 |
| 12.6 | 12.1 | 11.4 | 10.8 | 10.4 | 9.3 | 8.6 | 7.8 | 7.7 | 6.6 | 4.8 | 3.9 | 3.5 | 3.2 |
| 12.1 | 11.5 | 11.1 | 10.5 | 10.0 | 8.9 | 8.1 | 7.6 | 7.5 | 5.0 | 3.9 | 3.6 | 3.5 | 3.3 |
| 11.5 | 11.2 | 10.7 | 9.9 | 9.1 | 8.2 | 9.4 | 8.1 | 7.2 | 4.0 | 3.8 | 3.6 | 3.5 | 3.2 |

Figure 2.3. Sample temperature distribution of the thermal image at Figure 2.2, 30.4°C is the hottest part of the cat, close to ear.

Radiative energy measured by IR cameras is transformed to surface temperature value of the target area by using Stephan-Boltzmann equation, and this equation is formulized as:

$$\theta = \varepsilon \times \sigma \times T^4 \quad (1)$$

where,

θ : radiation energy, Wm^{-2}

ε : emissivity of the material, and it is written as a fraction of the energy emitted from the surface to the energy emitted by ideal black body at that temperature, unitless

σ : Stefan Boltzmann constant, $5,67 \times 10^{-8}$, $\text{Wm}^{-2} \text{T}^{-4}$

T: surface temperature, K

During imaging of the target area with thermal camera, radiation coming from target area, surroundings and atmosphere are collected by infrared sensor (Figure 2.4). Therefore, for infrared thermography, following parameters should be collected to estimate the surface temperature: (i) ambient temperature, (ii) reflected temperature, (iii) relative humidity, (iv) emissivity of the target area and (v) distance between target area and the camera sensor (Fokaides & Kalogirou, 2011; Asdrubali et al., 2012; Kylili et al., 2014; Albatici et al., 2015; Albatici & Tonelli, 2010). Equation of thermographic measurement is formulized as:

$$W_{tot} = \varepsilon \times \tau \times W_{target-area} + (1 - \varepsilon) \times \tau \times W_{reflected} + (1 - \tau) \times W_{atm} \quad (2)$$

where,

W : radiation power, W

ε : emissivity of the material, and it is written as a fraction of the energy emitted from the surface to the energy emitted by ideal black body at that temperature, unitless

τ : atmosphere radiation transfer, unitless

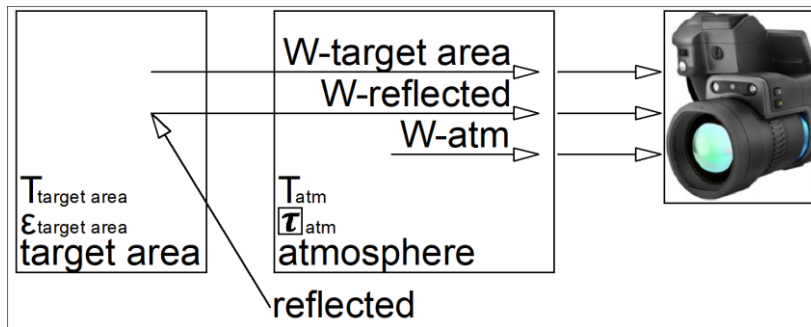


Figure 2.4. Schematic representation of thermographic measurement

Thermal cameras are suitable for either short (3-5 μm) or long (8-12 μm) wavelengths. Short wavelength cameras are suitable for hot surfaces and when the importance of contrast is higher than the sensitivity to ambient objects temperature. However, if the sensitivity to the ambient temperature and ambient objects temperature is important long wavelength type cameras should be used, in addition to this, long wavelength cameras are less affected by solar radiation and detection of small temperature differences is possible (Balaras & Argiriou, 2002; Lucchi, 2018; Martín Ocaña, Cañas Guerrero, & González Requena, 2004; Tejedor, Casals, Gangolells, & Roca, 2017).

2.2. Use of Heat Flow Meter for building diagnostics

Heat flow Meters (HFM), which are widely accepted for evaluation of thermal transmittance, can be used to measure in-situ thermal transmittance value of the building walls without destruction. Heat flow meter is a transducer and this device can directly transfer the electrical signals given by its temperature sensors to heat flow through the wall. Calculation of thermal transmittance value with HFM is described in the standard (TS EN ISO 9869, 2004). This device measure the average heat flux through wall, than this value is divided to the temperature difference between the two sides of the wall to calculate the overall thermal transmittance value. It is possible to measure only point base thermal transmittance value with this method, and in order to estimate transmittance value of another point another measurement is needed. Therefore measurement procedure is much longer than infrared cameras. Another limitation of this method is, heat flow meters does not calculate the radiative heat transfer, in other words this method ignores emitted energy from surfaces (Fokaides & Kalogirou, 2011; Nardi et al., 2014).

Although, thermal transmittance value of the walls can be calculated by heat flow meters, there are some restrictions of this building diagnostic method, these restrictions are as follows:

- The sensors must be located carefully to avoid from thermal bridges, construction joints and moist elements.
- The sensors located to outside wall surface must be away from rain, snow and solar radiation.
- The sensors located to inside wall surface must be away from heat sources like radiators or air conditioner.
- There should be a minimum 10 temperature difference between inside and outside of the walls, and this difference should be stable.
- Finally the minimum test duration is about 72 hours.

Otherwise, the result of the estimation will not represent the wall overall thermal transmittance value.

HFM is a point base device, therefore to estimation of the temperature distribution of the whole wall surface is not easy in comparison with IRT. One single image can be enough to estimate the temperature distribution of the whole wall surface with IRT method. However, for heat flow meter several data collection is needed, therefore more than one device should be used. Also, it is very difficult, even impossible, to reach some parts of the building: ceiling, roof, etc. Finally, if the façade of the building with multi-layered and therefore non-homogeneous, the data obtained with HFM is not reliable (Albatici & Tonelli, 2010; Grinzato, 2012; Tejedor et al., 2017).

Although, heat transfer through a medium is multi-dimensional, heat flow meter is based on the assumption that the heat flow through building wall is one dimensional. In other words, temperature of the medium varies in all direction through the wall,

however this device assume it to vary only one direction (Çengel & Ghajar, 2015). In addition to this assumption, this method neglecting the heat transfer with convection and radiation from wall surface. Therefore, with this method only heat transfer because of conduction can be estimated (Albatici & Tonelli, 2010).

There are two different data analyze method for heat flow meter. One is average and the other one is dynamic method. Former one needs more data to increase the possibility to get the correct result, therefore test duration is higher. For the following one, test duration is shorter by having less data, however again for increasing possibility to get correct result, temperature difference between two sides of the wall should be higher (Albatici & Tonelli, 2010).

2.3. Heat Transfer; Modes and Parameters

Heat transfer modes and some important parameters, such as; thermal resistance, thermal transmittance and temperature index are briefly discussed in this section. In this study, these parameters are calculated and used to make quantitative investigation of the building walls.

Transportation of energy due to a temperature difference between matters is defined as heat transfer, and this energy transfer occurs from more energetic towards less energetic ones. There are three modes of heat transfer: Conduction, Convection and Radiation (Figure 2.5) (Çengel & Ghajar, 2015; Davies, 2004; Modest, 2003).

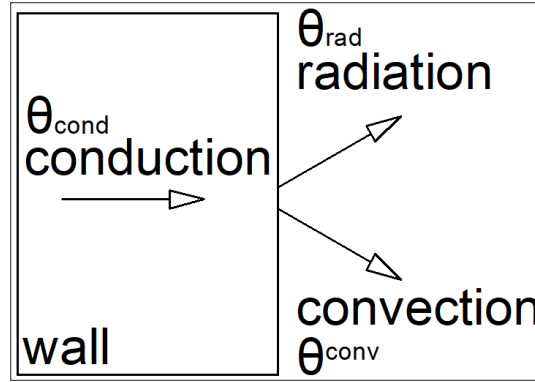


Figure 2.5. Energy interaction at wall surface

Energy balance at the wall surface, by assuming the heat diffusion through wall at third direction is negligible, is formulized as following (Çengel & Ghajar, 2015):

$$\theta_{cond} = \theta_{rad} + \theta_{conv} \quad (3)$$

where,

θ_{cond} : conduction, Wm^{-2}

θ_{rad} : radiation, Wm^{-2}

θ_{conv} : convection, Wm^{-2}

Heat transfer by **conduction** occurs because of the interactions of molecules with each other and heat transfer is defined as a measure the ability of the materials to transfer heat. This transfer is formulized in Fourier law of conduction as (Çengel & Ghajar, 2015):

$$\theta_{cond} = k \times \Delta T \quad (1)$$

where,

k: thermal conductivity of the material, $\text{Wm}^{-1}\text{K}^{-1}$, which is the measure of the ability of a material to conduct heat

ΔT : temperature difference between matters, K

Conductivity of the materials increases with the increased temperature, because, conductivity is the motion of the molecules and with increasing temperature, kinetic energy of the molecules increases. As a result, the material with higher temperature/energy conducts more heat (Çengel & Ghajar, 2015).

Heat transfer by **convection** occurs between a solid and the adjacent liquid or gas with different temperature. This transfer is formulized in Newton's law of cooling as (Çengel & Ghajar, 2015):

$$\theta_{conv} = h \times \Delta T \quad (4)$$

where,

h: convection coefficient, $\text{Wm}^{-2}\text{K}^{-1}$

ΔT : temperature difference between matters, K.

There are two methods to estimate convection coefficient of building envelope surfaces (Dall'O', Sarto, & Panza, 2013): (i) convection coefficient can be taken directly from related standards (TS 825, 2013), (ii) the Jurges equation can be used to calculate in-situ convection coefficient. Wind velocity (v , ms^{-1}) near building envelope should be measured to calculate convection coefficient with Jurges equation. Because, convective heat transfer depends on the wind velocity, and with

increasing wind velocity convective heat transfer also increases (Çengel & Ghajar, 2015). Calculation of convection coefficient by using Jurges equation is formulized as follows (wind velocity near building envelope should be smaller than 5ms^{-1}):

$$h_{OUT} = 5,8 + 38054 \times v \ (v < 5\text{ms}^{-1}) \quad (5)$$

where,

h_{out} : exterior surface convection coefficient, $\text{Wm}^{-2}\text{K}^{-1}$.

v : wind velocity near exterior wall surface. ms^{-1}

An existence medium is needed between heat source and the receiver both for conduction and convection heat transfer. On the contrary, radiative energy is transferred by electromagnetic waves and these waves can travel much longer distances without existence of an interacting medium between the source and the receiver. Heat transfer by **radiation** (θ , Wm^{-2}) occurs because of the energy transmission as electromagnetic waves, and unlike the other two heat transfer mechanisms radiative heat transfer does not need the existence of intervening medium, like sun energy reaching the earth. Bodies above absolute zero temperature (-273°C) radiate energy in the form of electromagnetic waves at a speed of light. This transfer is formulized in Stefan Boltzmann law as:

$$\theta = \varepsilon \times \sigma \times T^4 \quad (6)$$

where,

ε : emissivity of the material, and it is written as a fraction of the energy emitted from the surface to the energy emitted by ideal black body at that temperature, unitless

σ : Stefan Boltzmann constant, $5.67 \times 10^{-8} \text{Wm}^{-2}\text{T}^{-4}$

T: surface temperature, K

Another important difference between radiation and the other heat transfer modes is temperature proportionality. Conduction and convection are linearly proportional on the temperature. On contrary, radiation heat transfer is proportional to the fourth power (Equation 6) of the temperature, therefore especially for high temperatures radiative heat transfer is more influential than other two heat transfer modes (Çengel & Ghajar, 2015; Modest, 2003).

Thermal Resistance, R (m^2KW^{-1}), is defined as the resistance of the material against conductive (thermal conduction resistance), convective (thermal convection resistance) and radiative heat transfer (thermal radiation resistance) (Çengel & Ghajar, 2015).

Thermal Transmittance, U ($\text{Wm}^{-2}\text{K}^{-1}$), is rate at which thermal energy is transferred through unit area per unit temperature difference between either sides of the environment. This value can be estimated via infrared thermography method or can be calculated with using conduction and convection coefficients of the materials given in the relevant standards (Albatici & Tonelli, 2010; Çengel & Ghajar, 2015; Davies, 2004; Fokaides & Kalogirou, 2011; Modest, 2003; TS 825, 2013; TS EN ISO 6946, 2007).

In-situ Thermal Transmittance, U_{INSITU} ($\text{Wm}^{-2}\text{K}^{-1}$), value is assessed by quantitative infrared thermography (QIRT) method. Two different equations are used in the literature for assessing the in-situ thermal transmittance values: $U_{\text{INSITU-1}}$ and $U_{\text{INSITU-2}}$ (Albatici & Tonelli, 2010; Albatici et al., 2015; Fokaides & Kalogirou, 2011).

$$U_{INSITU-1} = \frac{5.67 \times \varepsilon \times \left(\frac{T_{SO}^4 - T_{OUT}^4}{100^4} \right) + 3.8054 \times v \times (T_{SO} - T_{OUT})}{(T_{in} - T_{out})} \quad (7)$$

where;

ε : emissivity of the wall surface (unitless)

T_{SO} : in-situ outside surface temperature of exterior wall, (K)

T_{OUT} : in-situ outside ambient temperature, (K)

T_{IN} : in-situ inside ambient temperature, (K)

v : in-situ local wind velocity, (m/s)

In that equation, there is necessity of measuring outside surface temperature of exterior walls, inside and outside ambient temperatures and as well, measuring the outside wind/air velocity near wall surface (Figure 2.6) (Albatici & Tonelli, 2010; Albatici et al., 2015).



Figure 2.6. Using handheld anemometer to measure wind velocity near wall surface

$$U_{INSITU-2} = \frac{4 \times \varepsilon \times 5.67 \times 10^{-8} \times T_{si}^3 \times (T_{si} - T_{in}) + h_{in} \times (T_{si} - T_{in})}{(T_{in} - T_{out})} \quad (8)$$

where;

ϵ : emissivity of the wall surface (unitless)

T_{SI} : in-situ inside surface temperature of exterior wall, (K)

T_{OUT} : in-situ outside ambient temperature, (K)

T_{IN} : in-situ inside ambient temperature, (K)

h_{IN} : thermal convection coefficient, ($Wm^{-2}K^{-1}$).

In that equation, there is necessity of measuring inside surface temperature of exterior walls, inside and outside ambient temperature, and using thermal convection coefficient values (h_{IN}) given in the relevant standards (Fokaides & Kalogirou, 2011; TS 825, 2013). The authors of this method decided to perform thermal transmittance estimation based on indoor measurements, because correct measurement of reflected temperature is very important to increase the reliability of IRT method, and measuring reflected temperature at the inside of the building is easier (Fokaides & Kalogirou, 2011).

Theoretical Thermal Transmittance, U_{CALC} ($Wm^{-2}K^{-1}$), value of the walls is calculated by using surface convection coefficient of interior wall (h_{SI}) and exterior wall (h_{SO}) and thermal conductivity values (k_i) given in relevant standards for each material and the thickness of wall layer (d_i) (Çengel & Ghajar, 2015; TS 825, 2013; TS EN ISO 6946, 2007).

$$U_{CALC} = \frac{1}{\frac{1}{h_{SI}} + \frac{d_1}{k_1} + \dots + \frac{d_n}{k_n} + \frac{1}{h_{SO}}} \quad (9)$$

where;

h_{SI} : inside wall surface thermal convection coefficient ($7.69 \text{ Wm}^{-2}\text{K}^{-1}$)

h_{SO} : outside wall surface thermal convection coefficient ($25 \text{ Wm}^{-2}\text{K}^{-1}$);

d_i : thickness of the wall layers (m)

k_i : thermal conductivity of the wall layers ($\text{Wm}^{-1}\text{K}^{-1}$).

The studies deal with the performance assessment of existing situation mention that, in-situ thermal transmittance value (U_{INSITU}) of the building walls is higher than the theoretical calculated U value (U_{CALC}) (Table 2.2) (Albatici & Tonelli, 2010; Albatici et al., 2015; Fokaides & Kalogirou, 2011; Kylili et al., 2014; Nardi et al., 2014).

Table 2.2. Comparison table of estimated U_{INSITU} and U_{CALC} values in related researches

| Reference | building type | studied wall type | measurement from | wind speed | | U _{INSITU-1} | | U _{CALC} | Rel.Change | |
|----------------------------|---------------|-------------------|------------------|--|---------------|----------------------------------|--------|-------------------|--|-----|
| | | | | m/s | | Wm ⁻² K ⁻¹ | | | U _{INSITU1} , U _{C2} | |
| | | | | | | winter | summer | | | |
| Albatici & Tonelli, 2010 | residential | light weighted | outside | assumed = 0 | | 0.38 | 0.29 | 31% | | |
| | | assumed = 0 | | assumed = 1 | 0.19 | 0.38 | 0.148 | 28% | 157% | |
| | | heavy weighted | | assumed = 0.2 | assumed = 0.1 | 0.27 | 0.3 | 0.225 | 20% | 33% |
| Albatici & Tonelli, 2015 | experimental | light weighted | outside | insitu measured | | 0.14 | 0.17 | -18% | | |
| | | 0.16 | | | | 0.18 | -11% | | | |
| | | 0.37 | | | | 0.3 | 23% | | | |
| | | 0.62 | | | | 0.57 | 9% | | | |
| | | 0.51 | | | | 0.44 | 16% | | | |
| Reference | building type | studied wall type | measurement from | wind speed | | U _{INSITU-2} | | U _{CALC} | Rel.Change | |
| | | | | m/s | | Wm ⁻² K ⁻¹ | | | U _{INSITU2} , U _{C1} | |
| | | | | | | winter | summer | | | |
| Fokaides & Kalogirou, 2011 | residential | heavy weighted | inside | surface convection is taken from related standards | | 2.35 | 2.32 | 2.1 | 12% | 10% |
| | | 1.56 | | | | 1.58 | 1.39 | 12% | 14% | |
| | | 0.47 | | | | 0.52 | 0.42 | 12% | 24% | |
| | | 1.39 | | | | 1.38 | 1.39 | 0% | -1% | |
| | | 1.52 | | | | 1.66 | 1.39 | 9% | 19% | |

Because of the difference between in-situ and theoretical calculated U values, the reliability to the theoretically calculated U values is under discussion. Some of the reasons that may change the expected thermal resistance performance are summarized below:

- The thermal conductivity values of building materials assigned in the standards are used for the theoretical calculations. However, thermal conductivity performance may differ in damp and wet conditions, which may occur real service life of building components. Therefore, the materials can perform less thermal resistive than expected in real case.
- The building components and their multi layered configurations are defining in working drawings (shop drawings) of the building. However, those components sometimes are not constructed in coherence with the architectural details given in working drawings. In addition to this case, especially for old buildings working drawings may be missing, so it is hard to define the multi layered configuration at the building envelope. Therefore, the building components can perform less thermal resistive than expected in real case (Albatici & Tonelli, 2010; Fokaides & Kalogirou, 2011; Nardi et al., 2014).
- Thermal transmittance values can be calculated theoretically based on the equation 7. Those values are used as design values to estimate the thermal resistivity on each component. However, the real performance and the theoretically calculated performance may differ and such difference may result in troublesome situations in buildings; thermal, moisture and material failures (Albatici & Tonelli, 2010; Albatici et al., 2015; Fokaides & Kalogirou, 2011).
- It is assumed that the materials always have the performance that is assigned according to relevant standards (TS 825, 2013), however because of aging effect on materials used at the façade of the buildings actual thermal performance of the buildings may be different.
- In addition to the aging effect, workmanship faults during construction of the walls may change the actual thermal performance of the materials.
- Thermal surface convection coefficient increases with increasing wind speed, therefore effect of changing wind speed should be taken into account, however for theoretical calculations thermal convection coefficient is constant and effect of changing wind speed is not taken into consideration.

- Thermal surface convection coefficient and conduction coefficient increases with increasing humidity level of the materials, therefore effect of changing relative humidity should be taken into account.

Temperature Index, (TI, unitless), is a parameter which is defined as insulation efficiency or condensation index in literature. TI value is calculated by using Equation 10 and there is necessity to measure the interior surface temperature of exterior wall together with inside and outside ambient temperatures. The data collected in 1980's show that TI value ranges between 0 to 1 and being away from 1 corresponds to decrease in thermal insulation performance of the wall (Stainton, 1980). The ranges in TI values given in the literature are not determinative enough to identify the type of defect.

$$TI = \frac{R_{SO} + R_W}{R_{SO} + R_W + R_{SI}} = \frac{T_{SI} - T_{OUT}}{T_{IN} - T_{OUT}} \quad (10)$$

where;

R_{SO}: outer surface convection resistance (m²KW⁻¹)

R_{SI}: interior surface convection resistance (m²KW⁻¹)

R_W: W conduction resistance (m²KW⁻¹)

T_{IN}: in-situ inside ambient temperature (K)

T_{SI}: in-situ interior surface temperature of exterior wall (K)

T_{OUT}: in-situ outside ambient temperature (K)

Another study defines a parameter called TI with the Equation 11 and uses that parameter to identify thermal and moisture defects (Koçkar, 2012; Tuğla & Tavukçuoğlu, 2016; Tuğla, Tavukçuoğlu, & Arslan, 2013). That TI value requires

the exterior surface temperature of exterior wall together with inside and outside ambient temperatures. Measuring exterior surface temperature of building walls is more practical than the measuring the interior surface temperatures. Therefore, the calculation of TI value introduced by Koçkar (Koçkar, 2012) is a more practical method than the calculation of TI value introduced by Stainton (Stainton, 1980). The values below 1 refers to the presence of heat loss through the wall component while the TI values below 0.6 signal air leakages from warm inside to cold outside. TI values above 1 signal the damp zones in building walls (Koçkar, 2012; Tuğla & Tavukçuoğlu, 2016; Tugla et al., 2013).

$$TI = \frac{R_{SI} + R_W}{R_{SO} + R_W + R_{SI}} = \frac{T_{SO} - T_{OUT}}{T_{IN} - T_{OUT}} \quad (11)$$

where;

R_{SO} : outer surface convection resistance (m^2KW^{-1})

R_{SI} : interior surface convection resistance (m^2KW^{-1})

R_W : W conduction resistance (m^2KW^{-1})

T_{IN} : in-situ inside ambient temperature (K)

T_{SO} : in-situ outer surface temperature of exterior wall (K)

T_{OUT} : in-situ outside ambient temperature (K)

Black body can be defined as an object which does not reflect any radiation at any wavelength, in other words black body absorbs maximum amount of thermal energy, and emissivity of ideal black body is assumed to be equal to 1 (Çengel & Ghajar, 2015).

Emissivity, ϵ (unitless), of a material is used to compare the energy emission of materials with ideal black body, in other words, emissivity is the difference of emitted energy between the material and the ideal black body at the same temperature (Balaras & Argiriou, 2002; Çengel & Ghajar, 2015; Rao P., 2008). In theory, emissivity can be between 0 (reflected material) and 1 (black body). Infrared cameras detect infrared radiation emitting from the target surface and transfer this data by using Stefan Boltzman equation (Equation 4) into surface temperature. Therefore, estimation emissivity of surface material is necessary. Emissivity of the building materials usually has a value about 0.95 (Table 2.3). However to increase reliability of IRT method obtaining real/as-is emissivity value is beneficial. Because, this value is not only depended on the material itself, but also is effected by; pollution, surface humidity, roughness of the surface and aging effect of material surface (Albatici & Tonelli, 2010; Avdelidis & Moropoulou, 2003; Barreira & de Freitas, 2007; Davies, 2004; Flir Systems, 2013). Emissivity of the surface materials can be estimated by IRT. One method to estimate surface emissivity is using a diffusive material fixed to building walls with known emissivity and compare the temperature of the surface and the fixed material (Figure 2.7). Other method is measuring the surface temperature with Surface Thermometer and adjusting the emissivity of the surface material accordingly (Table 2.3).

Relative humidity, RH, can be defined as the percentage of water-vapour in the mixture to the saturated water pressure. Water-vapour, in other words water droplets in air break up the radiative energy transferring from target area to infrared sensor. Therefore measuring relative humidity is necessary for infrared thermography method (Korukcu & Kilic, 2009).

Table 2.3. Emissivity values of some common materials (Flir Systems, 2013)

| material | specification | spectrum | emissivity |
|-------------|----------------------------------|----------|------------|
| brick | red, common | LW | 0.93 |
| concrete | dry | LW | 0.95 |
| fiber board | masonite | LW | 0.88 |
| gypsum | | LW | 0.8-0.9 |
| paint | 8 different colors and qualities | LW | 0.92-0.94 |
| paper | white | LW | 0.7-0.9 |
| plastic | laminated | LW | 0.91 |
| sandstone | rough | LW | 0.935 |
| skin | human | LW | 0.98 |
| wood | oak | LW | 0.88 |

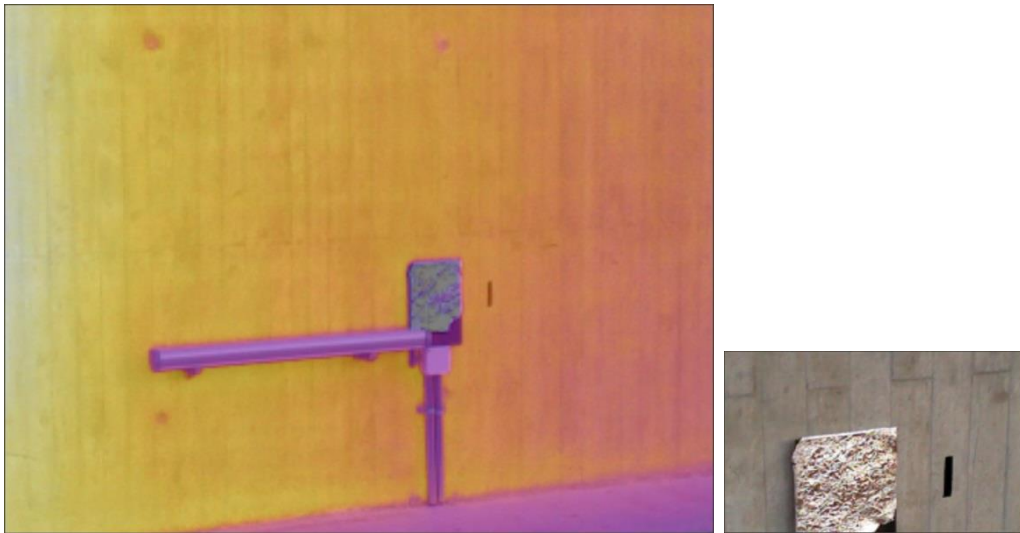


Figure 2.7. Using black electrical tape for surface emissivity measurement and aluminum foil for reflected temperature measurement.

Partial vapour pressure distribution calculation is used for assessment of condensation risk both at the surface and within the wall section, and RH percentage is also needed for this calculation. Mixture of dry air and water-vapour can be assumed as atmospheric air, and the pressure of atmosphere at a given relative humidity is defined as partial vapour-pressure and formulized as (Çengel & Ghajar, 2015):

$$P_v = RH * P_{sat} \quad (12)$$

where;

P_v : partial vapour-pressure (Pa)

P_{sat} : is saturation pressure of water at a specified temperature (Pa) (Table 3.3)

RH: is relative humidity, percentage of water-vapour in the mixture (%)

Reflected Temperature, T_{ref} (K), is also a necessary parameter for IRT method, because this value affects the radiative energy. Using a wood plate covered with aluminum foil can be very beneficial for measuring reflected temperature. During having the image of the target surface this plate can be fixed to the target area (Asdrubali et al., 2012). Reflected temperature for indoor measurement is very close to the ambient room temperature and is almost constant. However reflected temperature for outdoor measurement has wider range, because, outdoor ambient temperature changes during day and correspondingly reflection from objects changes (Fokaides & Kalogirou, 2011).

2.4. Types of Thermal Failures Observed in Buildings

Thermal Bridges are the places where the thermal resistance is lower in compare with the overall thermal transmittance value of the building facade. These low resisting places decrease the overall thermal efficiency of the walls (Figure 2.8, Figure 2.9). Parallel to the increasing energy efficiency of the buildings, overall effect of thermal bridges on energy performance of the buildings becomes much more influential (Asdrubali et al., 2012; DeÂqueÂ, Ollivier, & Roux, 2001; O'Grady, Lechowska, & Harte, 2017).

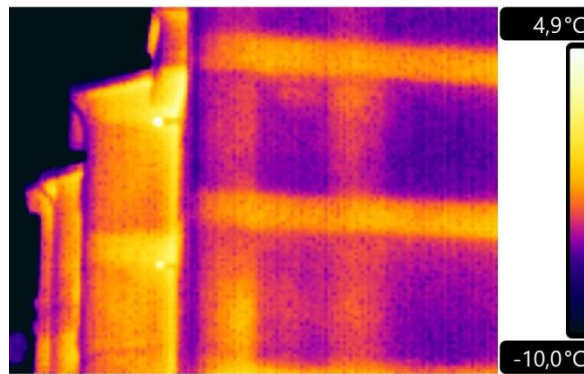


Figure 2.8. Thermal bridges occurring because of non-insulated surfaces at the façade of the building. ($T_{\text{out}} = 1.9^{\circ}\text{C}$ and $\text{RH} = 43\%$)

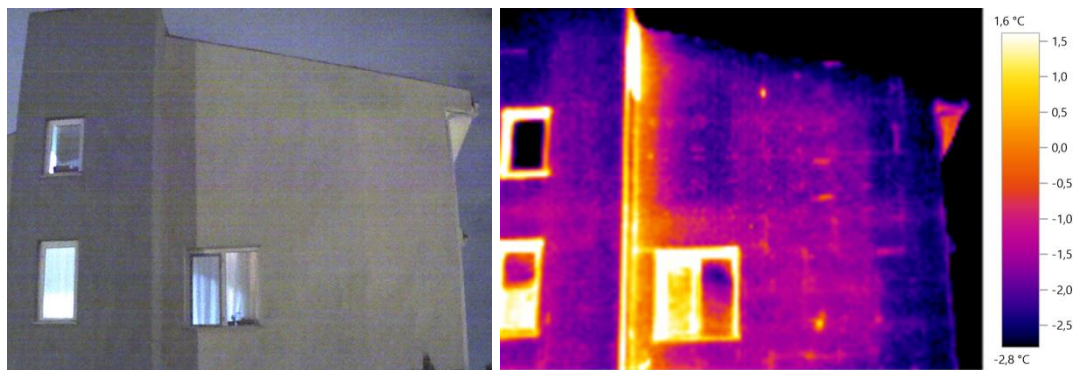


Figure 2.9. Thermal Bridges occurring due to the faults during fastening the thermal insulation boards to the backing wall, ($T_{\text{out}} = -3.9^{\circ}\text{C}$ and $\text{RH} = 60\%$)

Thermal bridges cause to, additional heat loss from building envelope, local condensation problems, internal condensation problems and growing mold on wall surfaces. Therefore, it is very important to locate and limit thermal bridges, and infrared thermography is widely used on this purpose (Asdrubali et al., 2012; DeÂqueÂ, Ollivier, & Roux, 2001; O'Grady, Lechowska, & Harte, 2017; Titman, 2001; Zalewski, Lassue, Rousse, & Boukhalifa, 2010)

With the help of qualitative infrared thermography, thermal bridges on the buildings can be determined practically, however the effect of these bridges on building

thermal performance cannot be evaluated. Quantitative Infrared thermography gives an opportunity to make a comparative analyze to each kind of thermal bridges. In the literature a parameter, which depends on inside and outside air and wall temperature, was calculated for the evaluation of thermal bridges, and this parameter was used for quantitative estimation of thermal performance (Asdrubali et al., 2012; O’Grady et al., 2017).

Another failure type is defined as **moisture problems**. Between two sides of the building façade, temperature and relative humidity levels are different, in other words vapor pressure is different between inside and outside of the buildings. Therefore, vapor molecules move from warm side to the cold side. During this movement if the temperature of the wall decreases under dew point temperature, vapor molecules condense, either on the surface (surface condensation) or within the section (interstitial condensation) of the building wall. Thermal performance of the building materials are directly affected by moisture content, therefore moisture transmission through building walls should be observed and controlled. Increase in moisture problems at the building envelope cause to, increase in heat transfer through building walls and decrease in thermal performance of the building. Because, with increasing moisture content thermal conductivity of the materials increases. Each percent change in moisture content by volume changes thermal conductivity of the material at a rate of 3-5 percent. In addition to this, as a result of moisture migration toward the surface evaporative cooling occurs and convective heat transfer increases from wall surface (Çengel & Ghajar, 2015; TS 825, 2013).

Air leakage is another thermal failure type observed in building. Heat transfer occurs through the windows of the building and most of this at the edges of the windows as air leakage. Wrong details especially at the joints of where buildings materials come together and workmanship failures increase the air leakage problems.

Apart from the negative effect of air leakage, necessary ventilation is supply by natural ventilation in most of the residential buildings. Therefore, air leakage is one of the most sensitive parameter that should be observed and controlled according to the needs of the building (Davies, 2004; Stainton, 1980).

2.5. Using Infrared Thermography for Thermal Transmittance Estimation

Energy usage of the buildings for heating and cooling purposes should be reduced. Therefore, research for estimating and decreasing this amount of energy usage is very important. Infrared Thermography Method is a non-destructive, non-invasive, reliable, effective and practical method. Therefore, the use of IRT in building diagnostics needs to be extended . Although it has been used over 40 years for building diagnostics, it has not fully investigated in quantitative bases yet and still needs research on it. Especially quantitative IRT method for building energy performance researches needs to be developed (Albatici & Tonelli, 2010; Albatici et al., 2015; Donatelli, Aversa, & Luprano, 2016; Fokaides & Kalogirou, 2011).

IRT is a gradual study and it combines following works: (i) scanning the target areas (building walls) with infrared cameras, (ii) obtain the IR image of these target areas and (iii) at the end analyzing these images. During thermal imaging, microclimatic measurements, such as ambient temperature, relative humidity and wind velocity near wall surface should be performed. In addition to these microclimatic measurements, optical parameters of the target area (emissivity), the heating and cooling conditions of the target area and the material variety of the building façade layer should be considered (Fokaides, Kalogirou, 2011; Tuğla, et al., 2013; Asdrubali, et al., 2012).

For in-situ researches following conditions should be carefully investigated before and during the imaging of the building and considered during the analyzing of the images (Albatici & Tonelli, 2010; Fokaides & Kalogirou, 2011):

- weather conditions (ambient temperature, wind speed, relative humidity etc.) before and during the IR imaging to have a steady state environment,
- effect of aging on the building materials,
- heating or cooling conditions of the building, being occupied or not, if there is an open window or not.

IRT is used to determine thermal and moisture problems at building façade of the existing buildings (Albatici et al., 2015; Asdrubali et al., 2012; Kylili et al., 2014; Lucchi, 2018; Martín Ocaña et al., 2004; Sayın, M. & Tavukçuoğlu, A., 2015, 2016b, 2016a, 2017; Tavukçuoğlu et al., 2005):

- wrong or missing heat insulation materials at the wall section,
- thermal bridges (which lead to additional heat loss, local condensation problems and mould growth) because of wrong or missing heat insulation,
- warm air leakage,
- moisture problems,
- material failures and
- and their probable causes and reasons

Thermal transmittance value of the building walls should be calculated for classification of the buildings according to their energy performance. Although, IRT method known as a qualitative technique, it is also possible to make quantitative research by it, therefore it is possible to calculate in-situ thermal transmittance values of the building walls by quantitative infrared thermography. There are some important quantitative researches in which IRT were used in laboratory conditions. In these studies to estimate the thermal performance of the buildings, thermal transmittance value of the walls are calculated with IRT method (Albatici & Tonelli,

2010; Albatici et al., 2015; Donatelli et al., 2016, 2016; Fokaides & Kalogirou, 2011; Tejedor et al., 2017).

There are two different approaches to calculate thermal transmittance value of the building walls by infrared thermography: one approach uses inside surface temperature of the exterior walls and the other approach uses outside surface temperature of exterior walls. In situ examination of thermal transmittance value is tried to be done by benefiting from these methods in this thesis study.

Albaciti et. al. used quantitative infrared thermography to investigate a building constructed for experimental purpose, which is consists of five different light and heavy weight external walls. This building was studied for three years, to calculate as-is thermal transmittance value of the building walls. For this purpose, the data collected by thermal cameras were analyzed by QIRT method. Thermal screening of the building walls is done from outside of the building at this method, therefore there is no need to enter the building. This situation makes screening easier, especially for existing occupied buildings. They concluded that: although the method gives suitable results for heavy walls further investigation is needed for light walls. (Albatici & Tonelli, 2010; Albatici et al., 2015) The reason of this difference is effect of the wind speed on the thermal transmittance value. This effect is higher for the walls with low thermal mass, since, with increasing wind speed they losses their energy easily (Tejedor et al., 2017).

Fokaides & Kalogirou (2011) conducted quantitative IRT method to calculate U value of the walls of five different existing buildings. In contrast with the former study, temperature measurements of exterior walls were done from inside of the building. Therefore, instead of outside wall surface temperature, inside wall surface temperatures were used for U value calculations. Unlike the former method, surface

convection coefficient values (h , $Wm^{-2}K^{-1}$) were not estimated by in-situ methods, instead the values given in the relevant standards were used (Fokaides & Kalogirou, 2011; TS 825, 2013).

There is an absolute deviation between in-situ U value which is calculated either using outer wall surface temperature or inner wall surface temperature and theoretical calculated U value. Rate of these deviations fluctuate according to the wall type: high/low/no insulated, light/heavy weight, one-layered/multi-layered, less-porous/porous (Albatici et al., 2015).

Parallel to result of this research, Lehmann (2013) says that, changing ambient temperature affects surface temperature of light weight walls more than heavy weight walls. Because, change in ambient temperature more effects the surface temperature of walls with lower inertia. Therefore, to have a steady state condition during imaging with infrared cameras, this fact should be taken into consideration (Lehmann, Wakili, Frank, Collado, & Tanner, 2013).

Tejedor (2017) used these two IRT methods, described at the studies of Albaciti and Fokaides, for calculation U -values in laboratory conditions and made a comparison between each other. It is obtained that, there is 1-2% deviations for one layered building walls and 3-4% for multi-layered building walls between these two methods (Tejedor et al., 2017).

Donatelli (2016) adapted the equation described in the study of Albaciti and then, set up an experimental procedure to calculate thermal transmittance value of a wall in laboratory conditions via IRT method. In this research, deviation between

theoretically calculated U value according to standard method and calculated U value with IRT method was calculated as -3.5% to 2.9% (Donatelli et al., 2016).

In this thesis study both of these approaches will be used for six wall types belonging to three different buildings, than the results of these approaches will be compared according the method described in the next chapter.

2.6. Physical parameters needed for Quantitative Infrared Thermography

Quantitative infrared thermography needs some physical parameters to calculate in-situ thermal transmittance value (U_{INSITU}) of the building walls.. Accuracy of obtaining these parameters directly affects the efficiency of this method (Albatici & Tonelli, 2010; Asdrubali et al., 2012; Dall'O' et al., 2013; Flir Systems, 2013). These parameters and reasons of necessity as follows:

- Inside and outside ambient temperature: temperature difference between inside and the outside ambient directly affects the thermal flow, and to calculate the thermal transmittance value, this difference is needed. Inside and outside ambient temperature values can be measured with separate devices and also can be measured with infrared thermography. For measuring inside ambient temperature from outside of the building, window should suddenly be opened for a short time and thermal image should be recorded in the same time. For the outside ambient temperature, a black body can be used, which should be located away from heat sources and building.
- Reflected ambient temperature: this value is needed to calculate for the radiation reflected on the target area. Especially for the materials which have lower thermal emissivity value it is much more important to set the reflected apparent temperature. Reflected temperature for indoor measurement is very close to the ambient room temperature and is almost constant. However, reflected

temperature for outdoor measurement has a wider range, because, ambient temperature changes during day and correspondingly reflection from objects changes. Therefore, especially for outdoor infrared imaging, to measure reflected temperature is very important to have a reliable measurement (Lehmann et al., 2013).

- Emissivity of the target surface: is used to compare the energy emission of materials with ideal black body, in other words, emissivity is the difference of emitted energy between the material and the ideal black body at the same temperature, because a black body, which is not exist in realty, emits %100 of all of its radiant energy.
- Relative humidity: thermal transmittance value changes with changing humidity level of the atmosphere, therefore relative humidity should be measured, and used during calculation of in-situ U value of the walls.
- Distance between camera sensor and the target area: with increasing distance, resolution of the camera decreases and every pixel at the digital image shows average temperature data of a larger area. (Balaras & Argiriou, 2002; Maldague, 2002). Therefore distance between camera sensor and the target are should be measured and for this purpose laser meters can be used.

Physical parameters should be considered to increase the sensitivity of the method. Inside and outside ambient temperature, reflected ambient temperature, emissivity of the target surface has higher importance on the estimated thermal transmittance value. However, the influence of the relative humidity and distance between camera sensor and the target area has lower significance, because these parameters are needed to estimate the atmosphere radiation and only a very small portion of the energy is absorbed by atmosphere (Fokaides & Kalogirou, 2011).

2.7. Certification of Building Energy Performance in Reference to Annual Total Energy Consumption

The overall energy consumption in a building is calculated by taking into consideration the annual energy use for heating, ventilating and air conditioning (HVAC) facilities, hot water generation and lighting systems of the buildings. Depending on the specified ranges of energy consumption in relation to the building type and its geometrical features, the energy efficiency scale of the building is certified with an energy identification document, namely Energy Performance Certification (EPC) (BEP, 2008; European Council, 2010; TS 825, 2013). The energy efficiency scale is given in a range from the letter “A” to “G” in which “A” refers to the most energy efficient building envelope while “G” refers to the worst case. The energy efficiency identification of the building envelope is also done by taken into consideration the annual energy consumption for heating and cooling purposes. Similar to the EPC scale, the energy efficiency performance of the building envelope is identified with an Energy Efficiency Index (EEI) within a range from “A” to “C” defined in the TS825:2013 standard. A building with EEI of “C” is accepted to be moderately energy efficient while energy efficiency of a building below the “C” scale is accepted to be inefficient (TS825, 2013). The main target is to achieve the least heat loss through the building envelope during winter and heat gain during summer that results in minimum energy consumption. In this regard, the common approach is highly-thermal resistive exterior building walls, ground floors and roofs forming the overall building envelope. Once EPC of a building is identified, the procedure for the energy efficiency performance assessment of the same building should be repeated for every 10 years.

Total heating energy needs of buildings can be calculated according to (i) hourly, (ii) monthly and (iii) seasonal time intervals and these calculation procedures are

defined at relevant standards (TS 825, 2013; TS EN ISO 6946, 2007; TS EN ISO 9869, 2004). The objectives of these calculations are as follows:

- to calculate the ideal design for a new building
- to calculate energy needs for heating of an existing building
- to decrease heating energy needs of the buildings
- to determine thickness, places and types of the heat insulation precautions
- to estimate future energy needs of the buildings
- to certificate Energy Performance of the buildings

The factors that affect the building heating loads are; (i) thermal performance of the building façade; both walls, windows, doors, roof and the basement floor, (ii) efficiency of the heating system, (iii) inside and outside microclimatic conditions; temperature, humidity and wind velocity, (iv) inside heat gain and (v) the heat gain from sun. And total heating energy need is calculated as follows,

$$\theta_{nd} = \theta_{ht} - \eta \times \theta_{gn} \quad (13)$$

where;

θ_{nd} : needed energy requirement for heating (Wm^{-2}).

θ_{ht} : total heat loss energy (Wm^{-2}).

η : utilization factor (unitless).

θ_{gn} : total heat gain (Wm^{-2}).

Annual energy consumption of the buildings (θ , kWh) is the energy amount that the heating system of the building requires. According to relevant standards, during calculation of this energy, solar energy gains of the building, internal heat gains from equipment's and humans are neglected (TS 825, 2013). Monthly energy consumption for heating purposes of a building is formulized as follows,

$$\theta_{\text{month}} = ((U_1 \times A_1) + \dots + (U_n \times A_n)) \times (T_{\text{IN}} - T_{\text{OUT}}) \times t \quad (14)$$

Annual energy consumption for heating purposes of a building is formulized as follows,

$$\theta_{\text{annual}} = \sum \theta_{\text{month}} \quad (15)$$

where;

U_n : is thermal transmittance value of the building component ($\text{Wm}^{-2}\text{K}^{-1}$),

A_n : is the surface area of walls

T_{IN} : is the inside ambient temperature (K).

T_{OUT} : is the outside ambient temperature (K).

t : time, one month as seconds = $24\text{h} \times 60\text{m} \times 60\text{s} \times 30\text{day}$ (s).

Maximum/Allowed annual energy consumption of the buildings (θ_{allowed} , kWh, year) is the allowed energy amount that the heating system of the building can consume to have C level energy efficiency index (EEI). Maximum/Allowed energy

consumption for heating purposes of a building is calculated by the method define in the standard and given in Table 2.4 (TS 825, 2013).

Table 2.4. *Maximum/Allowed annual energy consumption calculation table for different climatic regions according to standard TS825:2013.*

| climatic region | EEI (energy efficiency index) | | |
|-----------------|--|---------------------------------------|---------------------------------------|
| | C | B | A |
| 1. | $= 36.7 \times A_{\text{tot}}/V_{\text{gross}} + 6.0$ | | |
| 2. | $= 63.7 \times A_{\text{tot}}/V_{\text{gross}} + 14.9$ | | |
| 3.* | $= 74.2 \times A_{\text{tot}}/V_{\text{gross}} + 22.4$ | 90% of | 80% of |
| 4. | $= 83.4 \times A_{\text{tot}}/V_{\text{gross}} + 31.0$ | θ_{allowed} , kWh, year | θ_{allowed} , kWh, year |
| 5. | $= 88.7 \times A_{\text{tot}}/V_{\text{gross}} + 30.6$ | | |

* Ankara is in 3. climatic region.

A_{total} : total surface area of building envelope

V_{gross} : gross volume of building

CHAPTER 3

MATERIAL & METHOD

The in-situ IRT examinations involve the thermal performance assessment of two types of residential building and a faculty building in the campus of Middle East Technical University (Ankara, Turkey) (Figure 3.1, Figure 3.2, Figure 3.3, Figure 3.4). Those three buildings are briefly described below:

- One of the residential buildings is a villa type house (B1) composed of one basement, ground floor and first floor. Its exterior façades are composed of fair-faced (exposed reinforced concrete) structural elements, such as shear walls, column and beams, and solid brick cavity wall infill between the fair-faced structural elements (Figure 3.1). Due to the complaints of occupants, the fair-faced reinforced concrete surfaces underwent remedial renovation and externally-insulated with 5cm-thick extruded polystyrene (EPS) boards (Figure 3.2).
- The second residential building is a two-storey height reinforced concrete structure (B2). The infill walls between the reinforced concrete structural elements are made of autoclaved aerated concrete (AAC) masonry units and the whole wall surface is externally-insulated (Figure 3.3).
- The third structure is the Faculty of Architecture Building (B3) and its exterior walls are mainly composed of fair-faced shear walls and solid brick masonry infill walls at some parts (Figure 3.4).



Figure 3.1. Villa type house (B1) under examination in the campus of METU, construction time: 1998 (Ankara, Turkey)



Figure 3.2. Villa type house (B1) during and after externally-insulation of reinforced concrete walls, renovation time: 2014.



Figure 3.3. Two-storey height residential unit (B2) under examination in the campus of METU, construction time: 2001 (Ankara, Turkey).



Figure 3.4. Faculty of Architecture Building (B3) under examination in the campus of METU, construction time: 1962 (Ankara, Turkey).

The examinations were conducted on mainly six types of building walls belonging to those three buildings and including the fair-faced reinforced concrete walls before and after renovation. The main concerns of the in-situ examinations are the quantitative identification of thermal and moisture failures on building facades in terms of “temperature index” and the quantitative evaluation of their thermal transmittance value. In addition, the configuration of building wall types under examination and the methods used for the in-situ IRT studies are explained in detail under respective subheadings.

3.1. Building Wall Configurations under Examinations

The configuration of each building wall under examination is given in Figure 3.5 and their layer compositions are briefly described in Table 3.1. Mainly there are six types of walls, simply named as insulated cavity wall (W1), non-insulated reinforced concrete wall (W5, W6), externally-insulated shear wall (W2, W3), externally-insulated AAC wall (W4). Among them W2 represents the case after insulation treatment underwent at B1 (villa house in METU Campus) while W5 represents the case before insulation treatment.

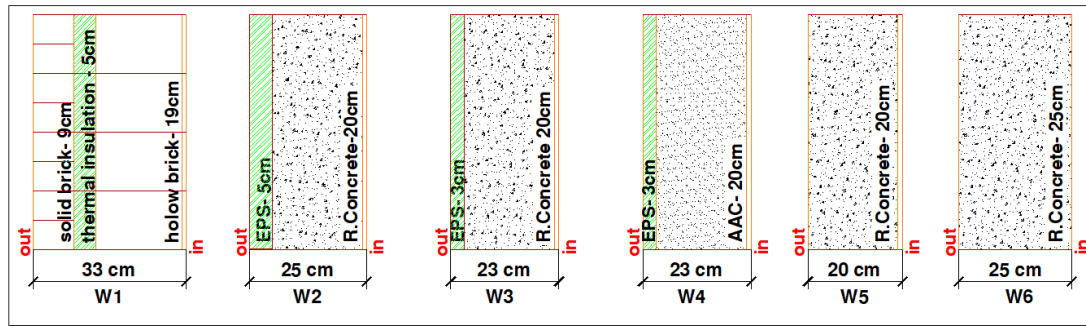


Figure 3.5. Wall configurations under examination

Table 3.1. List of wall types under examination including their codes, configuration descriptions and the buildings where the wall components belong to.

| Wall Type | Wall Configuration | Building Type | Season |
|--|--|--|---|
| W1 Insulated cavity wall | <ul style="list-style-type: none"> – 9cm-thick solid brick wall facing – 5cm-thick expanded polystyrene (XPS) cavity infill – 19cm-thick hollow brick internally-coated with gypsum-based plaster | B1 | Winter – when the outside is cold and inside is warm |
| W2 Externally-insulated shear wall | <ul style="list-style-type: none"> – 5cm-thick extruded polystyrene (EPS) board externally-coated with cement-based plaster – 20cm-thick reinforced concrete internally-coated with gypsum-based plaster | B1 after the insulation treatment (fair-faced reinforced concrete surfaces were externally-insulated) | Winter – when the outside is cold and inside is warm |
| W3 Externally-insulated shear wall | <ul style="list-style-type: none"> – 3cm-thick extruded polystyrene (EPS) board externally-coated with cement-based plaster – 20cm-thick reinforced concrete internally-coated with gypsum-based plaster | B2 | Winter – when the outside is cold and inside is warm |
| W4 Externally-insulated AAC wall | <ul style="list-style-type: none"> – 3cm-thick extruded polystyrene (EPS) board externally-coated with cement-based plaster – 20cm-thick autoclaved aerated concrete block internally-coated with gypsum-based plaster | B2 | Winter – when the outside is cold and inside is warm |
| W5 Non-insulated reinforced concrete wall | <ul style="list-style-type: none"> – 20cm-thick reinforced concrete internally-coated with gypsum-based plaster | B1 Before the insulation treatment | Winter – when the outside is cold and inside is warm |
| W6 Non-insulated reinforced concrete (fair-faced concrete) wall | <ul style="list-style-type: none"> – 25cm-thick fair-faced reinforced concrete | B3 | <p>Winter – when the outside is cold and inside is warm</p> <p>Summer – when the outside is warm and inside is cold</p> |

3.2. In-situ IR Imaging for Thermal Failure Assessment

Due to the complaints of occupants about thermal and moisture failures of residential buildings in METU Campus, there was necessity of accurate in-situ measurements for assessing actual thermal performance of existing building walls with non-destructive methods. In this regard, for the villa type house in METU, IRT method was used to inspect thermal and moisture failures and a proposal report was prepared by the author and the supervisor of this thesis study and submitted to University administration in 2013, and in 2014, partially rehabilitation was done by University administration based on the suggestions written in that report. Finally, a comparative report was prepared by using qualitative infrared thermography about the benefits gathered from partially rehabilitation, and submitted to the University administration.

A non-destructive in-situ survey was conducted on three buildings for the assessment of thermal transmittance value of the six wall types. In that purpose, in-situ IRT method was done by single IR imaging from both surfaces of the exterior walls. Those studies were performed for several times: winter 2013, 2015, 2016, 2017 and summer 2017. Following works were done in the given order:

- Site and building survey:
 - investigation of the building and the wall types in terms of architectural drawings.
 - knowing orientation of building with sun, because solar radiation before, during or after IR imaging may affect the performance of the assessment process.
- Heating and cooling facility (on/off time) information:
 - heating system of residential buildings (B1 & B2) usually active between 5PM to 8AM, therefore IR imaging was done late evening or night to have a

constant inside ambient temperature. Thus, steady state condition achieved by having constant heat transfer from inside to outside through wall section.

- Faculty building heating system is on during the day (usually from 7AM to 8PM), therefore IR imaging was done just early in the morning before the sunlight coming to wall surfaces. Because during night heating system is off and cooling starts inside the building and steady state heat transfer condition is corrupted.
- In-situ climatic history of the working environment: to increase the reliability of the IRT method in-situ climatic history of the working environment information is observed: snowy, rainy, windy etc.
- IR imaging: exterior building walls both from inside and outside were scanned with infrared cameras. IR imaging was done during cold weather conditions except W6. In addition to cold weather conditions IR imaging was done also in hot weather conditions for W6. Correspondingly real/digital images of the target areas were taken with digital camera.
- Microclimatic measurements: The microclimatic data including interior and exterior surface temperature, ambient temperature and relative humidity data which represent the actual conditions, were used for in-situ IRT analyses. Those data were achieved with the in-situ measurements and monitoring studies by using IR cameras and environmental anemometers.
- During IR imaging some precautions were taken to increase the possibility of having steady state heat transfer condition:
 - very early in the morning and at night,
 - when the exterior surfaces were not exposed to direct solar radiation and
 - when the exterior surfaces were not exposed to precipitation to increase the possibility of having steady state condition.
 - there should be an enough difference between inside and outside ambient temperature, in order to allow a measurable heat exchange through the target area.

- Finally, QIRT analyzes of these images were done and the U values of the walls were calculated by in-situ methods.

Unified Language Model (ULM) of in-situ IRT survey also shows the stages of in-situ measurements and the analyses of the IR data for the actual U values calculation of the exterior walls (Figure 3.6). Each stage defined in the model has roles to achieve the real surface temperature data on wall surfaces and complement each other to assess the real thermal performance of the exterior walls by means of IRT.

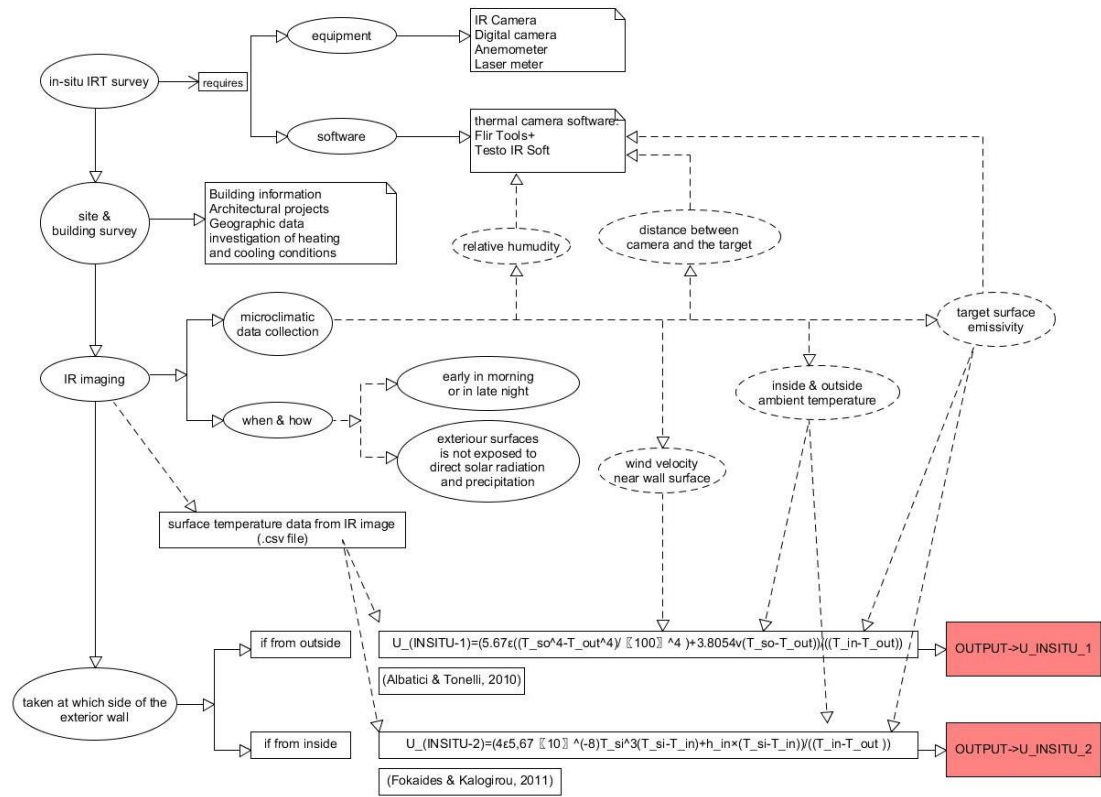


Figure 3.6. Unified Language Modeling (ULM) Diagram of in-situ IRT survey for the actual U-value assessment of exterior walls

Performance of the instrument used for in-situ data collection is important for increasing the reliability of the infrared study, therefore proper selection of equipment and software for the IRT method will improve quality of the results. Information of the equipment and software used in this thesis study is as follows:

- The in-situ examinations were done by monitoring actual inside/outside surface temperature of walls under examination by means of Flir E60 and Testo 875i thermal imaging cameras according to their availability (Appendix A).
- Because of the importance of the ambient temperature sensitivity for building diagnostics research, the infrared cameras used are long-wave type (7,5-13µm/8-14µm).
- During IR imaging, digital/real images of the buildings also taken with Canon 600D.
- The analyses of infrared images were done by using the software products; FLIR Tools+, FLIR Word add-in and TESTO IRTSoft 4.4 (Appendix B).
- MMO-TS:285 software is used for annual heating energy consumption calculations, which is released by Chamber of Turkish Mechanical Engineers (MMO, 2015).
- During thermal imaging, microclimatic measurements, such as ambient temperature, relative humidity and wind velocity near wall surface were taken by using handheld anemometers, Testo-410-2 and Testo-416.
- Distance between thermal camera sensor and the target area is measured with handheld laser meter, Bosch-PLR-50.

3.3. Condensation Analyses by the combined use of IRT & Partial Vapour Pressure Distribution Calculations

Partial vapour pressure distribution calculations (Equation 12) were done by using in-situ relative humidity, in-situ ambient temperature and in-situ surface temperature values, which are achieved via IRT method.

$$P_v = RH * P_{sat} \quad (12)$$

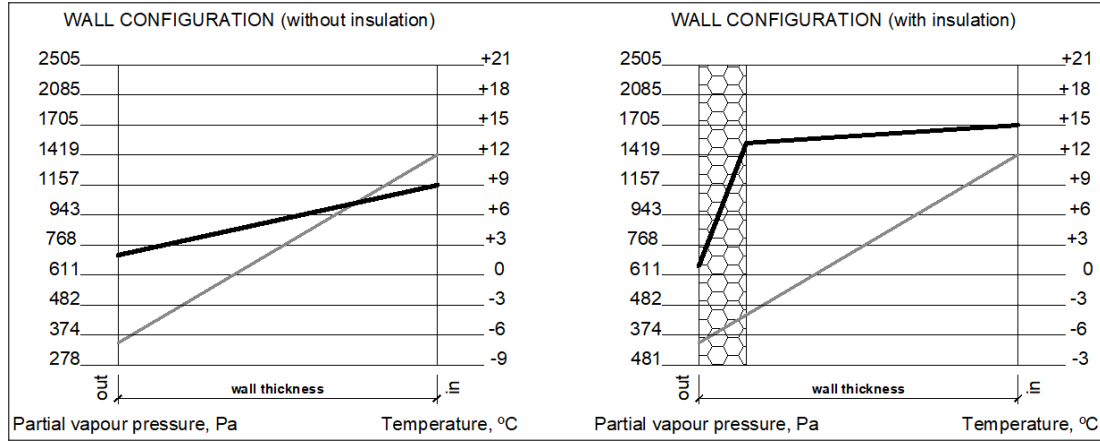
where;

P_v : partial vapour-pressure (Pa)

P_{sat} : is saturation pressure of water at a specified temperature (Pa) (Appendix C)

RH: is relative humidity, percentage of water-vapour in the mixture (%)

The condensation risk through the wall configuration is assessed by producing the profiles of partial and equilibrium water vapour pressures for each wall cross-section in relation to the temperature gradient and moisture content in the air varying from inside to outside of the wall cross-section (Çengel & Ghajar, 2015; TS 825, 2013). Similar to the vapour pressure analyses, the plot of the as-is temperature gradient through the wall cross-section in reference to the dew point temperature data in a graph is also used for the assessment of condensation risk within the wall section (Çengel & Ghajar, 2015; TS 825, 2013). The Figure 3.7 shows the plot of partial and equilibrium water vapour pressure profiles and the plot of temperature gradient and dew point temperature profile in the same graph produced for an externally-insulated and not-insulated reinforced concrete walls. Vapour pressure data and temperature data exhibit similar profiles for the same wall component as shown in Figure 3.7 since those data are derived from the same microclimatic conditions. The region in the wall section where the equilibrium water vapour pressure is lower than the partial water vapour pressure signals the risk of condensation at that region (Figure 3.7a). In other words, the region where the temperature gradient is below the dew point temperature, that region may suffer from condensation and entrapped moisture problems (Figure 3.7a). In case that equilibrium water vapour pressure is higher than partial water vapour pressure, those parts of the wall is not under risk of condensation at specified microclimatic conditions (Figure 3.7b). In other words, the regions where the temperature gradient is above the dew point temperature are kept away from surface and interstitial condensation problem (Figure 3.7b).



(a) not-insulated reinforced concrete wall

(b) externally-insulated reinforced concrete wall

Figure 3.7. Partial water vapour pressure distribution and temperature distribution profiles show if there is risk of condensation (a) or not (b).

The microclimatic data including interior and exterior surface temperature, ambient temperature and relative humidity data which represent the actual conditions were used for the analyses of condensation risk. Those data were achieved with the in-situ measurements and monitoring studies by using IR cameras and environmental anemometers.

3.4. Calculation of Temperature Index

The exterior surface temperature data collected by IR scanning are used for the determination of Temperature Index (TI) values by using the Equation 11. Surface temperature data collected from reference areas which do not suffer from thermal failures are used to calculate TI_{REF} values. Surface temperature data collected from thermal and/or moisture failure zones areas are used to calculate TI_{DEF} values.

$$TI = \frac{R_{SI} + R_W}{R_{SO} + R_W + R_{SI}} = \frac{T_{SO} - T_{OUT}}{T_{IN} - T_{OUT}} \quad (11)$$

where;

R_{SO} : outer surface convection resistance (m^2KW^{-1})

R_{SI} : interior surface convection resistance (m^2KW^{-1})

R_W : W conduction resistance (m^2KW^{-1})

T_{IN} : in-situ inside ambient temperature (K)

T_{SO} : in-situ outer surface temperature of exterior wall (K)

T_{OUT} : in-situ outside ambient temperature (K)

TI is used for the identification of problem type whether the defect area suffers from thermal failure, dampness or air leakage. TI_{REF} gives an idea about the thermal resistance performance of the wall component. TI_{DEF} values are the indicators that can be used to identify the type of defect quantitatively (Koçkar, 2012; Tuğla & Tavukçuoğlu, 2016; Tugla et al., 2013). For instances, TI_{DEF} values below 0.6 signal the airtightness problem while the TI_{DEF} values between 1 to 0.6 locate heat loss areas due to thermal bridges. TI_{DEF} values above 1 indicate damp zones.

3.5. In-situ Thermal Transmittance Estimation by Quantitative Infrared Thermography (QIRT)

The actual thermal transmittance values (U_{INSITU} , $Wm^{-2}K^{-1}$) of the walls were determined by using in-situ surface temperature data extracted from infrared/thermal images and microclimatic data together with relevant equations defined in the literature (Albatici & Tonelli, 2010; Albatici et al., 2015; Fokaides & Kalogirou, 2011). There are two calculation methods, referring to different in-situ IRT measurement methods, were conducted for the assessment of as-is thermal transmittance values.

The first calculation method uses the Equation 7 (method 1) and there is necessity of measuring outside surface temperature of exterior walls as well as measuring outside air velocity (Albatici & Tonelli, 2010; Albatici et al., 2015).

$$U_{INSITU-1} = \frac{5.67 \times \epsilon \times \left(\frac{T_{SO}^4 - T_{OUT}^4}{100^4} \right) + 3.8054 \times v \times (T_{SO} - T_{OUT})}{(T_{IN} - T_{OUT})} \quad (7)$$

where;

$U_{INSITU-1}$: in-situ thermal transmittance value $Wm^{-2}K^{-1}$

ϵ : thermal emissivity of the surface (unitless) which is assumed to be 0.95

T_{SO} : in-situ outside surface temperature of exterior wall (K)

T_{OUT} : in-situ outside ambient temperature (K)

T_{IN} : in-situ inside ambient temperature (K)

v : in-situ wind velocity near wall surface, m/s

Here, all data used in the Equation 7 are the in-situ data, representing the actual situation. The outside surface convection (h_{OUT} , $Wm^{-2}K^{-1}$) increases with wind velocity (v , m/s) (Balaras & Argiriou, 2002) and when the wind velocity higher than $2 ms^{-1}$, h_{OUT} coefficient given in the relevant standards, such as TS 825:2013, does not reflect the actual situation on site (Dall'O' et al., 2013). The Equation 7 includes the impact of the parameter “exterior surface convection” with the involvement of Jurges Equation (Equation 5) as explained in Section 2.4 (Çengel & Ghajar, 2015). That equation calculates the actual heat transfer from exterior wall

surface with convection (h_{OUT} , $Wm^{-2}K^{-1}$) in case that the wind velocity near exterior wall surface is below 5m/s. Therefore, a special care was given during the IRT measurements on site and all surface temperature measurements were done when the wind velocity is below 5m/s.

The second calculation method uses the Equation 8 (method 2) (Fokaides & Kalogirou, 2011) and there is necessity of measuring inside surface temperature of exterior walls and using the interior surface convection coefficient values (h_{IN} , $Wm^{-2}K^{-1}$) given in the standards (TS 825, 2013).

$$U_{INSITU-2} = \frac{4 \times \epsilon \times 5,67 \times 10^{-8} \times T_{SI}^3 \times (T_{SI} - T_{IN}) + h_{IN} \times (T_{SI} - T_{IN})}{(T_{IN} - T_{OUT})} \quad (8)$$

where;

$U_{INSITU-2}$: in-situ thermal transmittance value, $Wm^{-2}K^{-1}$

ϵ : thermal emissivity of the surface (unitless) which is assumed to be 0.95

T_{SI} : in-situ inside surface temperature of exterior wall (K)

T_{OUT} : in-situ outside ambient temperature (K)

T_{IN} : in-situ inside ambient temperature (K)

h_{IN} : surface convection coefficient, taken as $7.69Wm^{-2}K^{-1}$, since the building component is a wall .

Here, the interior surface temperature data used in the Equation 8 are measured on site while the h_{IN} data is an accepted value given in the standards (TS 825, 2013)

dependent on whether the building component has a vertical or horizontal exposed surface.

The actual/as-is thermal transmittance value (U_{INSITU}) of each wall type was calculated by using the in-situ temperature data. The data achieved from at least eight different areas representing the thermal performance of wall. The surface temperature values close to outside air temperature are used for estimation reference U_{INSITU} value, surface temperature values of thermally defect zones are used for calculation of defect U_{INSITU} value, and finally average surface temperature of the wall is used for average/actual U_{INSITU} value of the walls (Figure 3.8 and Figure 3.9). Here, there is necessity to identify the defect areas which suffer from thermal and moisture failures and the reference area which do not suffer from any failure. Since thermal failure zones are visible in IR images, those images allow identifying the reference areas and failure areas and acquisition of reliable data accordingly.

The thermal performance examination of each wall was done in terms of three parameters: $U_{\text{INSITU-REF}}$, $U_{\text{INSITU-AVG}}$ and $U_{\text{INSITU-DEF}}$. The definitions of those parameters are as follows:

- $U_{\text{INSITU-REF}}$: That U-value represents the actual thermal performance of the reference wall surfaces, which do not suffer from thermal failures. That value is used to assess the real thermal performance of the wall composition in comparison to the theoretical design values (U_{CALC}).
- $U_{\text{INSITU-AVG}}$: That U-values represents the actual thermal performance of the wall surfaces but differs from the $U_{\text{INSITU-REF}}$. Thermal and moisture failures adversely-effect the real thermal performance of walls. That effect is included in the $U_{\text{INSITU-AVG}}$ with the involvement of surface temperature data belonging to the areas both suffer and do not suffer from failures. That value is accepted to reflect the actual thermal performance of the wall composition to be used for

Energy Performance Certification (EPC) and to estimate annual energy consumption for heating.

- $U_{\text{INSITU-DEF}}$, That U-value represents the actual thermal performance of thermal and/or moisture failure zones. That value is an important parameter that allows the quantification of the heat loss through the defect areas acting as thermal bridges and the better-understanding the adverse-impact of thermal and moisture failures to the thermal performance of wall.

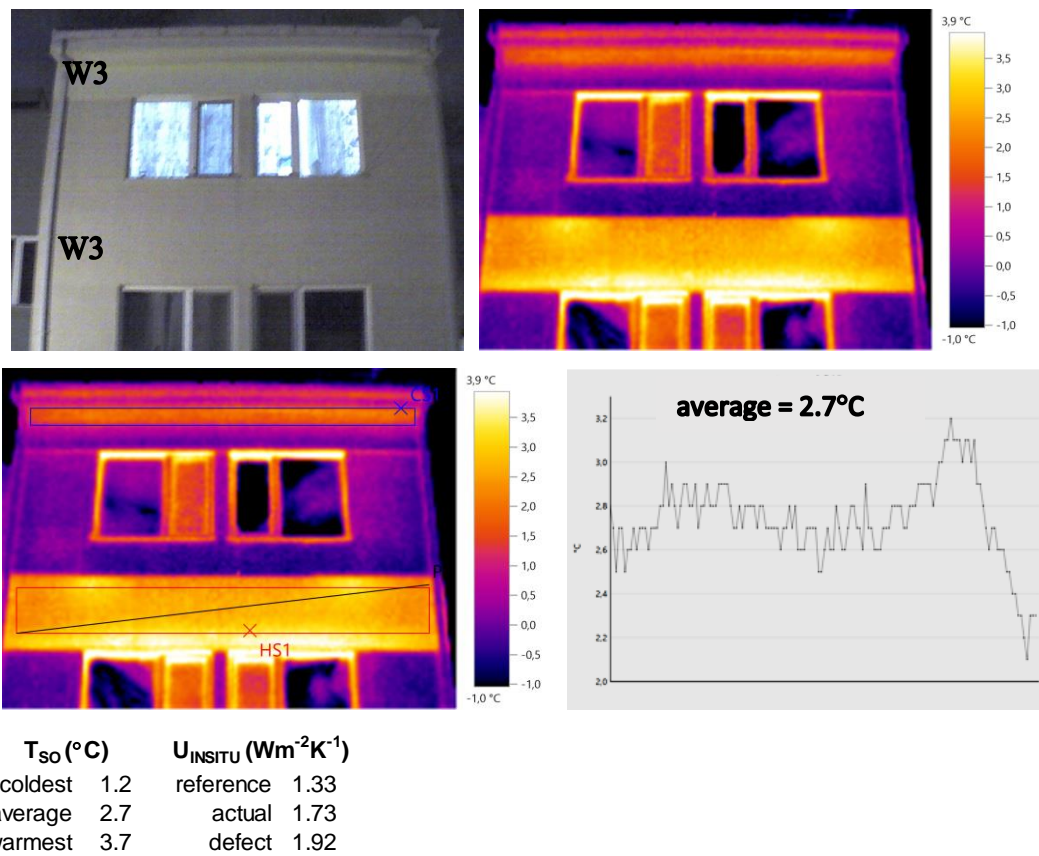


Figure 3.8. Obtaining surface temperature value close to outside air temperature cold spot tool of the software is used and CS1 shows the coldest surface temperature of W3 which represents the reference temperature value and $U_{\text{INSITU-REF}}$ is calculated accordingly. To obtain surface temperature value away from the outside air temperature hot spot tool is used and HS1 shows the warmest surface temperature of W3 which represents the defect temperature value and $U_{\text{INSITU-DEF}}$ is calculated accordingly. Finally, to obtain average surface temperature value temperature profile passing through W3 surface is used and the average surface temperature value is gathered and this value is used for calculation of $U_{\text{INSITU-AVG}}$ value. This method is repeated for eight times and average U values represent the in-situ thermal transmittance values.

The in-situ thermal transmittance values of six building walls types (W1-W6) belonging to three buildings (B1-B3) were determined with the use of in-situ quantitative IRT. The IRT measurements were done in winter when the outside is cold and inside is warm (when the heating system is functioning), in other words the heat transfer is expected from inside to outside in lack of satisfactory thermal insulation in wall component and causes heat loss.

In summer, the direction of heat transfer changes since the inside is warm and outside is hot, which may result in heat gain. In order to check the season dependency of the in-situ thermal transmittance measurement, QIRT method was also implemented to B3 (W6) during hot weather conditions, while heat is transferred from outside to inside. Steady state condition can only be achieved at one room at faculty building for hot weather condition, when heat is transfer from outside to inside. In that room a certain temperature difference between inside and outside can be achieved, because of existence of air conditioning.

Because of the complaints of occupants about thermal and moisture failures at B1, remedial renovation was done: fair faced reinforced concrete walls (W5) were covered with insulation material and these walls became insulated reinforced concrete walls (W2). To reveal the success of insulation applications & its adequacy in terms of temperature distribution on wall surfaces IR images taken before and after remedial renovation were quantitatively analyzed.

3.6. Thermal Transmittance Estimation with Standard Calculation Method

The theoretical performances (U_{CALC} , $W.m^{-2}K^{-1}$) of the same wall compositions were calculated as well by using thermal conductivity values given in standards for each

material layer according to project data of the buildings (Çengel & Ghajar, 2015; TS 825, 2013; TS EN ISO 6946, 2007).

The theoretical thermal transmittance values of the walls were calculated via Equation 9 by taking into consideration the layers forming the wall component together with their thicknesses, and thermal conductivity values of each layer and inside and outside thermal convection values given in the relevant standards (Table 3.2, Table 3.3) (Çengel & Ghajar, 2015; TS 825, 2013; TS EN ISO 6946, 2007).

$$U_{\text{CALC}} = \frac{1}{\frac{1}{h_{si}} + \frac{d_1}{\lambda_1} + \dots + \frac{d_n}{\lambda_n} + \frac{1}{h_{so}}} \quad (9)$$

where;

h_{si} : is the inside wall surface thermal convection coefficient ($7,69 \text{ Wm}^{-2}\text{K}^{-1}$)

h_{so} : is the outside wall surface thermal convection coefficient ($25 \text{ Wm}^{-2}\text{K}^{-1}$);

d : is the thickness of the wall layers (m)

λ_i : is the thermal conductivity of the wall layers ($\text{Wm}^{-1}\text{K}^{-1}$).

The differences between the as-is thermal transmittance and the theoretically-calculated one for each wall were discussed in terms of thermal failures determined on wall surfaces. The thermal transmittance of the wall surfaces suffering from thermal failures were examined in terms of thermal transmittance ($U_{\text{INSITU1-DEFECT}}$, $U_{\text{INSITU2-DEFECT}}$, $\text{Wm}^{-2}\text{K}^{-1}$) and Temperature Index ($TI_{\text{INSITU-DEFECT}}$, unitless) values, , and these values were obtained by IRT from problem area.

Table 3.2. Surface thermal convection coefficient (BS EN ISO 10456, 2007; TS 825, 2013)

| Type of construction component | surface thermal convection coefficient (h) | |
|---|--|----------|
| | $Wm^{-2}K^{-1}$ | |
| | h_{si} | h_{so} |
| External wall | 7.69 | 25 |
| Soil contacted external wall | 7.69 | 0 |
| Horizontal or inclined ceiling or roof forming the border of a living place with the external air (non-ventilated roof) | 7.69 | 25 |
| Unused attic or ceiling under a ventilated place (ventilated roof shell) | 7.69 | 12,5 |

Table 3.3. Theoretically-calculated thermal transmittance values of the walls according the thermal conductivity data given in the standards (BS EN ISO 10456, 2007; TS 825, 2013)

| Wall types | TS-825 | Layers | thickness | density (ρ) | water vapour diffusion (μ) | thermal conductivity (λ) | U _{CALC} |
|--------------------------------------|--------|-------------------------|-----------|-------------------|----------------------------|----------------------------------|----------------------------------|
| | No | | m | kg/m ³ | - | Wm ⁻¹ K ⁻¹ | Wm ⁻² K ⁻¹ |
| Insulated cavity wall (W1) | 4.4 | Plaster | 0.02 | 1200 | 10.00 | 0.51 | 0.50 |
| | 7.1 | Hollow brick | 0.20 | 1600 | 5.00 | 0.70 | |
| | 10.3 | Heat insulation layer | 0.05 | 15 | 80.00 | 0.04 | |
| | 11.3 | Air gap | 0.02 | - | 1.00 | 0.06 | |
| | 7.1 | Solid brick wall facing | 0.09 | 900 | 5.00 | 0.42 | |
| Externally-insulated shear wall (W2) | 4.4 | Plaster | 0.02 | 1200 | 10.00 | 0.51 | 0.60 |
| | 5.1 | R. Concrete | 0.20 | 2400 | 80.00 | 2.50 | |
| | 10.3 | Heat insulation layer | 0.05 | 15 | 80.00 | 0.04 | |
| | 4.10 | Plaster | 0.02 | 1200 | 5.00 | 0.10 | |
| Externally-insulated shear wall (W3) | 4.4 | Plaster | 0.02 | 1200 | 10.00 | 0.51 | 0.75 |
| | 5.1 | R. Concrete | 0.20 | 2400 | 80.00 | 2.50 | |
| | 10.3 | Heat insulation layer | 0.03 | 15 | 80.00 | 0.04 | |
| | 4.10 | Plaster | 0.02 | 1200 | 10.00 | 0.10 | |
| Externally-insulated wall (W4) | 4.4 | Plaster | 0.02 | 1200 | 10.00 | 0.51 | 0.39 |
| | 5.5 | AAC | 0.20 | 400 | 5.00 | 0.13 | |
| | 10.3 | Heat insulation layer | 0.03 | 15 | 80.00 | 0.04 | |
| | 4.10 | Plaster | 0.02 | 1200 | 10.00 | 0.10 | |
| Non-insulated shear wall (W5) | 4.4 | Plaster | 0.02 | 1200 | 10.00 | 0.51 | 3.46 |
| | 5.1 | R. Concrete | 0.20 | 2400 | 80.00 | 2.50 | |
| Non-insulated shear wall (W6) | 5.1 | R. Concrete | 0.25 | 2400 | 80.00 | 2.50 | 3.70 |

3.7. Annual Heating Energy Consumption Estimation with Standard Calculation Method and Identification of Building Performance Certification

The differences between the as-is thermal transmittance and the theoretically-calculated thermal transmittance were discussed in terms of Annual Heating Energy Consumptions (θ_{INSITU} and θ_{CALC} , kWhm⁻², year).

Calculated annual heating energy consumption values were evaluated in accordance with the reference annual heating energy consumption values defined in the standards, which are used for the Certification of Energy Performance (EPC) of buildings. EPC is assessed for buildings, according to their energy usage for following purposes: heating and cooling facilities, hot water generation and lighting systems of the buildings. There is an energy efficiency scale in these certificates, which spans from A to G: A means most efficient and G means the worst (Appendix D) (BEP, 2008; European Council, 2010; TS 825, 2013).

Maximum allowed annual energy consumption for heating purposes for buildings is calculated according to equation at the appendix A2 of TS 825 to get C level EPC. To get B and A level EPC this value should be %10 and %20 lower, and this C energy level is calculated as following:

$$\theta_{\text{max}} = 74.2 * A_n/V + 22.4 \quad (13)$$

where;

V volume of the house (m³),

A_n : is the total surface area of the building envelope (m^2),

The Equation 14 and 15 are used for the estimation of annual energy consumption. During the calculations of in-situ actual annual energy consumption, θ_{INSITU} , U_{INSITU} values, which are calculated via IRT method, were used. Annual energy consumption for heating purposes of a building is formulized as following:

$$\theta_{month} = ((U_1 \times A_1) + \dots + (U_n \times A_n)) \times (T_{in} - T_{out}) \times t \quad (14)$$

$$\theta_{annual} = \sum \theta_{month} \quad (15)$$

where;

U_n : is thermal transmittance value of the building component ($Wm^{-2}K^{-1}$),

A_n : is the surface area of walls (m^2),

T_{in} : is the inside ambient temperature (K),

T_{out} : is the outside ambient temperature (K),

t : time, one month as seconds = 86400×30 (s).

IRT method was used to calculate annual heating energy consumption for villa type houses during cold weather conditions. Heat is transferred in cold weather conditions from warm side to cold side of the wall in other words from inside to outside. In that purpose before renovation and after renovation IR images of different houses were taken at 18.12.2013 and then 26.01.2015 (early in the morning and in late evening: between 06:00-07:30 and 19:00-23:00). The buildings in which IR images were taken are marked in Figure 3.8.



Figure 3.9. Villa Type Houses (B1) that IR images were taken are marked at the site plan

Thermal transmittance values of the building components except studied walls via IRT, such as; roof (ventilated roof), basement wall, slab-on-ground, windows and doors were taken from the relevant standards. In other words their U_{INSITU} values are assumed to be same as the U_{CALC} values (Table 3.4). Therefore, thermal parameters of building components except studied walls were accepted to be same both for in-situ and theoretical calculated annual heating energy consumption, θ_{CALC} (TS 825, 2013). Annual heating energy consumption calculations were done by using MMO-TS285 software, which is released by Chamber of Turkish Mechanical Engineers (MMO, 2015).

Table 3.4. Theoretically-calculated thermal transmittance values (U_{CALC}) of the walls according the thermal conductivity data given in the standards

| Building Component | TS | layers | thickness | density (ρ) | water vapour diffusion (μ) | thermal | U_{CALC} | |
|-------------------------|------------------|------------------|-------------|-----------------------|--|----------------------------------|----------------------------------|------|
| | 825 | | | | | conductivity (λ) | | |
| | No | | m | kg/m ³ | - | Wm ⁻¹ K ⁻¹ | Wm ⁻² K ⁻¹ | |
| villa type (B1) | 4.4 | Plaster | 0.02 | 1200 | 10 | 0.51 | 0.63 | |
| | 5.1 | R. Concrete | 0.20 | 2400 | 80 | 2.50 | | |
| | 10.3 | Heat Insulation | 0.05 | 15 | 80 | 0.04 | | |
| | 9.1 | Carpet | 0.01 | 200 | 5 | 0.06 | 0.54 | |
| | 4.6 | Screed | 0.05 | 2000 | 15 | 1.40 | | |
| | 5.1 | Concrete | 0.10 | 2200 | 70 | 1.65 | | |
| | 5.2 | Concrete | 0.10 | 300 | 70 | 0.10 | | |
| | 3.1 | Filling Material | 0.30 | 1800 | 3 | 0.70 | 4.02 | |
| | 4.4 | Plaster | 0.02 | 1200 | 10 | 0.51 | | |
| | 5.1 | R. Concrete | 0.20 | 2400 | 80 | 2.50 | | |
| | Window | PVC | | | | | | 1.80 |
| | Door | Door | | | | | | 4.00 |
| 3 storey apartment (B2) | 4.4 | Plaster | 0.02 | 1200 | 10 | 0.51 | 0.96 | |
| | 5.1 | R. Concrete | 0.20 | 2400 | 80 | 2.50 | | |
| | 10.3 | Heat Insulation | 0.03 | 15 | 80 | 0.04 | | |
| | 9.1 | Carpet | 0.01 | 200 | 5 | 0.06 | 0.54 | |
| | 4.6 | Screed | 0.05 | 2000 | 15 | 1.40 | | |
| | 5.1 | Concrete | 0.10 | 2200 | 70 | 1.65 | | |
| | 5.2 | Concrete | 0.10 | 300 | 70 | 0.10 | | |
| | 3.1 | Filling Material | 0.30 | 1800 | 3 | 0.70 | 1.80 | |
| | Window PVC | | | | | | | |
| | Door | | | | | | | 4.00 |
| | faculty building | 4.4 | Plaster | 0.02 | 1200 | 10 | 0.51 | 0.63 |
| | | 5.1 | R. Concrete | 0.20 | 2400 | 80 | 2.50 | |
| 10.3 | | Heat Insulation | 0.05 | 15 | 80 | 0.04 | | |
| 9.1 | | Carpet | 0.01 | 200 | 5 | 0.06 | 0.54 | |
| 4.6 | | Screed | 0.05 | 2000 | 15 | 1.40 | | |
| 5.1 | | Concrete | 0.10 | 2200 | 70 | 1.65 | | |
| 5.2 | | Concrete | 0.10 | 300 | 70 | 0.10 | | |
| 3.1 | | Filling Material | 0.30 | 1800 | 3 | 0.70 | 2.70 | |
| Window Aluminum | | | | | | | | |
| Door | | | | | | 4.00 | | |

CHAPTER 4

RESULTS

The data collected from in-situ IRT measurements were used to identify thermal and moisture failure zones on various exterior building walls, to estimate their actual and theoretical thermal transmittance values and to determine actual thermal transmittance at thermal failure zones. The annual heating energy consumption was calculated only for one type of residential unit in order to interpret the impact of external insulation to energy efficiency of exposed concrete surfaces. The results are given under respective subheadings including related figures and tables.

4.1. Inspection of thermal and moisture failures with qualitative analyses of IR images

The infrared images taken from interior and exterior surfaces of exterior walls and their evaluation exhibited:-

- the problem areas suffering from thermal failures and causing serious heat loss while those failures zones are not visible by eye,
- distribution of those problem areas in the structure and their reasons.

Those evaluations are done for each building and summarized under respective subheading as follows:

4.1.1. Failures detected in villa type house (B1)

In villa type house (B1), its reinforced concrete walls were externally-insulated with 5cm-thick expanded polystyrene boards. Here:-

- thermal failures of its exterior wall surfaces (for the wall types W1 and W5) were inspected before insulation application (Figure 4.1, Figure 4.2, Figure 4.3, Figure 4.4 and Figure 4.5),
- the problem areas were confirmed with the IR images taken from the interior surfaces of those walls (Figure 4.6 and Figure 4.7), and
- the impact of thermal insulation were monitored in reinforced concrete walls (for the wall type W2) by the qualitative analyses of IR images (Figure 4.8, Figure 4.9, Figure 4.10, Figure 4.11).

The warmer exterior surfaces above the outside air temperature signal the thermal bridge zones where heat loss happens through the warmer inside to the colder outside. For the wall configurations with enough thermal resistance performances, exterior surfaces are expected to have similar surface temperatures with the outside air temperature. Here, Figure 4.1 and Figure 4.2 show that the surface temperature of non-insulated shear wall (W5) is about 7-8°C higher than the outside air temperature as well as about 4-5°C higher than the insulated cavity brick wall (W1). Those temperature differences demonstrate that there is a considerable heat loss through the fair-faced reinforced concrete structural elements (basement walls, columns and beams). Surface temperature of insulated cavity brick wall (W1) is about 4-5°C lower than the non-insulated shear wall (W5) while still above the outside air temperature with a temperature difference in the range of 3-5 °C. This temperature difference shows that W1 has not enough thermal resistance while it has higher thermal resistance performance than W5 because of the thermal insulation infill within the cavity of W1.

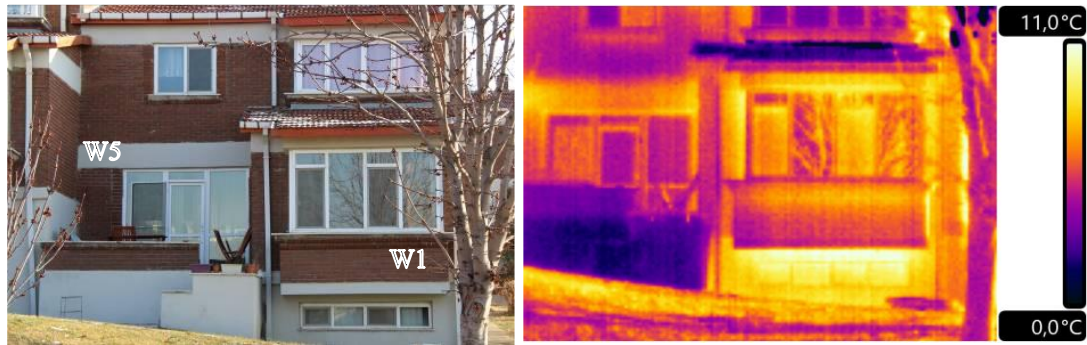


Figure 4.1. Surface temperatures of non-insulated shear wall (W5) and beams are about 4-5°C higher than the insulated cavity brick wall surfaces (W1). W5 surfaces are about 7-8°C higher than the outside air temperature. These temperature differences show that there is serious heat loss through the surfaces of non-insulated reinforced concrete wall and beams (W5). ($T_{out} = -3^{\circ}\text{C}$ and $RH = 43\%$)

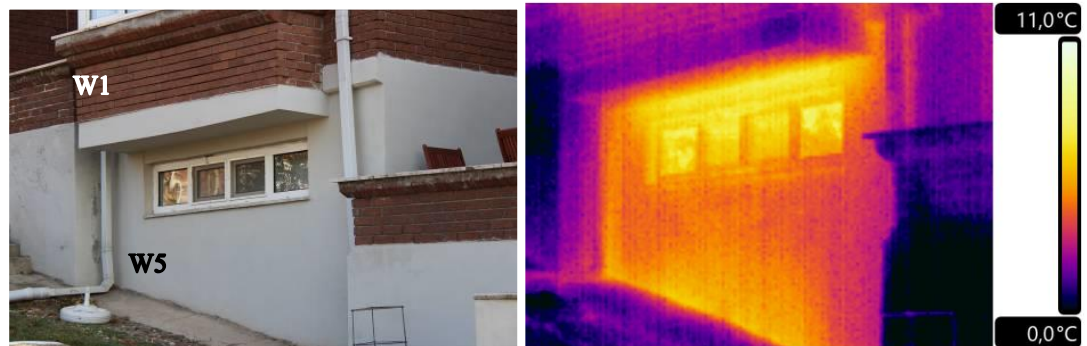


Figure 4.2. Surface temperature of W5 wall is about 7-8°C higher than the outside air temperature. This temperature difference demonstrates that there is a serious heat loss from non-insulated basement shear wall (W5). ($T_{out} = -3^{\circ}\text{C}$ and $RH = 43\%$).

Heterogeneous temperature distribution visible in the IR images in the form of warm patches, especially where there is a heat source (radiator) behind the wall, signals the insufficiency of the wall's thermal resistance. Here, Figure 4.3 and Figure 4.4 show that the warm areas have surface temperatures 4-5°C higher than the rest of the insulated cavity brick wall (W1) and that difference is due to the radiator positioned behind W1. Presence of such warm surfaces reveals significant heat loss through the parapet below the window and confirms that the insulation infill layer within the wall cavity does not provide enough thermal resistance. Figure 4.4 exhibits the considerable heat loss at the edges where window frame comes together with the structure due to the improper detailing at the joints.

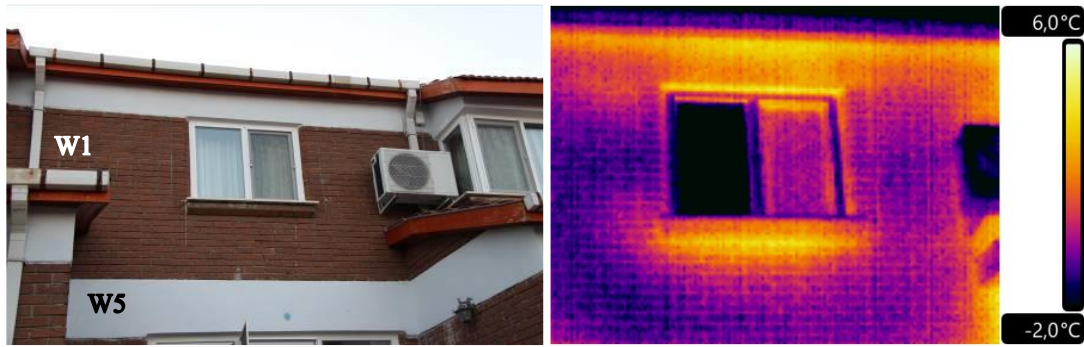


Figure 4.3. IR image showing the warm areas where radiator is positioned behind the insulated cavity walls. Those warm areas have surface temperatures 4-5°C higher than the rest of W1 surfaces. The surface temperatures of W1 being 3-5°C higher than the outside air temperature signal the insufficient thermal resistance of its composition ($T_{out} = 0.3^{\circ}\text{C}$, RH= 60%).



Figure 4.4. The warm edges reaching 6°C difference higher than the outside air temperature exhibit the significant heat loss through the edges where the window frames come together with the structure. The warmer surfaces of the uninsulated reinforced concrete beam (W5) and the insulated cavity brick wall (W1) where the radiator is positioned behind the parapet signal the inadequate thermal resistance of those walls ($T_{out} = 0.3^{\circ}\text{C}$, RH= 60%).

The villa houses are observed to suffer from thermal bridges at roof level (Figure 4.5). The edges where roof and gable wall come together act as thermal bridges and

those defect areas are visible in IR images as the warmest area with surface temperature reaching 8°C higher than the outside air temperature. The warmer pattern of the columns and beams show the heat loss through the columns hidden behind the brick wall facing and uninsulated (exposed) reinforced concrete beam surfaces due to their inadequate thermal resistances.

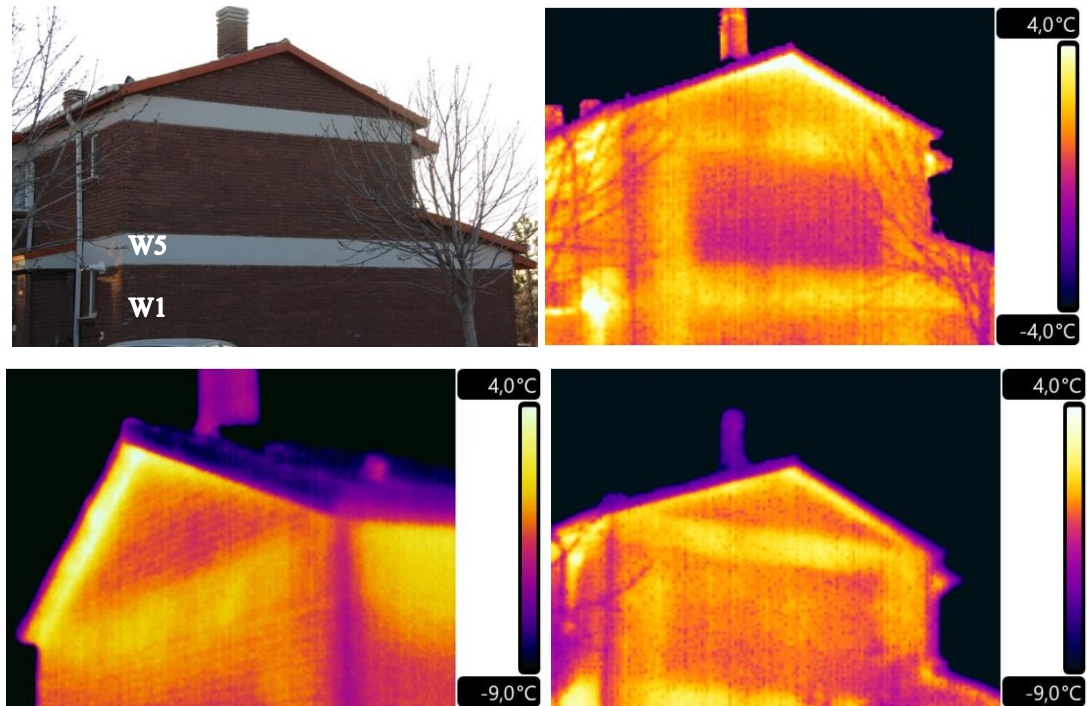


Figure 4.5. The warmest area with surface temperature reaching 8°C higher than the outside air temperature is the edge where roof and gable wall come together. Heat loss through the structural elements of the building (columns and beams) is also visible in IR images. ($T_{\text{out}} = -3^{\circ}\text{C}$, RH= 43%).

The colder interior surfaces below the indoor air temperature signal the thermal bridge zones where heat loss happens through the warmer inside to the colder outside. For the wall configurations with enough thermal resistance performances, interior surfaces are expected to have similar surface temperatures with the indoor air temperature. The coldest patches at the edges where the building components come together or window frames come together may indicate the problem of air leakage through those edges, if the surface temperatures of the problem area are getting close to outside air temperature. Considerable heat loss at the edges, due to

air leakages and insufficient thermal resistance, may result in condensation at thermal failure zones.

The heat loss through the uninsulated reinforced concrete beam surfaces is visible in IR images as colder zones having surface temperatures about 7°C colder than the inside ambient temperature (Figure 4.6). The coldest zones having interior surface temperatures almost 10°C colder than indoor air temperature are observed at the corners where building wall and ceiling comes together and those coldest zones are under risk of condensation as shown in Figure 4.6, Figure 4.7 and Figure 4.8. The condensation analysis for the actual case representing the coldest interior zones of the uninsulated reinforced concrete wall (W5) verifies the risk of condensation at colder surfaces to a depth of 5cm (Figure 4.7).

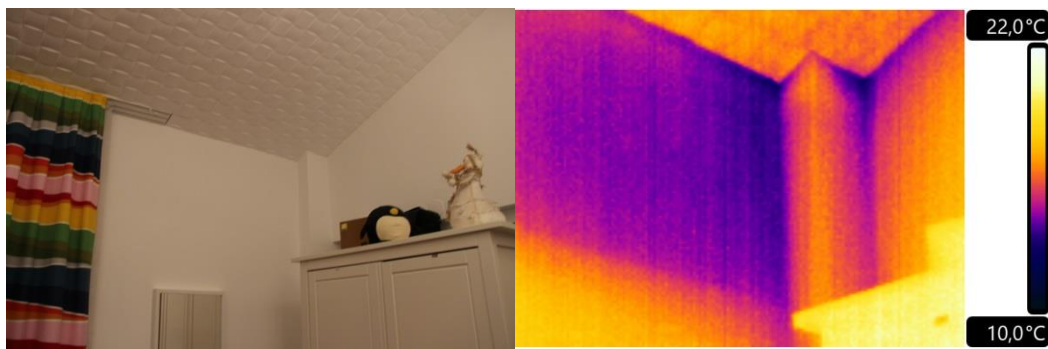


Figure 4.6. The coldest zones having interior surface temperatures almost 10°C colder than indoor air temperature are observed at the corners where building wall and ceiling comes together and those coldest zones are under risk of condensation ($T_{in} = 19.5^{\circ}\text{C}$, $\text{RH} = 45\%$).

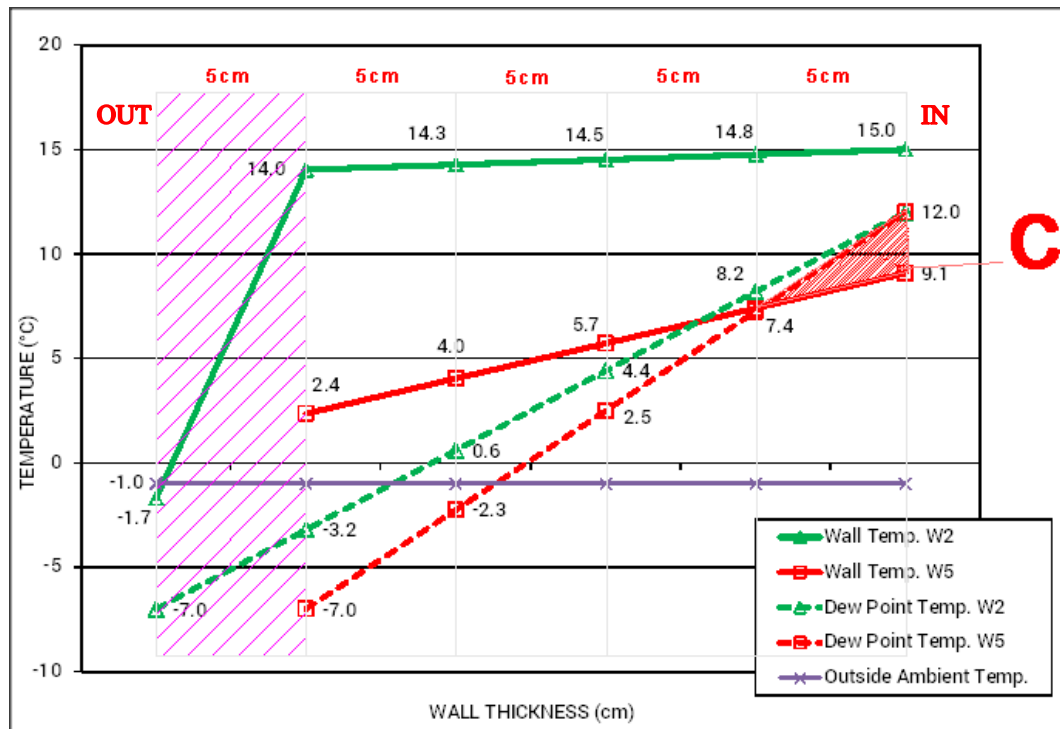


Figure 4.7. Temperature and dew point temperature profiles of non-insulated reinforced concrete surface (W5) and insulated reinforced concrete surface (W2), showing the risk of interstitial condensation (C) in W5, reaching to 5cm depth from interior surface while that risk was eliminated for the same wall after it was externally-insulated (W2) ($TI_{W5-REFERENCE} = 0.75$; $TI_{W5-DEFECT} = 0.58$; $TI_{W2-REFERENCE} = 0.94$; $TI_{W2-DEFECT} = 0.71$) ($T_{in} = 20^{\circ}\text{C}$, $RH_{in} = 45\%$ and $T_{out} = -1^{\circ}\text{C}$, $RH_{out} = 60\%$).

IR image taken from interior surfaces shows the thermal bridges and even air tightness problems through window frame or edges where window frame and building wall come together. These areas are 10°C - 15°C colder than the inside ambient temperature and those coldest zones are under risk of condensation (Figure 4.8).



Figure 4.8. The window frames, especially the edges where window frame and building wall come together are the coldest zones with surface temperatures 15°C colder than the indoor air temperature. That temperature difference signals the risk of condensation and air tightness problems occurring at the coldest zones ($T_{in} = 19.5^{\circ}\text{C}$, RH= 45%).

Thermal imaging was conducted on the exterior and interior surfaces of the same villa houses after reinforced concrete surfaces are externally-insulated with 5cm-thick expanded polystyrene. The qualitative analyses of IR images and the comparison of IR data taken before and after the insulation treatment show that heat loss through the reinforced concrete structural elements of the villa house is eliminated.

The impact of thermal insulation treatment in IR images is visible when thermal bridge areas identified as warmer exterior surfaces above the outside air temperature are eliminated. The success of insulation treatment is confirmed when the exterior surface temperatures reaches to similar values with the outside air temperature. In other words, the insulated wall configurations with enough thermal resistance performances exhibit exterior surface temperatures similar to outside air temperature. For instance, improvement in thermal resistance for the reinforced concrete basement wall is visible in IR images which were taken from the uninsulated reinforced concrete wall (W5) surfaces (before treatment) and insulated reinforced concrete wall (W2) surfaces (after insulation treatment). The Figure 4.9 shows that the exterior surface temperature of insulated shear basement wall (W2) is

close to the outside air temperature; however those temperatures are still above the outside air temperature with a temperature difference in the range of 1-2 °C. The comparison of IR images given in Figure 4.3 and figure 4.9 confirms that heat loss through uninsulated shear wall is reduced significantly; however thermal resistance of 5cm-thick insulated shear wall (W2) still needs to be increased. The Figure 4.10 presents similar exterior surface temperature data achieved from the rear side of the villa house at the same indoor and outdoor climatic conditions. The data obtained from IR scanning before and after insulation treatment revealed the improvement provided with external insulation of reinforced concrete walls.



Figure 4.9. Surface temperature of W2 being close to the outside air temperature shows the improvement in thermal resistance while being still 1-2°C higher than the outside air temperature ($T_{\text{out}} = -3.1^{\circ}\text{C}$, RH= 65%).



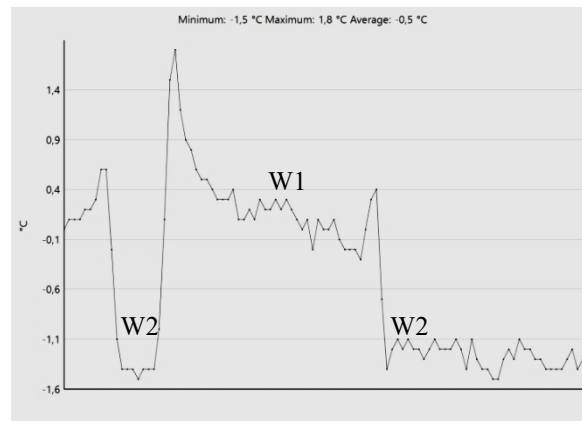


Figure 4.10. The IR image and temperature profile on Line P1 showing the exterior temperature distribution on the insulated cavity brick wall (W1) and insulated reinforced concrete wall (W2). The average surface temperature of W2 is close to the outside air with a temperature difference of 1-2°C. The thermal resistance of W2 seems to be better than the thermal resistance of W1 that is provided by the insulation treatment ($T_{out} = -3.1^{\circ}\text{C}$, RH= 65%).

Before insulation treatment, the coldest zones at the immediate periphery of reinforced concrete structural elements were under risk of condensation (Figure 4.7). The condensation analysis for the rehabilitated actual case representing the interior and exterior surfaces of the insulated reinforced concrete wall (W2) shows that the risk of condensation is eliminated (Figure 4.7).

Thermal failures on wall surfaces are noticeable in IR images with a certain temperature difference between non-problem and problem areas. After the thermal insulation treatment, the thermal imaging of the walls with a close view exhibited the thermal failure zones in the form of warm edges corresponding to the parts of walls where reinforced concrete surfaces externally-covered with thermal insulation boards and existing brick walls come together (Figure 4.11). Those edges are visible in IR images with surface temperatures about 5-6°C warmer than the insulated walls surfaces (non-problem area) as well as about 7°C warmer than outside air temperature. The Figure 4.12 presents similar thermal failures observed at the rear side of the villa house at the same indoor and outdoor climatic conditions. Those

thermal failure zones occur because of the discontinuity in external insulation, in other words partial insulation of the building envelope during remedial renovation (Figure 4.11 and Figure 4.12).

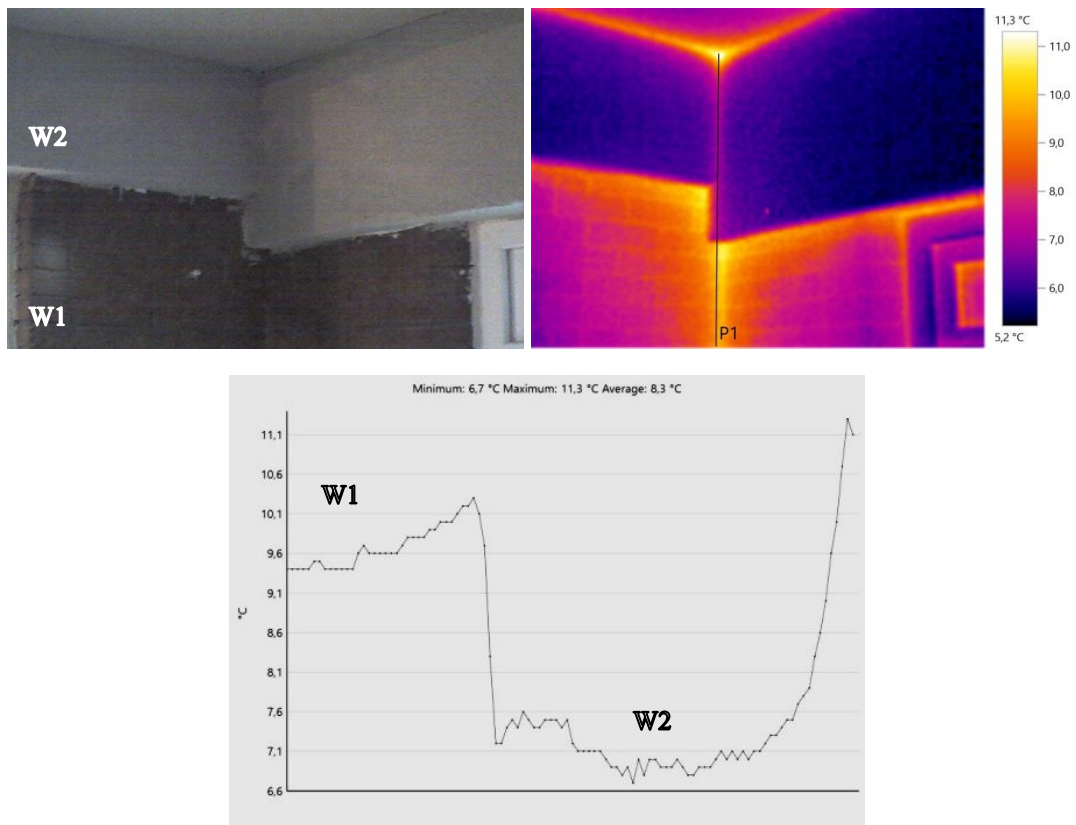


Figure 4.11. IR image taken from the exterior building envelope of villa house and temperature profile on Line P1 showing that thermal bridges occurs because of the discontinuity of insulation material. Thermal bridges are visible in IR images with surface temperatures about 5-6°C warmer than the insulated walls surfaces (non-problem area) as well as about 7°C warmer than outside air temperature. ($T_{\text{out}} = 5.0^{\circ}\text{C}$, RH= 65%).

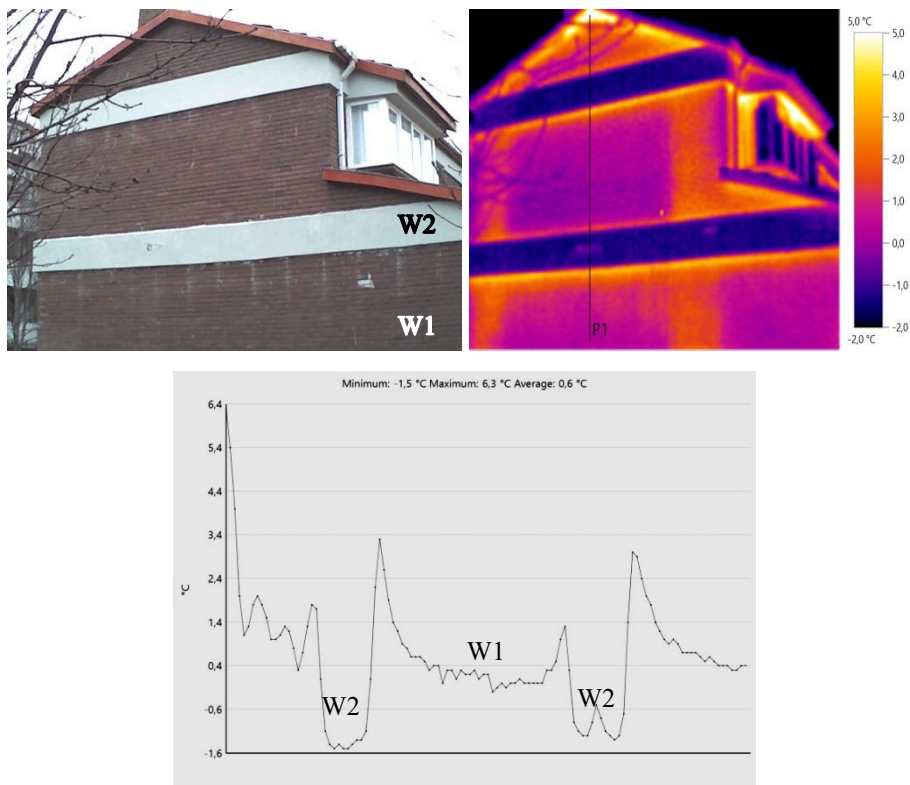


Figure 4.12. The IR image taken from the rear side of the villa house and temperature profile on Line P1 showing that, thermal bridges occur because of the discontinuity of insulation material. Thermal bridges with surface temperatures about 4-5°C higher than the externally-insulated concrete surfaces (non-problem areas) and 6-7°C higher than the outside ambient temperature ($T_{\text{out}} = -3.1^{\circ}\text{C}$, RH= 65%).

4.1.2. Failures detected in two-storey height residential unit (B2)

In two-storey height residential unit (B2), thermal failure and moist zones of its externally-insulated shear wall (W3) and externally-insulated autoclaved aerated concrete (AAC) wall (W4) were inspected, and the problem areas were confirmed with the qualitative analyses of relevant IR images taken from exterior and interior surfaces of walls (Figure 4.13, Figure 4.14, Figure 4.15 and Figure 4.16).

Figure 4.13 shows that, surface temperature of externally-insulated shear wall (W3) is about 3°C warmer than the surface temperature of externally-insulated AAC wall (W4) and 4°C warmer than the outside air temperature. Those temperature

differences demonstrate that there is a considerable heat loss through the externally-insulated shear wall (W3), and this heat loss shows that 3cm-thick extruded polystyrene (EPS) insulation layer of W3 is not enough. In other words, W3 thermal resistivity is insufficient because of inadequate-thick insulation board (Figure 4.13). Heterogeneous temperature distribution visible in the temperature profile (P3) in the form of peak temperature values shows heat source (radiator) behind the wall and this situation signals the insufficiency of the wall's thermal resistance. Here, Figure 4.13 shows that the warm areas have surface temperatures 1-2°C higher than the rest of the externally-insulated shear wall (W3) and that difference is due to the radiator positioned behind W3.

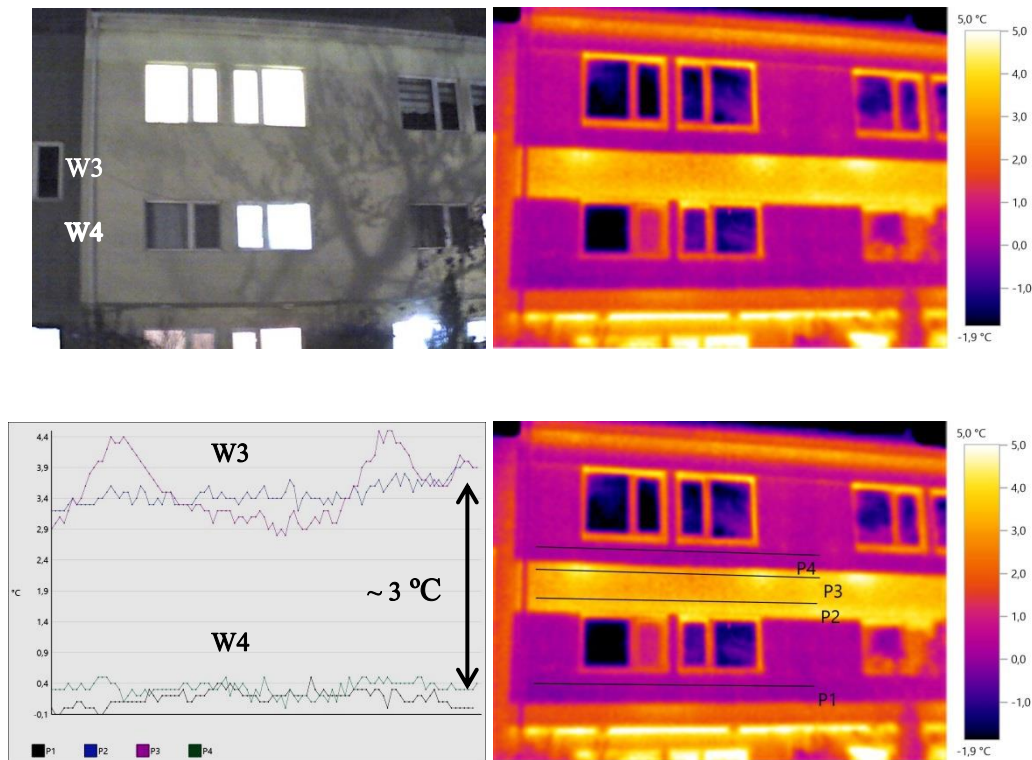


Figure 4.13. Externally-insulated shear wall (W3, P2&P3 profiles) surface temperature is 3,2°C higher than the surface temperature of externally-insulated autoclaved aerated concrete wall (W4, P1&P4 profiles). Heterogeneous temperature distribution visible in the temperature profile (P3) in the form of peak temperature values shows heat source (radiator) behind the wall and this situation signals the insufficiency of the wall's thermal resistance. ($T_{\text{out}} = -3.9^{\circ}\text{C}$, RH= 60%).

Thermal bridges of W3 and W4 are visible in IR images in the form of a pattern following the edges where two insulation board come together. These patterns of warmer patches are due to the clearances between the insulation boards left during their fastening to the backing wall and indicate poor workmanship (Figure 4.14). These thermal bridges at the edge of the thermal insulation materials, in other words discontinuities in thermal insulation layer cause a heterogeneous temperature distribution on wall surface and decreases the thermal performance of the walls. Temperature profiles that pass through these discontinuities in thermal insulation layer of W3 and W4 signal that these defect zones surface temperature are about 3-4°C warmer than the rest of the wall (Figure 4.14). In other words overall thermal performance of the walls decreases because of these clearances.

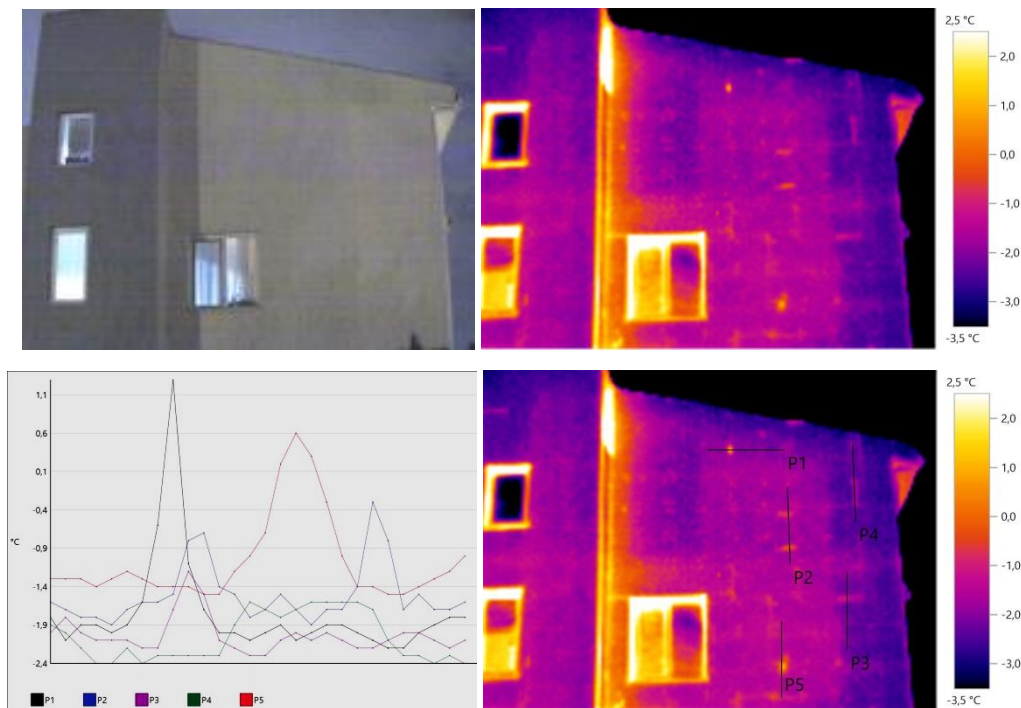


Figure 4.14. Heterogeneous temperature distribution is visible in the IR images in the form of warm patches at the intersection of thermal insulation boards and Temperature profiles passing through these zones shows that, surface temperature at the bridge zones are up to 3-4°C higher than surface temperature without defect ($T_{out} = -3.9^{\circ}\text{C}$, RH= 60%).

The heat loss through externally-insulated shear wall (W3) because of insufficient insulation material thickness is verified with the IR images taken from interior surfaces as well for B2 (Figure 4.15). Temperature profiles show that surface temperature difference between W3 and W4 reaches to 3-4°C (Figure 4.15).

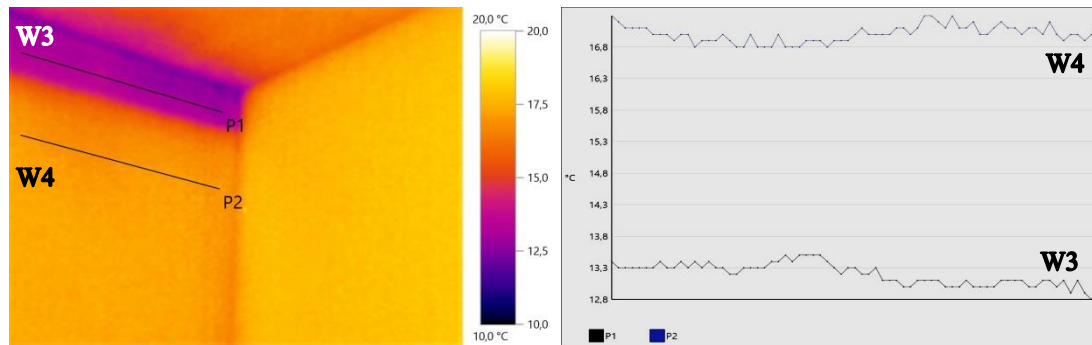


Figure 4.15. IR image and temperature profile taken from inside of the building show the thermal performance difference between W3 and W4 ($T_{in} = 19^{\circ}\text{C}$, RH= 55%).

The coldest zones having interior surface temperatures almost 10°C colder than indoor air temperature are observed at the corners where building wall and ceiling comes together (Figure 4.16). Those coldest zones are under risk of condensation as shown in Figure 4.17.

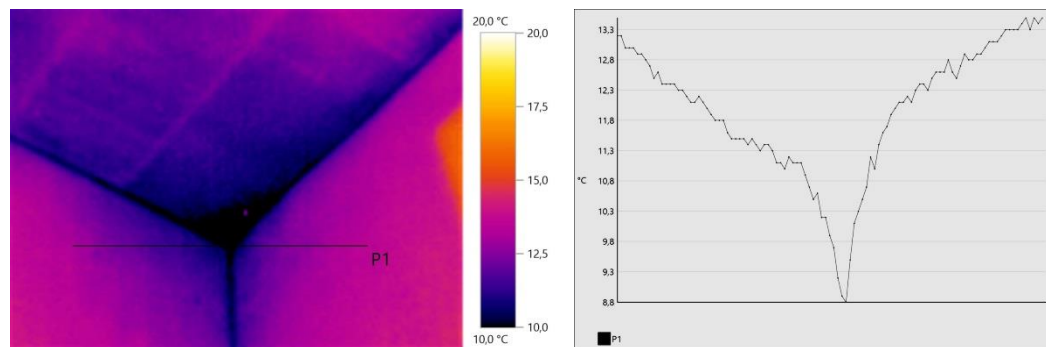


Figure 4.16. Temperature profile of B2 shows the possibility of the surface and interstitial moisture problem ($T_{in} = 19^{\circ}\text{C}$, RH= 55%).

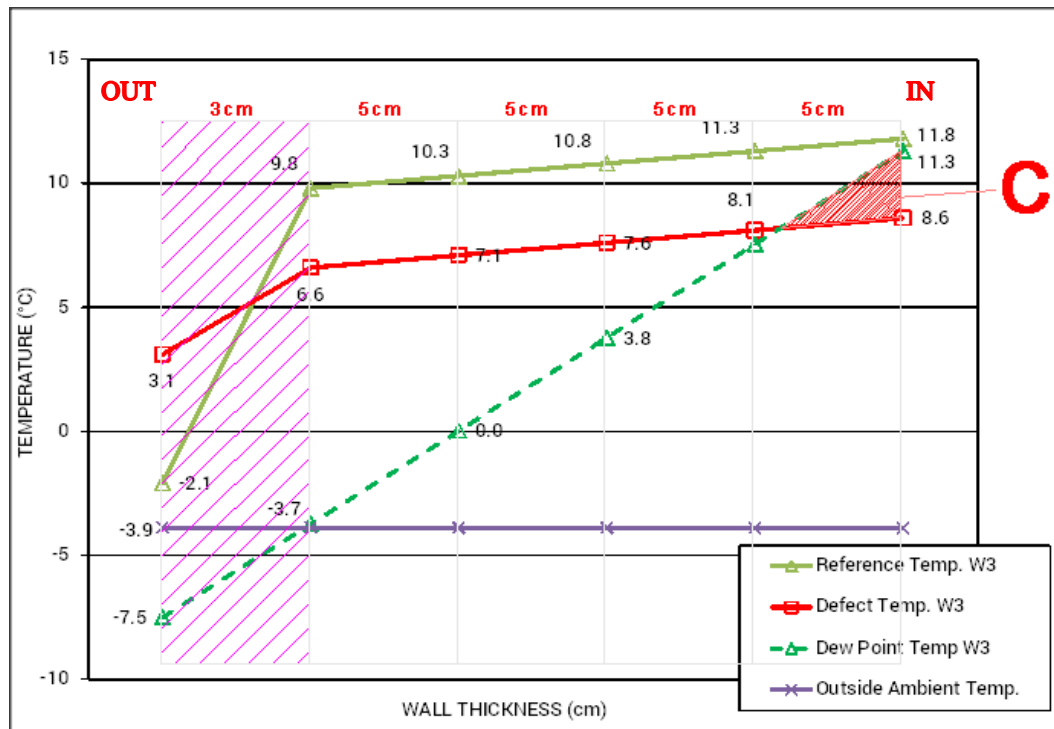


Figure 4.17. Temperature and dew point temperature profiles of insulated reinforced concrete wall (W3) show the risk of interstitial condensation (C) reaching to 4 cm depth from interior surface ($TI_{W3-DEFECT} = 0.71$) ($T_{in} = 20^{\circ}\text{C}$, $RH_{in} = 45\%$ and $T_{out} = -1^{\circ}\text{C}$, $RH_{out} = 60\%$).
REFERENCE = 0.92; $TI_{W3-DEFECT} = 0.71$) ($T_{in} = 20^{\circ}\text{C}$, $RH_{in} = 45\%$ and $T_{out} = -1^{\circ}\text{C}$, $RH_{out} = 60\%$).

4.1.3. Failures detected in Faculty of Architecture Building (B3)

In Faculty of Architecture Building (B3), thermal failure and moist zones of its non-insulated shear wall (W6) were inspected, and the problem areas were confirmed with the qualitative analyses of relevant IR images taken from exterior and interior surfaces of walls (Figure 4.18, Figure 4.19, Figure 4.20 and Figure 4.21).

Surface temperature of non-insulated shear wall (W6) being about 4°C warmer than the outside air temperature signal that heat loss happens through the warmer inside to the colder outside due to the insufficient thermal resistance performance of the fair-faced shear wall (Figure 4.18). The same walls are observed to suffer from thermal bridges at window frames. Temperature profile passing along aluminum

window frame and building wall shows that surface temperature reaches 4°C warmer than wall surfaces and 8°C warmer than outside air temperature (Figure 4.18). Such temperature differences may signal air tightness problem at the where window frame and building wall come together.

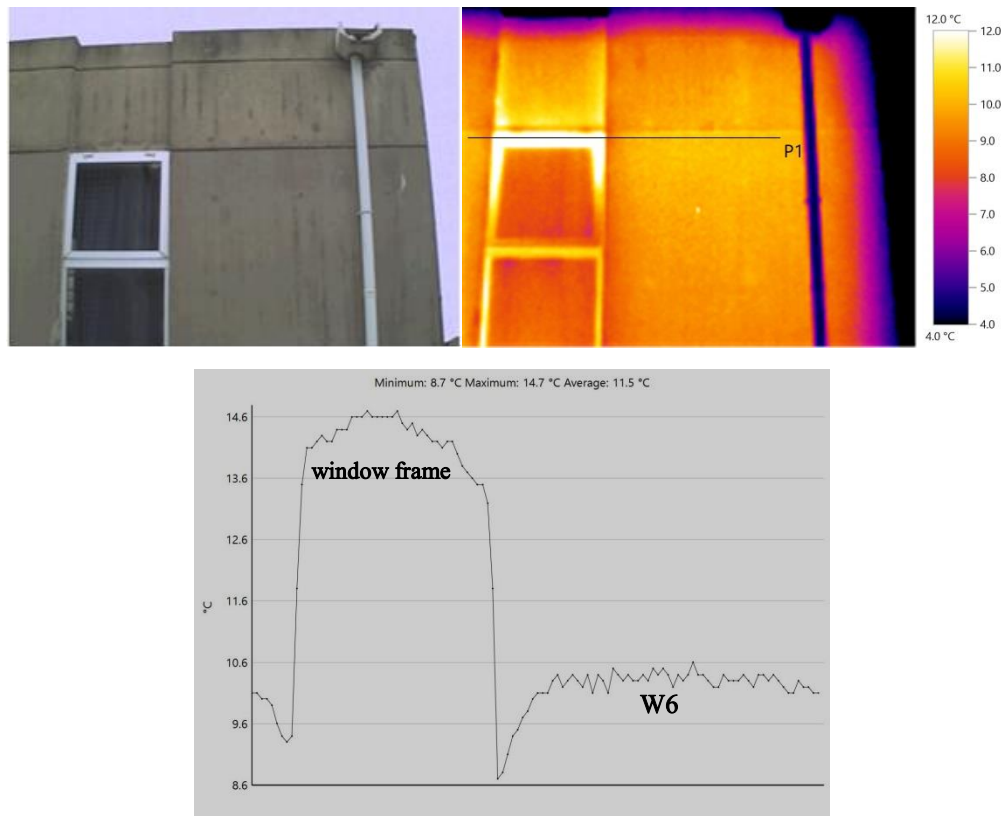


Figure 4.18. Exterior surface temperature of non-insulated shear wall (W6) is about 4°C higher and surface temperature of aluminum window frame is about 8°C higher than the outside air temperature. These temperature differences shows that there are serious heat loss through the wall and aluminum window frame surfaces ($T_{out}=6.4^{\circ}\text{C}$ and $\text{RH}= 65\%$).

The low thermal resistance of the uninsulated reinforced concrete wall (W6) is verified with the IR images taken from its interior surfaces (Figure 4.19). The heat loss through the wall surfaces is visible in IR images as colder surfaces with an evenly-distributed surface temperature about 4°C colder than the inside ambient temperature. The condensation analysis for the actual case of the uninsulated shear

wall (W6) shows that the temperature gradient throughout the wall section is very close to the dew point temperature profile; therefore, the wall is under risk of surface and interstitial condensation (Figure 4.20).

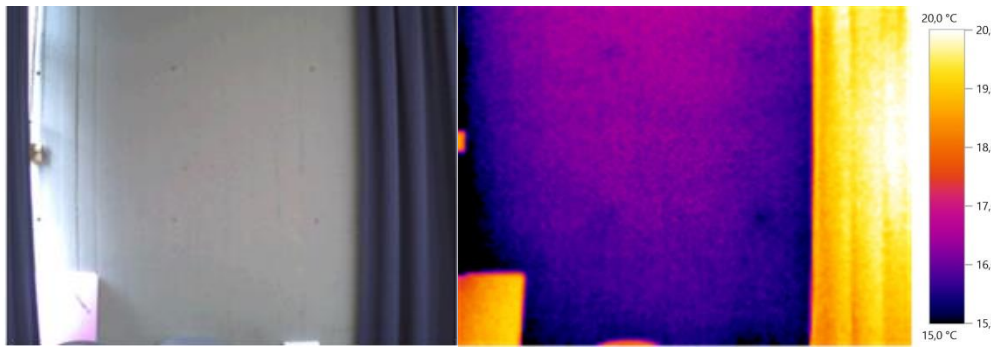


Figure 4.19. IR image shows that surface temperatures of W6 is about 4°C colder than the inside ambient temperature and tie-rod holes can be seen in thermal images in the form of circular colder patches ($T_{\text{out}}=6.4^{\circ}\text{C}$ and RH= 45%).

The exterior surfaces colder than outside air temperature may signal the damp zones getting colder due to evaporative cooling (Figure 4.20 and Figure 4.21). Damp zones are the failure areas acting as thermal bridges and causing excessive heat loss. The coldest areas observed at the lower parts of the wall having surface temperatures up to 2 °C colder than the outside air temperature signal the presence of rising damp problem (Figure 4.20 and Figure 4.21).

Any anomalies, such as tie rod holes existing on the fair faced concrete wall are visible in the IR images taken from the interior surfaces of the W6 in the form of circular patches with surface temperatures about 0.5°C colder than the rest of the wall surface (Figure 4.19). That presents that the tie rod holes have slightly lower thermal resistance than the fair-faced shear wall.

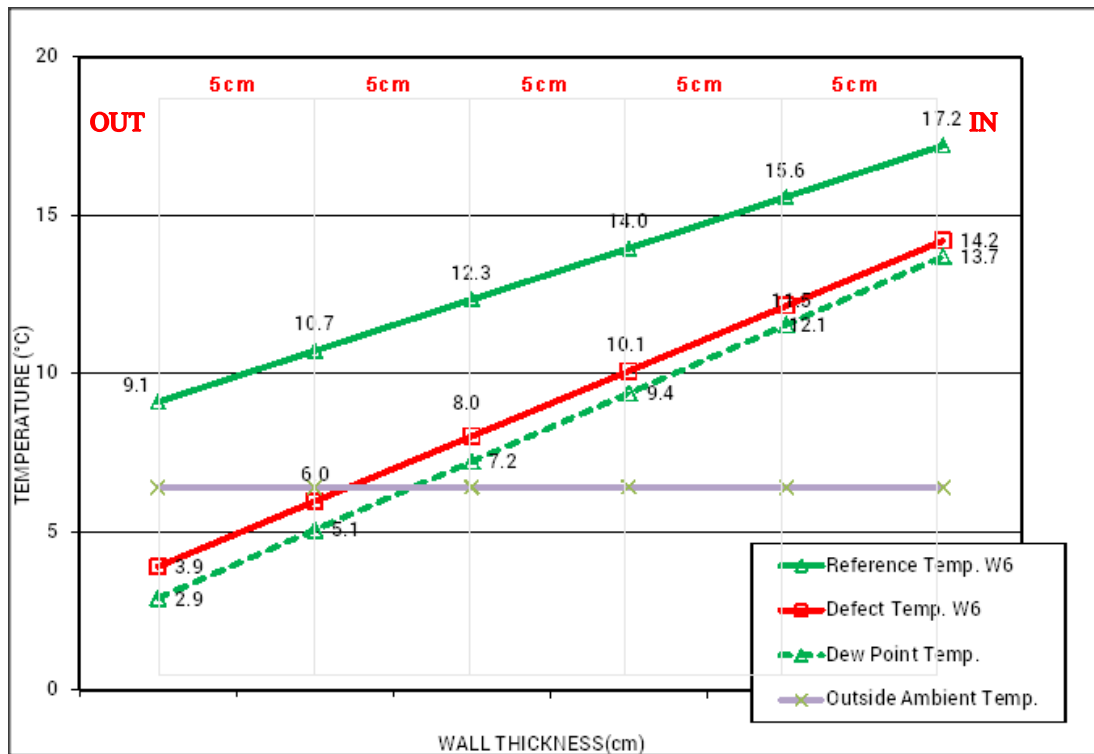


Figure 4.20. Temperature and dew point temperature profiles of W6 showing that temperature gradient throughout the wall section is very close to the dew point temperatures curve, therefore, the wall is under risk of surface and interstitial condensation ($TI_{W6-REFERENCE} = 0.84$; $TI_{W6-DEFECT} = 0.72$) ($T_{in} = 20^{\circ}C$, $RH_{in} = 45\%$ and $T_{out} = -1^{\circ}C$, $RH_{out} = 60\%$).

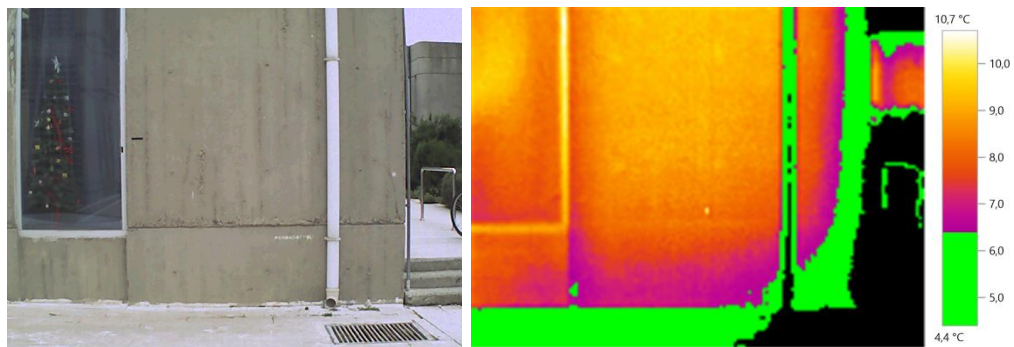


Figure 4.21. Green painted area at IR image shows the surfaces colder than outside air temperature and at the lower corner of W6 there is possibility of evaporative cooling due to damp zones. ($T_{out} = 6.4^{\circ}C$ and $RH = 65\%$).

4.2. Identification of thermal and moisture failures in terms of TI

The qualitative evaluation of IR images taken from interior and exterior surfaces of three building types allowed the identification of thermal and moisture failures existing in six building wall compositions.

The TI values of building surfaces which do not suffer from heat loss is accepted as 1.0 “one”. Considering that, TI_{REF} gives an idea about the as-is thermal resistance performance of the wall component. The TI_{REF} values of all the examined walls are below “1.00” and determined to be in the range of 0.75 and 0.94 (Table 4.1, Figure 4.22). This means that heat loss occurs through the wall components from warm side to the cold sides depending on thermal resistance performance of those wall components. That conclusion was checked with the as-is thermal transmittance (U_{INSITU}) values of the wall components. Supporting their TI_{REF} values, all six walls have U_{INSITU} values above the threshold level of $0.50 \text{ Wm}^{-2}\text{K}^{-1}$ showing that those wall components perform lower thermal resistance than an energy efficient wall component defined in TS 825:2013 for Ankara region. The lowest TI_{REF} values correspond to the non-insulated reinforced concrete walls which perform the lowest thermal resistance (Figure 4.22: See W5 and W6).

The TI_{DEF} values corresponding to the types of thermal and moisture failures are summarized as follows (Table 4.1, Figure 4.22).


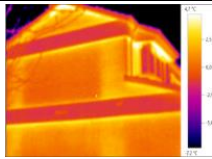

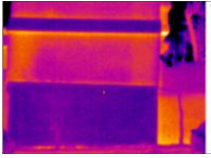
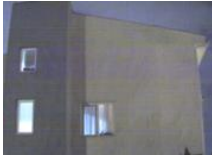
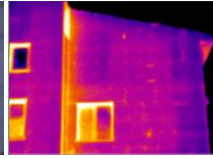

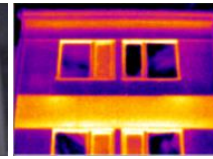

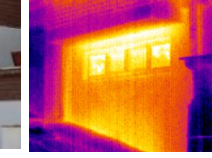

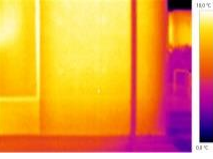
- Thermal bridges due to insufficient thermal resistance of wall composition, sourced from lack of thermal insulation layer (See W5, W6 with TI values in the range of 0.75-0.84).
- Thermal bridges due to the faults occurred during fastening the thermal insulation boards to the backing wall (See W3, W4 with TI values of 0.80 and 0.79).

- Thermal bridges due to discontinuities in partially-insulated exterior walls (See W2 with TI value in the range of 0.71-0.76)
- Warm air leakages through the edges where window frame and building wall come together and through the edges where roof and gable wall come together (See W1, W3 with TI values in the range of 0.53-0.60).
- Damp surfaces due to rising damp (See W6 with TI values of 1.15 – higher than 1.0).

Those TI_{DEF} values correspond to the ranges of TI values obtained for the thermal and moisture failure areas given in the literature (Koçkar, 2012; Tuğla & Tavukçuoğlu, 2016; Tugla et al., 2013).

The problem areas in building walls can be easily detected in infrared images, therefore the problem areas suffering from thermal failures and the reference areas representing the thermal performance of wall composition can be differentiated in the same target area of IR image. The TI_{REF} and TI_{DEF} values were calculated by using the actual exterior surface temperature data corresponding to the reference wall surfaces and thermal failure surfaces. The results show that thermal bridges, air infiltration and damp zones can be identified with TI values and TI_{DEF} values can be used as the indicators that can be used to identify the type of defect quantitatively. For instances, TI_{DEF} values in the range of 0.53 and 0.80 represent thermal bridge zones causing heat loss through exterior building walls areas while the TI_{DEF} values below 0.60 signal air leakage zones of the exterior wall due to poor airtightness. TI_{DEF} values above 1.00 indicate damp surfaces of building walls which might be due to rising damp or surface condensation problems resulting in evaporative cooling on damp wall surfaces.

Table 4.1. Temperature index(TI) values of six walls with and without defect areas corresponding to the thermal failure and reference points in each IR image

| Wall Type | Digital Image | IR Image | Thermal Failure | TI_{INSITU} unitless |
|---------------------------------------|---|---|--|---------------------------|
| W1 Insulated cavity brick wall |  |  | REFERENCE Wall composition with insufficient thermal resistance | 0.88 |
| | | | WARM AIR LEAKAGE through the edge where gable wall and roof come together | 0.57 |
| | | | | |
| W2 Externally-insulated shear wall |  |  | REFERENCE Wall composition with 5 cm-thick EPS board | 0.94 |
| | | | THERMAL BRIDGE Discontinuity in external insulation | 0.76 |
| | | | THERMAL BRIDGE Discontinuity in external insulation | 0.71 |
| W3 Externally-insulated shear wall |  |  | REFERENCE Wall composition with 3 cm-thick EPS board | 0.92 |
| | | | THERMAL BRIDGE Clearances between two insulation boards due to poor workmanship | 0.80 |
| | | | WARM AIR LEAKAGE through the edges where window frame and building wall come together | 0.60 |
| W4 Externally-insulated AAC wall |  |  | REFERENCE Wall composition suffering from entrapped moisture | 0.87 |
| | | | THERMAL BRIDGE Clearances between two insulation boards due to poor workmanship | 0.79 |
| | | | THERMAL BRIDGE at the edge where building wall and roof at eaves level come together | 0.69 |
| | | | THERMAL BRIDGE through the edges where window frame and building wall come together | 0.64 |
| W5 Non-insulated shear wall |  |  | REFERENCE Wall composition without any insulation layer | 0.75 |
| | | | THERMAL BRIDGE at the edge where building wall and ground slab come together | 0.58 |
| | | | THERMAL BRIDGE at the edge where building wall and cantilever slab come together | 0.53 |
| W6 Non-insulated shear wall |  |  | REFERENCE Wall composition without any insulation layer | 0.84 |
| | | | THERMAL BRIDGE at the edge of aluminum metal frame of fenestration unit | 0.72 |
| | | | DAMP ZONES at lower parts | 1.15 |

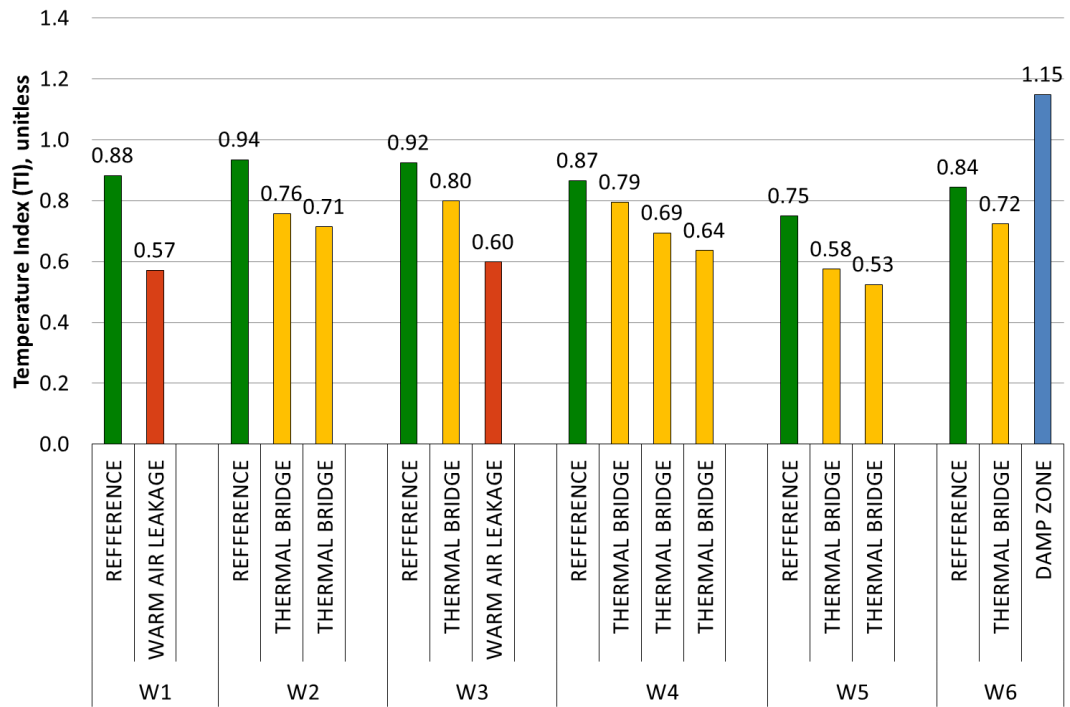


Figure 4.22. Temperature index values calculated for the wall surfaces without any defect and wall surfaces suffering from thermal bridges and air leakages.

4.3. Thermal transmittance values of wall configurations determined with in-situ QIRT ($U_{\text{INSITU-REF}}$) and standard calculation method (U_{CALC})

The $U_{\text{INSITU-REF}}$ values represent the actual thermal transmittance through the existing wall components for their zones, which do not suffer from thermal failures. The comparison of that value with the theoretical thermal transmittance values (U_{CALC} , $\text{W}\cdot\text{m}^{-2}\text{K}^{-1}$) of the same wall compositions allows assessing whether the real thermal performance of the wall compositions are in coherence with the theoretical ones.

Two $U_{\text{INSITU-REF}}$ values, specifically $U_{\text{INSITU-1-REF}}$ and $U_{\text{INSITU-2-REF}}$, are calculated by using Equation 7 in which exterior surface temperature data and outside air velocity are used, and by using Equation 8 in which interior surface temperature. Those

values together with theoretical U_{CALC} values calculated (Equation 9) for six types of wall components are summarized in Figure 4.23. For the comparison and evaluation of the U_{INSITU} and U_{CALC} values, reference thermal transmittance ($U_{\text{INSITU-REF}}$) values, which represent the actual thermal performance of the reference wall areas, are used. The results are given below (Figure 4.23, Figure 4.24).

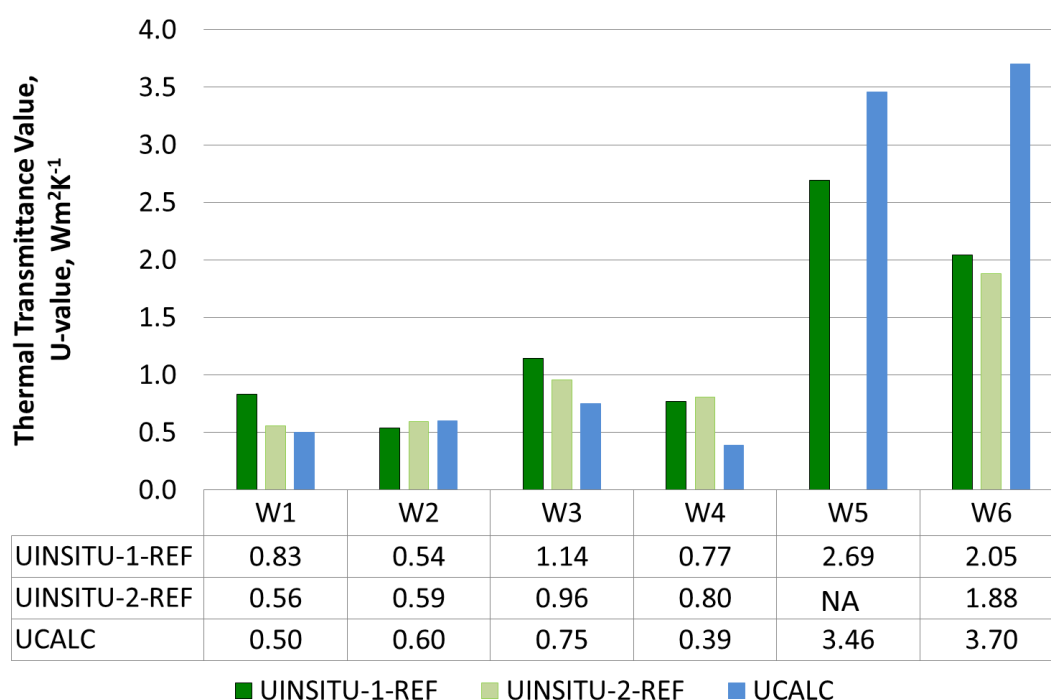


Figure 4.23. Reference in-situ thermal transmittance ($U_{\text{INSITU-1-REF}}$ and $U_{\text{INSITU-2-REF}}$) and the theoretically calculated (U_{CALC}) thermal transmittance values of the walls

The thermal transmittance values ($U_{\text{INSITU-1}}$) based on the calculations using exterior wall surface temperatures were found to be more sensitive than the calculations based on the internal surface temperatures ($U_{\text{INSITU-2}}$). The reasons that provide this sensitivity are explained below:

- In the thermal images showing temperature distribution on exterior surfaces of building walls, thermal and moisture failures zones where the thermal bridges

occur can be distinguished. Thermal images taken from exterior surfaces allow distinguishing problem and non-problem (reference) areas; therefore, that technique does not allow data acquisition from misleading problem areas while allow extracting the exterior surface temperature data only from the evenly-distributed non-problem regions of the wall.

- In Equation 7, the calculations are based on actual exterior surface temperature as well as the actual wind velocity affecting outside surface convection (h_{OUT} , $Wm^{-2}K^{-1}$). That equation increases the accuracy in thermal transmittance calculations by involvement of actual heat transfer from exterior wall surface with convection (h_{OUT} , $Wm^{-2}K^{-1}$), in other words, the impact of wind velocity near exterior wall surface.
- Since the thermal imaging is done on the warm side, any differences on the interior surface, such as paintings, wall clock, and any delamination/detachment in finishing layers plaster layers or surface defects; will be visible in IR images. That situation which involves many disturbances in IR images is not appropriate to distinguish the problem and non-problem (reference) zones which has crucial importance for thermal transmittance measurements.
- In Equation 8, the calculations are based on actual interior surface temperature of exterior walls. Since the surface temperature distribution is disturbed by the presence of surface differences/anomalies, the surface temperature data which has to be obtained from problem and/or non-problem areas for thermal transmittance estimation can be misleading. In addition, that equation uses the interior surface convection coefficient data (h_{IN} , $Wm^{-2}K^{-1}$) as an accepted value given in the standards, while this coefficient does not represent the real situation. Therefore, actual heat transfer with convection neither from exterior nor interior wall surfaces are not involved in the Equation 8.
- Considering all, the $U_{INSITU-1-REF}$ values using external thermal images and Equation 7 are considered to represent the actual thermal performance of the wall

composition with more accuracy than the alternative method using internal thermal images and Equation 8.

- For the reliability confirmation of QIRT method, the measurements repeated for several times both in winter and summer. $U_{\text{INSITU-REF}}$ measurements for W6 (fair-faced concrete shear wall) in B3 (Faculty of Architecture Building) were repeated during cold weather conditions for two times in winter 2016 and winter 2017. The winter measurements were done when the outside was cold and inside was warm, and when IR images were taken at the colder side (outdoor side). The $U_{\text{INSITU-REF}}$ measurements for W6 were also repeated in hot weather conditions in summer 2017. The summer measurements were done when the outside was warm and inside was cold and when IR images were taken at the colder side (indoor side). The results obtained are given in Figure 4.24. For the W6, the $U_{\text{INSITU-REF}}$ values achieved in winter seasons are almost the same and the $U_{\text{INSITU-REF}}$ value achieved in summer season is very similar with the winter data. The achievement of similar values in a range of $\pm 5\%$ difference signals the repeatability of the method in the same and different seasons, therefore, shows the reliability of the QIRT method for the actual U-value estimation.

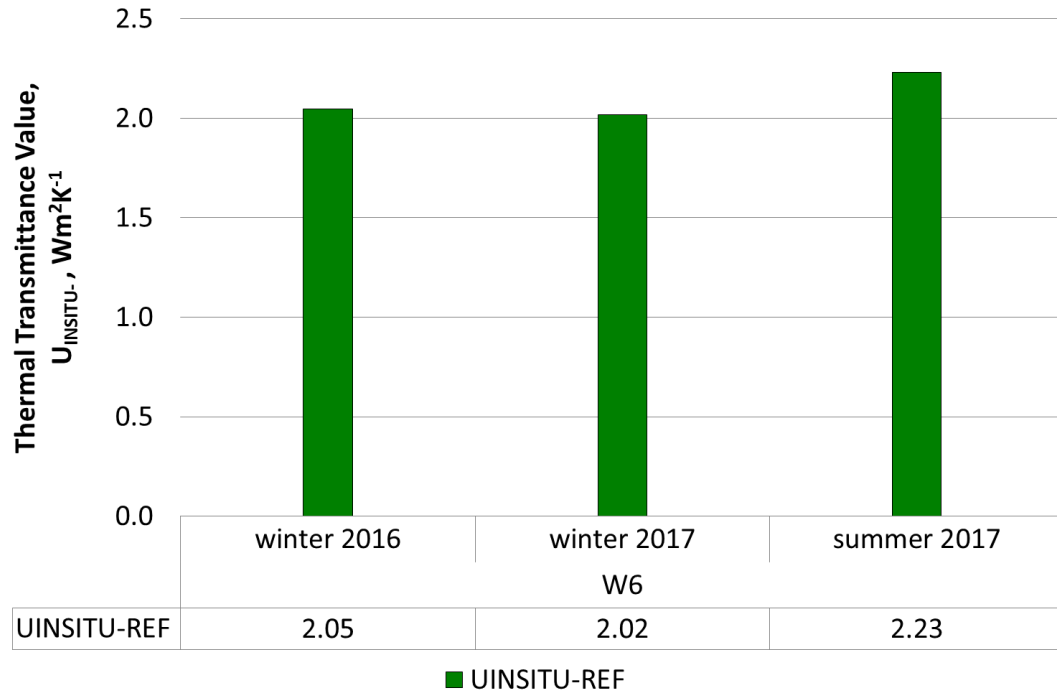


Figure 4.24. In-situ U values of W6, obtained at hot and cold weather conditions

The comparison of U_{INSITU} values and the theoretically-calculated U values have shown that (Figure 4.23):

- All types of walls have U_{INSITU} values above the level of $0.50 \text{ W.m}^{-2}\text{K}^{-1}$ assigned as the threshold level for an energy efficient wall component in TS 825:2013 for Ankara region. That conclusion is also supported with the walls' TI_{REF} values below 1.0 (Table 4.1, Figure 4.22). It means that exterior surfaces of walls, especially the zones which do not suffer from a specific thermal failure, have surface temperatures above the outside air temperature; in other words, heat loss in varying ranges are observed to occur in all six wall component depending on their thermal resistance performances. All data signals that the thermal resistances of the walls are not sufficient to cope up with the existing climatic conditions.
- The actual thermal transmittance values of all insulated walls (multi-layered walls), except W2 (shear wall externally-insulated with 5cm-thick EPS boards) are higher than the theoretically calculated ones ($U_{\text{INSITU}} > U_{\text{CALC}}$). It means that

the actual thermal resistivity of these walls (W1, W3 and W4) is lower than expected.

- *The actual and theoretical thermal transmittance values belonging to W2 (shear wall externally-insulated with 5cm-thick EPS) are almost the same ($U_{\text{INSITU}} \cong U_{\text{CALC}}$). That consistency between the actual and expected thermal resistance performances show that newly-applied external insulation layer functions well enough to meet the expected thermal resistance, and the W2 wall component is not under adverse effect of any thermal and moisture failure at the moment.*
- According to theoretically-calculated U_{CALC} values, insulated aerated concrete wall (W4) is expected to perform the highest thermal resistance among six wall components. However, *actual thermal transmittance of aerated concrete wall (W4) is higher than, almost twice the theoretical one* (Compare $U_{\text{CALC-W4}}$ and $U_{\text{INSITU-1-REF-W4}}$). Possible reasons of achieving lower thermal resistance from W4 compositions are explained below:
 - Discontinuities at thermal insulation material due to the faulty fastening the thermal insulation boards to the backing wall cause thermal bridges (Figure 4.14) followed by interstitial condensation problems within the multi-layered aerated concrete wall component and then, this resulted in considerable heat loss and decreasing thermal resistivity.
 - In addition, the input data on thermal conductivity of aerated concrete given in the relevant standards can be a reason for the calculation of misleading theoretical U-value. According to TS 825:2013 standards thermal conductivities of the materials being in equilibrium with 80% relative humidity have to be used for theoretical calculations. However, the thermal conductivity of aerated concrete infill block is given as $0.13\text{Wm}^{-1}\text{K}^{-1}$ in TS 825:2013 which is a misleading data since the value belongs to the AAC material in dry state. Therefore, its use for theoretical calculations may result in misleading lower U values in a certain range particularly for very porous materials well-known with their high moisture intake capacities. For

instance, the analyses in literature report that thermal conductivity of AAC increases with the increase in moisture content (Jin, Yao, Fan, Xu, & Yu, 2016). The thermal conductivity of an AAC block in damp state (which is a similar type of AAC used in W4 with bulk density of 0.6g/cm^3) is $0.55\text{Wm}^{-1}\text{K}^{-1}$ when the sample is in equilibrium at 80%RH while its thermal conductivity in very dry state is $0.18\text{Wm}^{-1}\text{K}^{-1}$ when the sample is in equilibrium at 0%RH. In short, the reference thermal conductivity values of porous materials given in the standard, especially for the one having high portion of micro pores need to be revised by taking into consideration the values at 80%RH conditions.

- Since AAC is very porous and highly-breathable masonry unit, its external covering with a less breathable insulation layer, expanded polystyrene (EPS) is expected to accelerate the entrapped moisture problem within the wall section. The occurrence of condensation is proved in the same building wall, specifically at the neighboring concrete wall parts (Figure 4.17). The covering of a building wall with a non-breathable insulation material does not allow moisture escape through the wall. Confirmation of that problem requires further analyses, but its presence at least show that selection of materials compatible with each other has vital importance for the multi-layered wall components, especially for their long-term energy efficiency and durability performances.
- The actual thermal resistivity of W3 (shear wall externally-insulated with 3cm-thick EPS boards) is considerably lower than expected resistivity since *the theoretically-calculated thermal transmittance of the W3 is half of its actual higher thermal transmittance* (Compare $U_{\text{CALC-W3}}$ and $U_{\text{INSITU-1-REF-W3}}$). Thermal and moisture failures due to the inadequate thermal resistance of wall composition, discontinuities between the edges of thermal insulation boards, and air leakages through the edges where window frame and wall come together, result in surface and interstitial condensation within the multi-layered wall component (Figure 4.14 and Figure 4.17). Presence of such failures causes

reduction in overall thermal resistivity of the wall component and result in heat loss in an unexpected level through wall surfaces.

- According to its theoretically-calculated U_{CALC} value of $0.50\text{Wm}^{-2}\text{K}^{-1}$, the cavity brick wall with 5cm-thick thermal insulation infill (W1) is expected to perform as an energy efficient wall in Ankara climate. However, *actual thermal transmittance of insulated cavity brick wall (W1) is higher than the theoretical one* (Compare $U_{\text{CALC-W4}}$ and $U_{\text{INSITU-1-REF-W4}}$). Thermal and moisture failures due to the partial-lack of insulation infill within the cavity due to workmanship faults or deterioration of cavity insulation in time (Figure 4.3, Figure 4.4 and Figure 4.5), air leakages through the edges where window frame and wall come together (Figure 4.4 and Figure 4.8) and being in contact with damp parts of uninsulated shear wall (W5) (Figure 4.6 and Figure 4.7) are expected to result in moisture problems within the multi-layered wall component. Those failures reduce the overall thermal resistivity of the wall component and result in heat loss in more than expected level.
- Among six different types of walls, the lowest thermal efficiency is expected from non-insulated fair faced shear walls (W5 and W6) according to their theoretically calculated thermal transmittance values (Figure 4.23, See $U_{\text{CALC-W5}}$, $U_{\text{CALC-W6}}$). However, *as-is thermal performances of those single layered solid walls are noticeably better than the expected performances* (Compare $U_{\text{CALC-W5}}$ and $U_{\text{CALC-W6}}$ with $U_{\text{INSITU-W5}}$ and $U_{\text{INSITU-W6}}$). Those values signal that the reinforced concrete materials used in the constructions of W5 (B1 - Villa house in METU Campus) and W6 (Faculty of Architecture building in METU Campus), exhibit lower thermal conductivity values than the reference value given in the standard TS 825:2013. Since the W5 and W6 are a single-layered solid wall, their actual thermal conductivity values can be estimated by using the data on their actual thermal transmittance value and actual thickness based on Equation 9 (page 26). The reference thermal conductivity value of reinforced concrete is given as $2.50\text{Wm}^{-1}\text{K}^{-1}$ in the standard TS825:2013 while the estimated thermal conductivity values for the W5 and W6 are $1.75\text{Wm}^{-1}\text{K}^{-1}$ and

1.10 Wm⁻¹K⁻¹, respectively. The analyses on the original concrete used in the construction of Faculty of Architecture Building report that its particular properties, such as its total effective porosity being about 13% by volume, the abundance of individual large-sized pores and aggregates, and quite a low portion of cement binder, are expected to contribute to the lower thermal transmittance performance of the original concrete in comparison to today's concrete (Savaş, A., in the process of publication). Specifically for the W6, it is understood that a qualified concrete performing low thermal conductivity has been used in the construction of the reinforced concrete wall. Further analyses are needed to better understand the thermal performance properties of that original concrete type and compositional properties contributing to that particular thermal performance.

4.4. Actual thermal transmittance values determined for the thermal failure zones ($U_{\text{INSITU-DEF}}$)

In order to better-understand the adverse impact of thermal bridges due to thermal and moisture failures occurred in time at existing building walls, thermal transmittance at those problem zones were determined in terms of $U_{\text{INSITU-DEF}}$ values. The surface temperature data extracted from defect zones were used for the calculation of $U_{\text{INSITU-DEF}}$ values. Those problem areas and non-problem/reference areas in building walls could be detected and located in IR images for data extraction (Table 4.1).

The data on the $U_{\text{INSITU-DEF}}$ values corresponding to thermal bridge areas existing on walls components and the increase in reference values of actual thermal transmittance at thermal bridge zones are summarized in Figure 4.25, respectively. The $U_{\text{INSITU-DEF}}$ values corresponding to thermal bridge zones reveal the extremely-considerable heat loss through those local problem areas. Increase in thermal

transmittance at thermal bridges in reference to $U_{\text{INSITU-REF}}$ values are higher at insulated wall components (W1, W2, W3 and W4) than at non-insulated wall components (W5 and W6) (Figure 4.26 and Figure 4.27). At insulated wall components, the increase in their reference actual thermal transmittance values are in the range of 56% and 135%. Such a considerable increase in thermal transmittance at defect areas signal that extreme heat loss may occur even at small sized thermal bridge zones and may destroy thermal resistance of those wall components although thermal insulation exists within their multi-layered compositions. That adverse impact of thermal bridge zones at not-insulated reinforced concrete walls (W5 and W6) are also noticeable, as an increase in actual thermal transmittance in the range of 23% and 31%. The overall wall surfaces of W5 and W6 walls already act as thermal bridges due to their considerably-high thermal transmittance, and thermal transmittance values at defect areas reaches to $2.67\text{--}3.37 \text{ Wm}^{-2}\text{K}^{-1}$ which highlight heat loss at extreme levels.

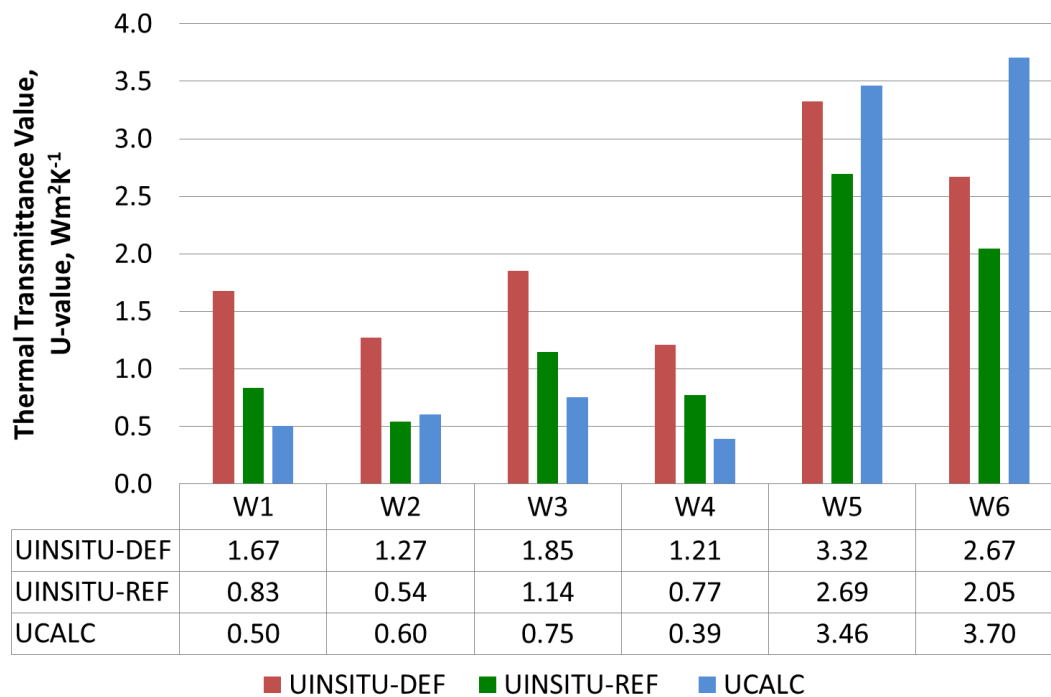


Figure 4.25. The reference value of actual thermal transmittance ($U_{\text{INSITU-REF}}$), the actual thermal transmittance at thermal bridge zones ($U_{\text{INSITU-DEF}}$) and the theoretically calculated thermal transmittance (U_{CALC}) values of the six wall components under examination.

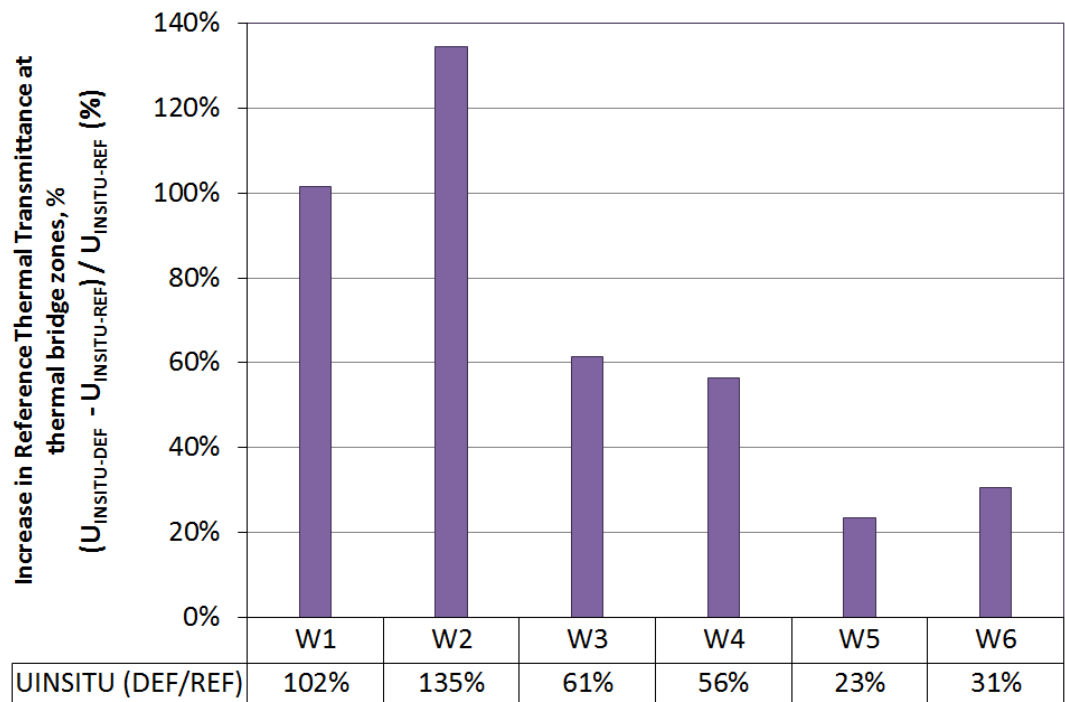


Figure 4.26. The increase in reference values of actual thermal transmittance at thermal bridge zones ($U_{\text{INSITU-REF}}$) in percentages

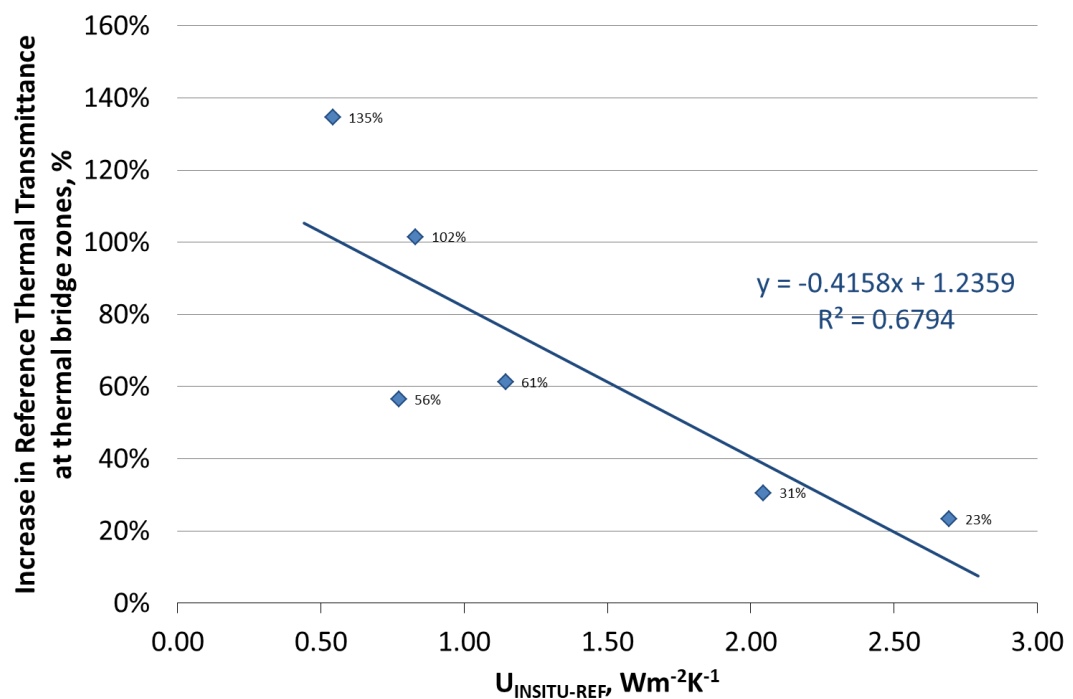


Figure 4.27. The plot of increase in the reference values of actual thermal transmittance values at thermal bridge zones (in percentages) versus $U_{\text{INSITU-REF}}$ values of existing building walls.

4.5. Actual thermal transmittance values ($U_{\text{INSITU-AVG}}$) of wall configurations to be used for Energy Performance Certification

The evaluation of $U_{\text{INSITU-REF}}$ and $U_{\text{INSITU-DEF}}$ values reveal that thermal bridges on wall surfaces significantly reduce the overall thermal resistance of a wall component. If Energy Performance Certification (EPC) is expected to reflect the actual thermal performance of building components, the adverse impact of thermal bridges has to be involved in thermal transmittance assessment of wall components. For that purpose, $U_{\text{INSITU-AVG}}$, which involves thermal transmittance of the areas both suffer and do not suffer from thermal bridges, is proposed for its use to estimate annual energy consumption and to energy performance certification (EPC) of an existing building.

The data on the $U_{\text{INSITU-AVG}}$ values of the wall components and difference between $U_{\text{INSITU-AVG}}$ and $U_{\text{INSITU-REF}}$ values in percentage are summarized in Figure 4.28 and Figure 4.29, respectively. The adverse impact of thermal bridges, which occur in existing building wall in time, reduces the actual thermal resistance of six building walls and that adverse impact is visible with an increase in their actual thermal transmittance in the range of 11% and 37% (Figure 4.29). That adverse impact is lower at not-insulated reinforced concrete walls (W5 and W6) than insulated wall components (W1, W2, W3 and W4) (Figure 4.29 and Figure 4.30). The overall wall surfaces of the uninsulated exterior walls already act as thermal bridges due to their considerably-high thermal transmittance. In cases of insulated walls, although thermal insulation exists within their multi-layered compositions, the adverse impact of thermal bridges to their overall thermal performance is considerable and accelerates the overall transmittance around 33% (Figure 4.29).

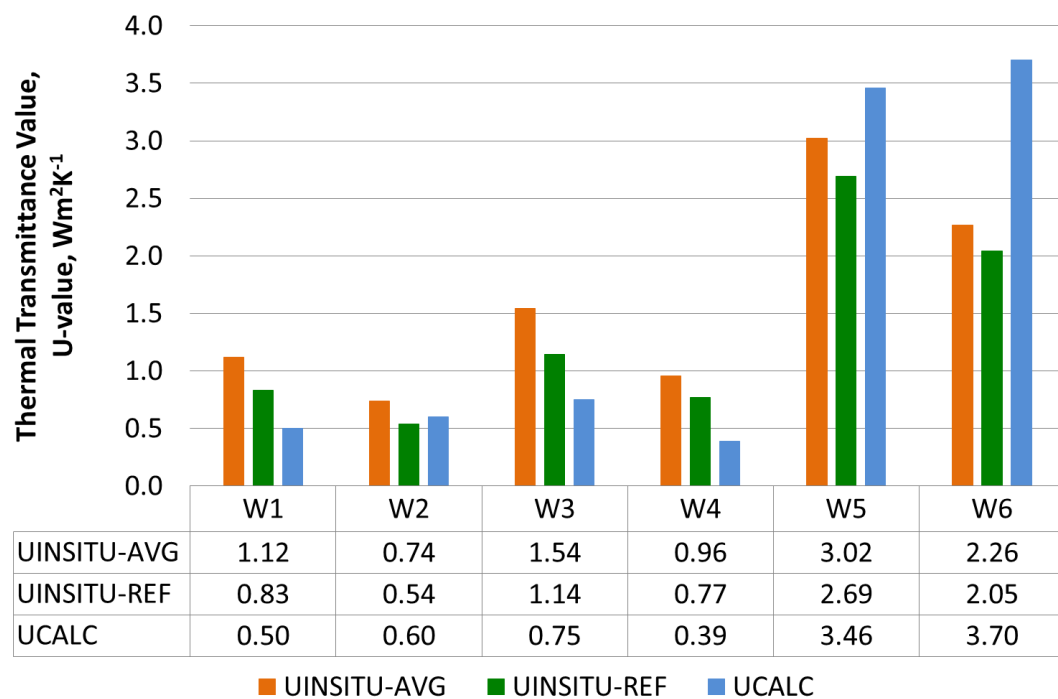


Figure 4.28. The reference value of actual thermal transmittance ($U_{\text{INSITU-REF}}$), the average value of actual thermal transmittance ($U_{\text{INSITU-AVG}}$) and the theoretically calculated thermal transmittance (U_{CALC}) values of the six wall components under examination.

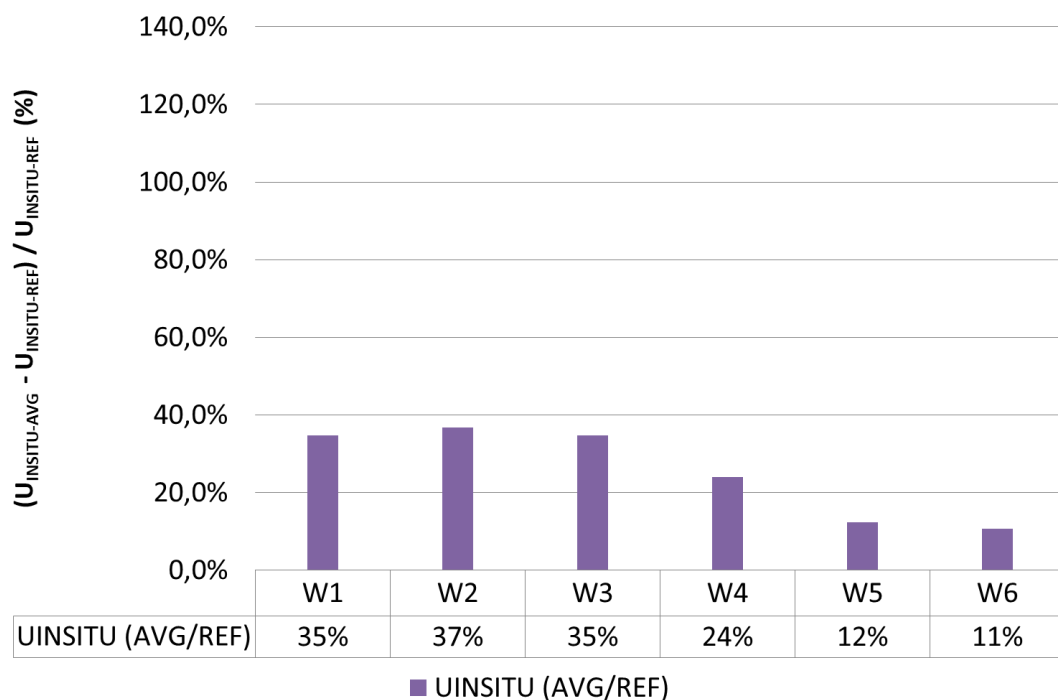


Figure 4.29. The increase in percentages, which were observed in the reference values of actual thermal transmittance ($U_{\text{INSITU-REF}}$) due to the thermal bridges occurred in time in existing building walls

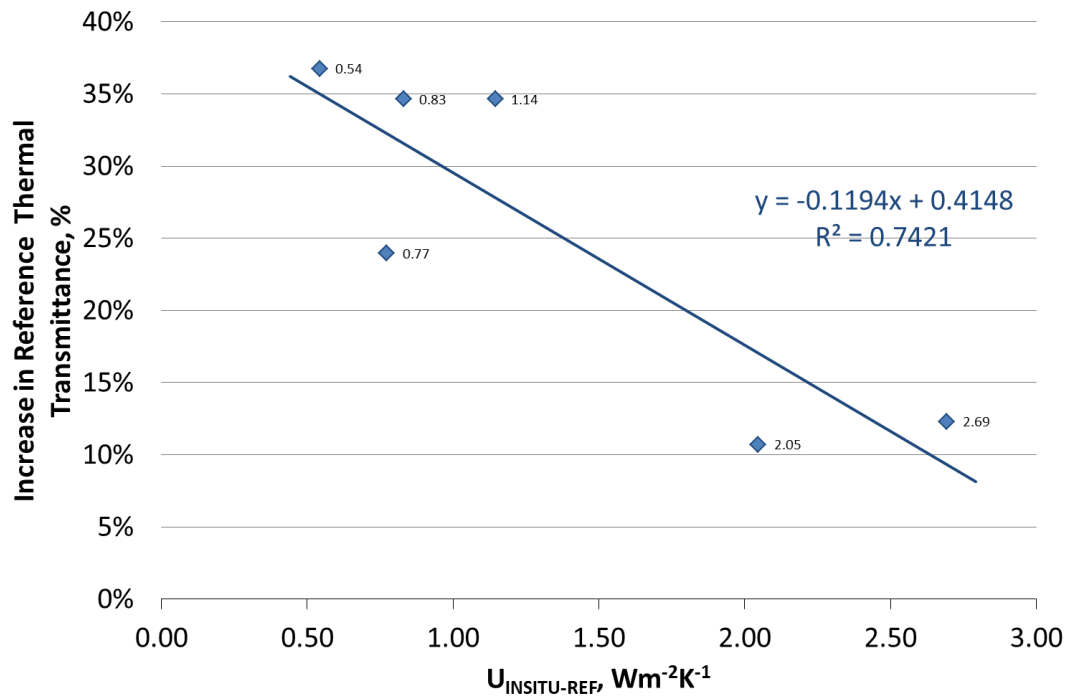


Figure 4.30. The plot of increase in the reference values of actual thermal transmittance values in percentages versus $U_{\text{INSITU-DEF}}$ values of existing building walls

4.6. Estimation of Annual Heating Energy Consumption and identification of Energy Performance Rating: Case B1 - before and after insulation treatment

Differences between as-is and theoretically-calculated thermal transmittance values were discussed in terms of Annual Heating Energy Consumption (θ_{INSITU} and θ_{CALC} , $\text{kWhm}^{-2}\text{-year}$) of Villa Type House (B1): before and after remedial renovation.

Maximum allowed annual heating energy consumption for Villa Type Building (B1) was calculated as 94.10kWhm^{-2} to be a C type energy performance according to relevant standard (TS:825, 2013) (Table 4.2).

Table 4.2. *Maximum allowed annual energy consumption for heating purposes for B1 calculated according to relevant standard (TS 825, 2013)*

| Total surface area of building envelope | Total gross volume of building | $A_{\text{total}}/V_{\text{gross}}$ | allowed annual heating energy consumption | | |
|---|--------------------------------|-------------------------------------|---|--------|--------|
| | | | θ_{annual} | | |
| A_{total} | V_{gross} | | A type | B type | C type |
| m^2 | m^3 | m^{-1} | kWhm^{-2} | | |
| 402 | 416 | 0.97 | 75.28 | 84.69 | 94.10 |

$U_{\text{INSITU-AVG}}$ value is accepted to reflect the actual thermal performance of the wall composition to be used for Energy Performance Certification and to estimate annual heating energy consumption calculations (Figure 4.28). During calculation of actual (in-situ) annual heating energy consumption, thermal transmittance values of the building components except studied walls (W1, W2 and W5) were calculated according to thermal conductivity values and equations given in relevant standards by using MMO-TS285 software. In other words, their U_{INSITU} values are assumed to be same as these U_{CALC} values. Calculated U_{CALC} values according to relevant standards of these components (roof, slab on ground, windows, doors) are given in Table 3.4 (MMO, 2015; TS 825, 2013). These $U_{\text{INSITU-AVG}}$ and U_{CALC} values of the villa type house (B1) which are used for annual heating energy consumption calculations for the cases of before and after insulation treatment are given in Table 4.3.

Table 4.3. *In-situ and theoretical calculated thermal transmittance values of B1 façade elements, before and after remedial renovation*

| Villa Type House (B1) | $U_{\text{INSITU-AVG}} (\text{Wm}^{-2}\text{K}^{-1})$ | | | $U_{\text{CALC}} (\text{Wm}^{-2}\text{K}^{-1})$ | | | | | | | |
|----------------------------|---|------|------|---|------|------|--|------|----------------|--------|------|
| | W1 | W2 | W5 | W1 | W2 | W5 | Basement Wall (wall with earth contact) | Roof | Slab on ground | Window | Door |
| before remedial renovation | 1.12 | - | 3.02 | 0.50 | 0.60 | 3.46 | 0.54 | 0.63 | 0.54 | 1.80 | 4.00 |
| after remedial renovation | | 0.74 | - | | | | | | | | |

Villa Type House (B1) thermal performance was calculated in terms of estimated annual energy consumption (θ_{INSITU} , kWh) and theoretical annual energy consumption (θ_{CALC} , kWh). The Equation 14 and 15 and the MMO-TS285 software were used for these calculations (MMO, 2015). These calculations were done both for actual and theoretical cases. The results of these calculations are given in Figure 4.31 and summarized below:

- Villa Type House (B1) walls; W1, W2 and W5 have U_{CALC} and U_{INSITU} values above the level assigned as the threshold level ($0.50\text{Wm}^{-2}\text{K}^{-1}$) for an energy efficient wall component in related standards for Ankara region (TS 825, 2013). Therefore, it is obvious that the thermal performance of B1 is not sufficient to cope up with the existing climatic conditions and having a proper energy performance both before and after remedial renovation.
- Before remedial renovation θ_{INSITU} (233.6kWhm^{-2}) of B1 is lower than θ_{CALC} (281.5kWhm^{-2}). Because, in-situ thermal performance of W5 is higher than the expected thermal performance (Compare $U_{\text{CALC-W5}}$ with $U_{\text{INSITU-W5}}$ in Figure 4.25).
- After remedial renovation θ_{INSITU} value (152.2kWhm^{-2}) of B1 is higher than θ_{CALC} value (137.2kWhm^{-2}), vice versa the previous case. Because, W1 in-situ thermal performance is lower than the expected thermal performance (Compare $U_{\text{CALC-W1}}$, with $U_{\text{INSITU-W1}}$ in Figure 4.25).
- Difference between θ_{INSITU} and θ_{CALC} values expected to be higher, if the thermal actual transmittance values ($U_{\text{INSITU-AVG}}$) of the all façade elements, like; cold roof, basement wall, slab on ground, windows and doors also calculated via QIRT method. However, these values are assumed to be same with U_{CALC} values (Table 4.3).
- Remedial renovation increases the thermal performance of the B1, in other words, annual heating energy needs of the B1 decreases with the help of the thermal insulation treatment. This increase in energy performance is valid for both in-situ and theoretical cases:

- Before renovation θ_{INSITU} was 233.6kWhm⁻² and after renovation works this consumption decreases to 152.2kWhm⁻².
 - Before renovation θ_{CALC} was 281.5kWhm⁻² and after renovation works this consumption decreases to 137.2kWhm⁻².
- Before remedial renovation, θ_{INSITU} is lower than θ_{CALC} . In other words actual thermal performance of building is higher than the expected. This unexpected result is because of the fact that, in-situ performance is higher than the theoretical performance for W5, which is a one layered element.
- After remedial renovation, θ_{INSITU} is higher than θ_{CALC} . In other words actual thermal performance of building is lower than the theoretically calculated, which is an expected result.
- Although remedial renovation increases the thermal performance of B1, it is still not enough for an energy efficient building. Because, both before and after remedial renovation annual heating energy needs of B1 is higher than the threshold level for this building (94.1kWhm⁻²).

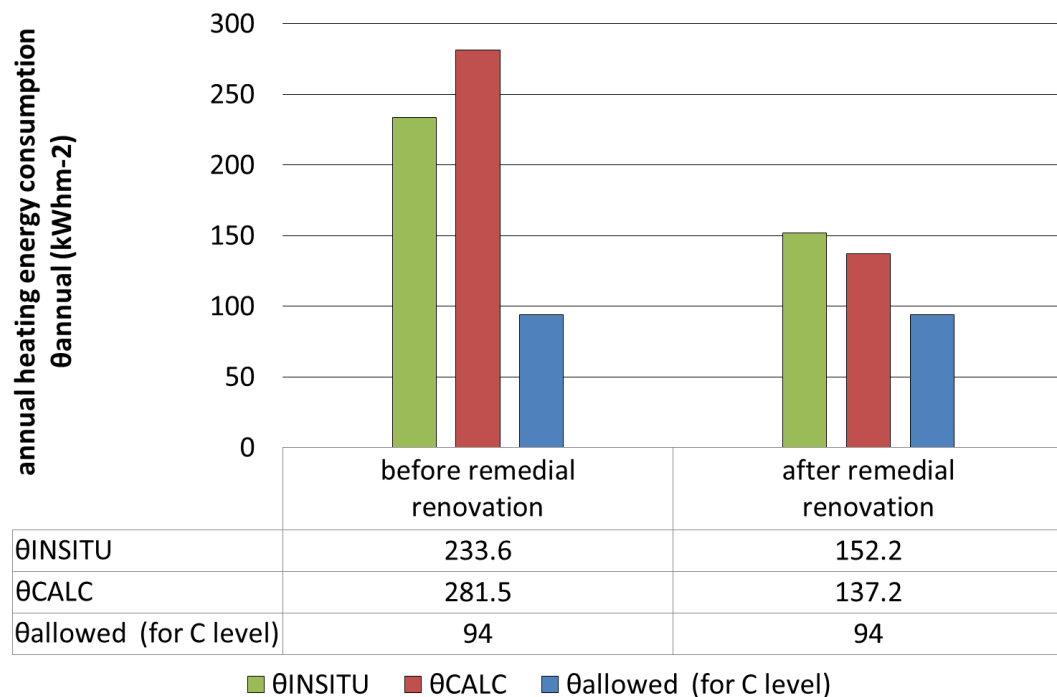


Figure 4.31. Comparison of annual energy consumption for heating purposes for Villa Type Building (B1): theoretically and in-situ θ_{annual} values for both before and after renovation works.

CHAPTER 5

DISCUSSION

The results of the in-situ studies were interpreted together in order to discuss the performance of in-situ QIRT method developed in the study for the assessment of thermal performance of building walls on quantitative basis, specifically in terms of thermal transmittance and temperature index values. The knowledge and experience achieved during in-situ Quantitative Infrared Thermography (QIRT) studies were evaluated and then the guiding remarks for the effective use of QIRT method on site and reliable data acquisition were explained.

5.1. Performance evaluation of in-situ QIRT method for thermal transmittance assessment

IR imaging of building surfaces allows gathering actual surface temperature and inside and outside air temperatures representing the actual cases in buildings. In addition, IR imaging allows detection of visible and invisible thermal and moisture failures existing in building envelope and exact locations of those failures. Therefore all data extracted from IR images are valuable and should be used to assess the actual thermal performance of building walls. The results of field studies show that the quantitative analysis of the actual surface temperature data is possible for the determination of thermal performance parameters in terms of thermal transmittance value and temperature index. Use of QIRT on site to assess the actual state of building wall is, in fact, a necessity and the QIRT method developed in the study as an in-situ testing method fill that gap for actual thermal performance assessment of building walls. Supportive heat transfer equations given in literature allow using in-

situ data for the calculation of real thermal transmittance values of building walls, and the quantitative identification of thermal failures and their severeness.

The results of the in-situ QIRT studies revealed and confirmed that the quantitative identification of thermal and moisture failures is possible in terms of TI values. The adverse impact of thermal failures, in other words the severeness level of thermal failures can be measured in terms of $U_{\text{INSITU-DEF}}$ values. For instance, the TI values below 1 refers to the presence of heat loss through the wall component while the TI values below 0.6 signal air leakages from warm inside to cold outside and TI values above 1 signal the damp zones in building walls. This means that if the temperature data in IR images can be transferred to a computer-based models of building surfaces pixel by pixel, it is possible to identify the TI values at each pixel of the target area by means of practical calculations. Therefore it is possible to produce the map of thermal and moisture failures in terms of TI values. In addition, it is possible to produce the map of the target area showing the distribution of U values by processing the in-situ IR data with the Equation 7 and to analyze the severeness of the problem areas in terms of $U_{\text{INSITU-DEF}}$ value.

The results of the in-situ QIRT studies revealed and confirmed that the accurate estimation of actual thermal transmittance values of the wall components is possible. The analyses show that the theoretical U values of wall components do not reflect the actual thermal performance of walls due to the thermal failures occurred at building component in time. This signals that the annual energy consumption values calculated by using the theoretical U values can be misleading in certain extent. Being able to measure the actual thermal transmittance of building walls has vital importance in this regard since using actual $U_{\text{INSITU-AVG}}$ values make the estimation of annual energy consumption in buildings more reliable as well as allow the certification of a building's Energy Efficiency Rating more accurate. In addition, the

use of QIRT in-situ testing method for actual $U_{\text{INSITU-AVG}}$ measurements provides a practically-applied repeatable technique of monitoring the changes in thermal performance of building envelope in time.

Achieving Energy Performance Certification (EPC) for a building, even at moderate levels, requires a certain amount of additional cost for the insulation of wall components. Therefore, instead of using theoretical U_{CALC} values, a strong resistance is expected when actual $U_{\text{INSITU-AVG}}$ values are used as input data in EPC system. In other words, the actual situation presents lower thermal resistance than expected, therefore requires thicker thermal insulation renovations resulting in higher costs. For benefitting from EPC system which will result in much more energy saving and energy efficiency in construction sector, there is necessity to improve the consciousness of the occupants and the professionals working in the fields of building inspection and construction market. Otherwise, it can be difficult to put that approach into practice; in other words to integrate QIRT in-situ testing method to the building inspection works related with energy efficiency assessment.

The integration of QIRT analyses to the EPC systems, without doubt, will contribute to the development of our country. As much as the QIRT in-situ testing methods are widely-involved in energy efficiency monitoring works in buildings, a real success in energy saving can be achieved in new and existing buildings. In this regard, there is necessity for IRT experts that is a recently-introduced profession working in research studies and field surveys related with energy efficiency monitoring and certification works.

In addition, the temperature data extracted from IR images can be processed to determine $U_{\text{INSITU-REF}}$ value of building components, which allows the estimation of the thermal conductivity of the overall building component.

The results of the in-situ QIRT studies revealed and confirmed that the using surface temperature data extracted from the IR images of exterior building surfaces is the most appropriate approach for accurate and reliable data acquisition from the multi-layered and single-layered building wall. However, there are restrictions of using exterior surface temperature data for the thermal performance and energy efficiency assessment of ventilated facades and ventilated cavity walls since the heat transfer mechanisms change with the presence of a ventilated cavity within the wall composition. Further studies are needed to develop most effective and efficient in-situ testing method by using QIRT especially for the ventilated facades in which some layers are not in direct contact with each other.

Since there are so many potentials of adapting QIRT to the quantitative thermal performance analyses, its integration into the in-situ analyses and its common-use are necessary. However, its common use necessitates collaborative work among research institutes, municipalities and ministries with focuses on training experts.

5.2. Considerations for in-situ thermal transmittance measurements with the use of QIRT

Guidelines to achieve reliable in-situ surface temperature data to establish the reference data were described under respective subheadings: method and analysis of data. These guidelines are expected to be useful to develop the simulation software and allow advanced computer based modelling & simulation analyses only by IR images taken from building surfaces. Today, the experts should be trained for

quantitative infrared thermography for assessment of Energy Performance Certification (EPC). In future, the approach in data acquisition and data analyses by use of QIRT is expected to lead fast and accurate performance assessment. Approach the logic behind data acquisition and data analyses will be transferred to simulation analyses and result in advance in-situ thermal performance monitoring in quantitative bases.

Thermal transmittance measurement with QIRT method has several steps, and there are some important aspects that should be taken into consideration before and during IR imaging, which are indicated below.

Before IR imaging:

- Experienced specialists are needed for infrared thermograph with having sufficient building science knowledge and understanding effects of thermal and moisture failures.
- Investigation of building envelope will be helpful, composition of exterior walls, roofs or other elements that will be studied via IRT.
- The geographical orientation of the building, including other buildings, vegetation and landscaping will be helpful.
- Surface temperature values may change because of direct solar radiation on the target area; therefore, the knowledge about the sun orientation is necessary. In other words solar radiation before or during IR imaging may affect the performance of the assessment process and should be taken into consideration.
- Visually determining the areas that may need further examination related to thermal bridging, moisture problems and air infiltration will be helpful during analyzing the IR images.
- Estimation thermal transmittance value with Infrared Thermography is based on the assumption that the building and its environment are in steady state heat transfer equilibrium, in other words there is a steady heat transfer between two

sides of the building façade. Therefore, heating and cooling facility on/off time information is necessary.

- It is suggested that, heating system (cooling system for hot weather conditions) of the building is operational to make the inside ambient temperature constant before 24 hours performing IRT (this time is approximate and depends on the thermal properties of the building envelope, inertia, thermal mass etc.).
- In-situ climatic history of the working environment should be observed to increase the reliability of the IRT method: snowy, rainy, windy etc.
- Thermal cameras should have some technical properties:
 - It is recommended that minimum camera resolution should be 160*120.
 - Thermal resolution or sensitivity, must be less than or equal to 0.10°C at 30°C (0.18°F at 86°F).”
 - Long wavelength type cameras should be used for in-situ studies, because the sensitivity to the ambient temperature and ambient objects temperature is important and long wavelength (8-12 µm) cameras are less affected.
 - Temperature range should be suitable for in-situ inside and outside air temperature ranges.

During IR imaging:

- The following in-situ data should be collected with data loggers before and during IR imaging: inside and outside ambient temperature, relative humidity and outside wind velocity near wall surface. In addition to this, using handheld anemometers is recommended during imaging for following instantaneous climatic changes.
- The quality of thermal images are depended on the temperature variation on target area, in other words contrast in temperature distribution is needed. Therefore for efficient building diagnostics with IRT, having a temperature difference between ambient and targeted surface is compulsory.

- Although most of IR cameras have digital image lens in addition to IR image lens, it is still recommended to take photos of the buildings with digital cameras also. Because resolution of digital cameras sensors are higher than the sensors of IR cameras.
- It is recommended that, the artificial lights during IR imaging should be off, because these lights are warmer than the target area. Therefore adjusting temperature scale of IR images during analyzing might be difficult.
- Estimation emissivity of the target surface improves the quality of the IRT method. Emissivity of the surface materials can be estimated by IRT, for that purpose, a material with known emissivity should be fixed to building walls. After that, temperature of the target area and the temperature of the fixed material should be compared with each other. Finally, emissivity value of the camera should be adjusted until the surface temperature of the target area is equal to fixed material with known emissivity, and that value is equal to emissivity of the target area.
- During IR imaging, radiation coming from surroundings and atmosphere is also collected by infrared sensor in addition to radiation coming from target area, Therefore, reflected ambient temperature should be measured to estimate radiation reflected on the target area from surroundings and atmosphere. Especially for the materials which have lower thermal emissivity value, measuring reflected temperature is much more important. Reflected temperature for indoor measurement is very close to the ambient room temperature and is almost constant. However, reflected temperature for outdoor measurement has a wider range, because, ambient temperature changes during day and correspondingly reflection from objects changes. Therefore, especially for outdoor infrared imaging, to measure reflected temperature is very important to increase the reliability of the method.
- To use IRT method for materials with low emissivity (like, glass, reflected metals etc.), emission tape or painting the surface is needed. Because, reflected

radiation coming from other surfaces will affect the temperature reading by the camera sensor.

- Precautions during exterior visual and/or thermal examination of a building based on site conditions:
 - Adjusting the viewing position of the thermal camera relative to the wall surfaces is important to ensure that data has acceptable quality and the target area is properly imaged
 - Obtain your thermal images as close to perpendicular to the surfaces you're examining as possible to minimize the reflected radiation coming from surroundings.
 - Where there is the possibility of reflected radiation change your position and view the same area again if necessary. Document the areas and location of surfaces obscured by mirrors, metal, reflective tile or other low emissivity coverings that affect thermal interpretations.
 - To increase steady state condition and the reliability of the method at least 10°C temperature difference between inside and outside air is necessary for a period of minimum 4 hours. In other words, Heating or cooling system of the building should be operated at least 3-4 hours before data collection to achieve .
 - Verify that no direct solar radiation has heated the surfaces to be examined for a period. This period is depended on the thermal inertia of the material used for the building façade.
 - Exterior investigation is recommended after sunset, before sunrise, or on a cloudy day when the influence of solar radiation can be determined to be minimal.
 - Convective heat transfer is depended on the wind speed near wall surface, therefore, verification of wind speed is less than 5m/s is necessary during IR imaging.

- To minimize the effect of evaporative cooling on the wall surfaces, IR imaging should be done when the exterior surfaces were not exposed to precipitation, in other words when the surfaces are not wet.
 - During cold weather conditions (in winter), when inside was warm while outside was cold, data should be collected very early in the morning or at night to increase the possibility of having steady state condition. Because during day temperature of the outside conditions and inside may not be stationary.
 - There should not be any operated air handling unit blowing directly to the wall surface.
 - In conclusion, the effect of the non-steady heat flow through building walls should be reduced with establishing the periods in which especially outdoor weather conditions has maximum stability.
- During IR imaging some of the building components may seen as anomalies, such as: heating systems, ductwork, plumbing pipes, electrical lines. The basic determining factor for correct interpretation is if the temperature distribution differs from that expected for the type of construction being viewed with the infrared imaging system. If the apparent anomaly can't be explained by the design of the building envelope, effects of heat sources, variations of emissivity, or by the physics of heat transfer, then the anomaly may require further investigation.

CHAPTER 6

CONCLUSION

6.1. Conclusion

The actual thermal performance of a wall can be identified in terms of thermal transmittance value only by using surface temperature data obtained by infrared thermography. The quantitative analyses of the surface temperature data is a promising approach for the thermal performance assessment and energy efficiency rating identification of new and existing buildings. Therefore, in-situ practical testing methods benefiting from quantitative infrared thermography (QIRT) should be developed and those methods should be commonly used in diagnostic and monitoring studies related with building inspection.

The recent studies proposing in-situ use of QIRT for thermal performance assessment were investigated. According to the evaluation of results the combined method using external thermal images for in-situ data acquisition and using Equation 7 for thermal transmittance calculation is the most appropriate approach for the thermal performance and energy efficiency assessment of multi-layered and single-layered building walls. That QIRT in-situ testing method using exterior surface temperature data was conducted on six different wall types belonging to three different buildings.

Results of the study showed that actual thermal performances of the walls are poorer than their theoretically-expected thermal performances, and the followings are the main findings:

- (i) Thermal failures weaken the thermal resistivity of a wall and their adverse impacts can be assessed in terms of measurable parameters by using QIRT.
- (ii) The walls designed with low thermal resistance were observed to be highly-susceptible to thermal failures resulting in considerable heat loss.
- (iii) Temperature Index (TI) is a useful parameter for identification of thermal and moisture failure types and for definition of thermal problems and their reasons.
- (iv) The actual thermal performance of a wall can be identified in terms of thermal transmittance value only by using actual exterior surface temperature data and inside and outside air temperatures.
- (v) The actual thermal transmittance calculation method can be used to estimate the real thermal conductivity value of single layered wall components.
- (vi) The achievements of QIRT method, mainly in-situ estimation and monitoring of the actual thermal transmittance of wall components, make QIRT method preferable for the studies on energy performance certification (EPC) of buildings.

The QIRT method, which can be practically used on site, is promising for the studies on Energy Performance Certification (EPC) of buildings, and in future:

- the common use of QIRT in building diagnostics needs to be extended,
- the approach in data acquisition and data analyses by use of QIRT is expected to lead fast and accurate performance assessment,
- it should be noted that brief and simple explanation of the developed in-situ experimental setups and practical evaluation of surface temperature data have vital importance to train experts and researchers from many disciplines/professions who work in relevant ministries, private and academic institutions and deal with energy performance control in buildings,
- such an improvement in building inspection skills is also expected to enhance thermal performance quality of buildings in Turkey and to improve a

consciousness in design and construction of energy efficient buildings and their monitoring,

For that purpose, a simulation software need to be developed, that allows advanced computer-based modelling and simulation analyses only using IR images taken from building surfaces. Experts should be trained for quantitative infrared thermography to assessment of Energy Performance Certification (EPC). In the future, approach the logic behind data acquisition and data analyses should be transferred to simulation analyses and result in advance in in-situ thermal performance monitoring in quantitative bases.

In conclusion, this study could be useful for developing a standard for measuring thermal transmittance values of the building façade with QIRT method. This technique of investigation, therefore, is very suited to perform thermal mapping of a large number of buildings. IR imaging can provide useful information to local Administrations, for example Municipalities, to carry out assessment of the energy quality of new and existing buildings.

6.2. Expected impacts

This study shows that it is possible to assess buildings thermal performance by using QIRT method and the followings are the expected impacts:

- The in-situ practice and experience achieved by the study is guiding for the training of experts working in governmental institutes and private sector for the building research and practice studies related with energy efficiency in buildings.
- The common and effective use of in-situ QIRT method in the Energy Performance Certification of the buildings will contribute to sustainable energy development in Turkey, by improving consciousness in design and construction

of energy efficient buildings and enhancing thermal performance quality of buildings in Turkey.

- Increase in QIRT use for diagnostic and monitoring studies in Turkey necessitates the training of experts and researchers in this field; such a demand, therefore, encourages the formation of such a profession which can be charged in relevant ministries, private and academic institutions.
- Development of advanced computer-based modelling and simulation software(s) allowing practical, fast and accurate thermal performance and energy efficiency analyses only using IR images taken from building surfaces.
- Knowledge produced on in-situ examination methods by QIRT and the experience/impressions achieved during in-situ examinations will be useful for training experts dealing with building inspection, particularly energy performance assessment.
- The quantitative analyses of thermal failures observed in IR images of building walls, actual thermal resistance performances of those walls and their impact on estimated annual energy consumption for heating purposes highlighted :
 - the importance of sufficiently-designed insulated wall compositions, proper detailing and workmanship for constructions for energy efficient building construction
 - the importance of building inspection in the form of non-destructive monitoring thermal performance of existing wall components for planning maintenance works and sustaining and improving their state of energy efficiency.
- The reference thermal conductivity values of materials given in the relevant standards (TS825, 2013), especially for the one having high portion of micro pores need to be revised by taking into consideration the values at 80%RH conditions.

6.3. Further studies

In this study solid walls with having highly emissive surfaces, above 0.90, were examined by using QIRT method. Comprehensive further studies are needed to develop its effective use for thermal performance and energy efficiency assessment curtain walls and ventilated facades. Examination of the building envelopes having low surface emissivity characteristics, such as glazed surfaces and curtain walls, by QIRT method is the other challenging research topic.

QIRT method should be further extended with using lock-in thermography and having sequential imaging with infrared cameras on site. These two advanced investigation methods commonly used on laboratory conditions for different sectors. Therefore, in-situ using of these methods is missing, especially for building diagnostics. It is possible to gather information about the thermal and moisture problems lying deep inside the wall section with lock-in thermography and sequential imaging. Therefore, specializing on these subjects, and focusing on developing energy performance assessment of buildings with QIRT method is very important.

REFERENCES

- Alastair Fothergill. (2006). *Planet Earth Deserts* [Documentary]. BBC.
- Albatici, R., & Tonelli, A. M. (2010). Infrared thermovision technique for the assessment of thermal transmittance value of opaque building elements on site. *Energy and Buildings*, 42(11), 2177–2183.
<https://doi.org/10.1016/j.enbuild.2010.07.010>
- Albatici, R., Tonelli, A. M., & Chiogna, M. (2015). A comprehensive experimental approach for the validation of quantitative infrared thermography in the evaluation of building thermal transmittance. *Applied Energy*, 141, 218–228.
<https://doi.org/10.1016/j.apenergy.2014.12.035>
- Amon, F., Hamins, A., Bryner, N., & Rowe, J. (2008). Meaningful performance evaluation conditions for fire service thermal imaging cameras. *Fire Safety Journal*, 43(8), 541–550. <https://doi.org/10.1016/j.firesaf.2007.12.006>
- Asdrubali, F., Baldinelli, G., & Bianchi, F. (2012). A quantitative methodology to evaluate thermal bridges in buildings. *Applied Energy*, 97, 365–373.
<https://doi.org/10.1016/j.apenergy.2011.12.054>
- Avdelidis, N. P., & Moropoulou, A. (2003). Emissivity considerations in building thermography. *Energy and Buildings*, 35(7), 663–667.
- Balaras, C. A., & Argiriou, A. A. (2002). Infrared thermography for building diagnostics. *Energy and Buildings*, 34(2), 171–183.
- Barreira, E., & de Freitas, V. P. (2007). Evaluation of building materials using infrared thermography. *Construction and Building Materials*, 21(1), 218–224.
<https://doi.org/10.1016/j.conbuildmat.2005.06.049>

BEP. (2008). *BEP, Building Energy Performance Regulation by Ministry of Public Works*. Official Newspaper No: 27075.

Berry, R. J., Kennedy, A. D., Scott, S. L., Kyle, B. L., & Schaefer, A. L. (2003). Daily variation in the udder surface temperature of dairy cows measured by infrared thermography: Potential for mastitis detection. *Canadian Journal of Animal Science*, 83(4), 687–693.

Bortolin, A., Cadelano, G., Ferrarini, G., Bison, P., Peron, F., & Maldague, X. (2013, May 22). *High-resolution survey of buildings by lock-in IR thermography* (G. R. Stockton & F. P. Colbert, Eds.). <https://doi.org/10.1117/12.2016592>

Brogi, G., & Pietranera, L. (1995). *Infrared sensor suitable for fire fighting applications*.

BS EN ISO 10456. (2007). *Building materials and products. Hygrothermal properties. Tabulated design values and procedures for determining declared and design thermal values*.

Çengel, Y. A., & Ghajar, A. J. (2015). *Heat and mass transfer: Fundamentals & applications* (5th edition). New York, NY: McGraw-Hill Education.

Center for History and New Media. (n.d.). Çabuk Başlama Rehberi. Retrieved from http://zotero.org/support/quick_start_guide

Chen, Q., Zhang, C., Zhao, J., & Ouyang, Q. (2013). Recent advances in emerging imaging techniques for non-destructive detection of food quality and safety. *TrAC Trends in Analytical Chemistry*, 52, 261–274. <https://doi.org/10.1016/j.trac.2013.09.007>

Cilulko, J., Janiszewski, P., Bogdaszewski, M., & Szczygielska, E. (2013). Infrared thermal imaging in studies of wild animals. *European Journal of Wildlife Research*, 59(1), 17–23. <https://doi.org/10.1007/s10344-012-0688-1>

- Costa, J. M., Grant, O. M., & Chaves, M. M. (2013). Thermography to explore plant–environment interactions. *Journal of Experimental Botany*, 64(13), 3937–3949. <https://doi.org/10.1093/jxb/ert029>
- Dall'O', G., Sarto, L., & Panza, A. (2013). Infrared Screening of Residential Buildings for Energy Audit Purposes: Results of a Field Test. *Energies*, 6(8), 3859–3878. <https://doi.org/10.3390/en6083859>
- Davies, M. G. (2004). *Building heat transfer*. John Wiley & Sons.
- DeÂqueÂ, F., Ollivier, F., & Roux, J. J. (2001). Effect of 2D modelling of thermal bridges on the energy performance of buildings Numerical application on the Matisse apartment. *Energy and Buildings*, 5.
- Djupkep, F. B. D., Maldague, X., Bendada, A., & Bison, P. (2013). Analysis of a new method of measurement and visualization of indoor conditions by infrared thermography. *Review of Scientific Instruments*, 84(8), 084906. <https://doi.org/10.1063/1.4818919>
- Donatelli, A., Aversa, P., & Luprano, V. A. M. (2016a). Set-up of an experimental procedure for the measurement of thermal transmittances via infrared thermography on lab-made prototype walls. *Infrared Physics & Technology*, 79, 135–143. <https://doi.org/10.1016/j.infrared.2016.10.005>
- Donatelli, A., Aversa, P., & Luprano, V. A. M. (2016b). Set-up of an experimental procedure for the measurement of thermal transmittances via infrared thermography on lab-made prototype walls. *Infrared Physics & Technology*, 79, 135–143. <https://doi.org/10.1016/j.infrared.2016.10.005>
- Doulos, L., Santamouris, M., & Livada, I. (2004). Passive cooling of outdoor urban spaces. The role of materials. *Solar Energy*, 77(2), 231–249. <https://doi.org/10.1016/j.solener.2004.04.005>
- Esposito, G., Nakazawa, J., Ogawa, S., Stival, R., Putnick, D. L., & Bornstein, M. H. (2015). Using infrared thermography to assess emotional responses to infants.

Early Child Development and Care, 185(3), 438–447.
<https://doi.org/10.1080/03004430.2014.932153>

European Council. (2010). *Directive 2010/31/EU of the European Parliament and of the Council of 19 May 2010 on the energy performance of buildings (recast)*. *Official Journal of the European Union*, 18(06), 2010. 23.

Ficco, G., Iannetta, F., Ianniello, E., d'Ambrosio Alfano, F. R., & Dell'Isola, M. (2015). U-value in situ measurement for energy diagnosis of existing buildings. *Energy and Buildings*, 104, 108–121.
<https://doi.org/10.1016/j.enbuild.2015.06.071>

Flir Systems. (2013). *EXX series user manual*. Retrieved from
<https://www.flir.com/globalassets/imported-assets/document/flir-exx-series-user-manual.pdf>

Fokaides, P. A., & Kalogirou, S. A. (2011a). Application of infrared thermography for the determination of the overall heat transfer coefficient (U-Value) in building envelopes. *Applied Energy*, 88(12), 4358–4365.
<https://doi.org/10.1016/j.apenergy.2011.05.014>

Fokaides, P. A., & Kalogirou, S. A. (2011b). Application of infrared thermography for the determination of the overall heat transfer coefficient (U-Value) in building envelopes. *Applied Energy*, 88(12), 4358–4365.
<https://doi.org/10.1016/j.apenergy.2011.05.014>

Fokaides, P. A., & Kalogirou, S. A. (2011c). Application of infrared thermography for the determination of the overall heat transfer coefficient (U-Value) in building envelopes. *Applied Energy*, 88(12), 4358–4365.
<https://doi.org/10.1016/j.apenergy.2011.05.014>

González-Aguilera, D., Lagüela, S., Rodríguez-Gonzálvez, P., & Hernández-López, D. (2013). Image-based thermographic modeling for assessing energy efficiency of buildings façades. *Energy and Buildings*, 65, 29–36.
<https://doi.org/10.1016/j.enbuild.2013.05.040>

- Gowen, A. A., Tiwari, B. K., Cullen, P. J., McDonnell, K., & O'Donnell, C. P. (2010). Applications of thermal imaging in food quality and safety assessment. *Trends in Food Science & Technology*, 21(4), 190–200. <https://doi.org/10.1016/j.tifs.2009.12.002>
- Grinzato, E. (2012). State of the art and perspective of infrared thermography applied to building science. In *Infrared Thermography: Recent Advances and Future Trends* (pp. 220–229).
- Grinzato, E., Bison, P., Cadelano, G. ., & Peron, F. (2010, April 23). *R-value estimation by local thermographic analysis* (R. B. Dinwiddie & M. Safai, Eds.). <https://doi.org/10.1117/12.850729>
- Grinzato, E., Vavilov, V., & Kauppinen, T. (1998). Quantitative infrared thermography in buildings. *Energy and Buildings*, (29), 1–9.
- Hazenbergh, C. E. V. B., van Netten, J. J., van Baal, S. G., & Bus, S. A. (2014). Assessment of Signs of Foot Infection in Diabetes Patients Using Photographic Foot Imaging and Infrared Thermography. *Diabetes Technology & Therapeutics*, 16(6), 370–377. <https://doi.org/10.1089/dia.2013.0251>
- Hoyano, A., Asano, K., & Kanamaru, T. (1999). Analysis of the sensible heat flux from the exterior surface of buildings using time sequential thermography. *Atmospheric Environment*, 11.
- Jin, H.-Q., Yao, X.-L., Fan, L.-W., Xu, X., & Yu, Z.-T. (2016). Experimental determination and fractal modeling of the effective thermal conductivity of autoclaved aerated concrete: Effects of moisture content. *International Journal of Heat and Mass Transfer*, 92, 589–602. <https://doi.org/10.1016/j.ijheatmasstransfer.2015.08.103>
- Jones, H. G. (2002). Use of infrared thermography for monitoring stomatal closure in the field: Application to grapevine. *Journal of Experimental Botany*, 53(378), 2249–2260. <https://doi.org/10.1093/jxb/erf083>

- Knížková, I., Kunc, P., Gürdil, G. A. K., Pinar, Y., & Selvi, K. C. (2007). Applications of infrared thermography in animal production. *Journal of the Faculty of Agriculture*, 22(3), 329–336.
- Koçkar, R. (2012). Duvarlardaki Isıl Özelliklerin Ve Sorunların Kızıl Ötesi Isıl Görüntüleme Ve Sıcak Kutu Yöntemleriyle İncelenmesi (Thesis). Gazi University, Ankara.
- Korukcu, O., & Kilic, M. (2009). The usage of IR thermography for the temperature measurements inside an automobile cabin. *International Communications in Heat and Mass Transfer*, 36(8), 872–877. <https://doi.org/10.1016/j.icheatmasstransfer.2009.04.010>
- Kylili, A., Fokaides, P. A., Christou, P., & Kalogirou, S. A. (2014). Infrared thermography (IRT) applications for building diagnostics: A review. *Applied Energy*, 134, 531–549. <https://doi.org/10.1016/j.apenergy.2014.08.005>
- Lehmann, B., Wakili, K., Frank, T., Collado, B., & Tanner, C. (2013). *Effects of individual climatic parameters on the infrared thermography of buildings*. (110), 29–43.
- Lucchi, E. (2018). Applications of the infrared thermography in the energy audit of buildings: A review. *Renewable and Sustainable Energy Reviews*, 82, 3077–3090. <https://doi.org/10.1016/j.rser.2017.10.031>
- Lucchi—2018—Applications of the infrared thermography in the e.pdf. (n.d.).
- Maldague, X. P. (2002). Introduction to NDT by active infrared thermography. *Materials Evaluation*, 60(9), 1060–1073.
- Martín Ocaña, S., Cañas Guerrero, I., & González Requena, I. (2004). Thermographic survey of two rural buildings in Spain. *Energy and Buildings*, 36(6), 515–523. <https://doi.org/10.1016/j.enbuild.2003.12.012>

Mccafferty, D. J. (2007). The value of infrared thermography for research on mammals: Previous applications and future directions. *Mammal Review*, 37(3), 207–223. <https://doi.org/10.1111/j.1365-2907.2007.00111.x>

MMO, C. of T. M. E. (2015). *MMO-TS285 software*.
<https://www.mmo.org.tr/merkez/isi-yalitim>.

Modest, F. M. (2003). *Radiative Heat Transfer*. Elsevier.

Nakanishi, R., & Imai-Matsumura, K. (2008). Facial skin temperature decreases in infants with joyful expression. *Infant Behavior and Development*, 31(1), 137–144. <https://doi.org/10.1016/j.infbeh.2007.09.001>

Nardi, I., Sfarra, S., & Ambrosini, D. (2014). Quantitative thermography for the estimation of the U-value: State of the art and a case study. *Journal of Physics: Conference Series*, 547, 012016. <https://doi.org/10.1088/1742-6596/547/1/012016>

Nemrut dag stone ayse t..pdf. (n.d.).

O’Grady, M., Lechowska, A. A., & Harte, A. M. (2017). Infrared thermography technique as an in-situ method of assessing heat loss through thermal bridging. *Energy and Buildings*, 135, 20–32.
<https://doi.org/10.1016/j.enbuild.2016.11.039>

Owrutsky, J. C., Steinhurst, D. A., Minor, C. P., Rose-Pehrsson, S. L., Williams, F. W., & Gottuk, D. T. (2006). Long wavelength video detection of fire in ship compartments. *Fire Safety Journal*, 41(4), 315–320.
<https://doi.org/10.1016/j.firesaf.2005.11.011>

Palyvos, J. A. (2008). A survey of wind convection coefficient correlations for building envelope energy systems’ modeling. *Applied Thermal Engineering*, 28(8–9), 801–808. <https://doi.org/10.1016/j.applthermaleng.2007.12.005>

- Panayiotou, G. P., Kalogirou, S. A., Florides, G. A., Maxoulis, C. N., Papadopoulos, A. M., Neophytou, M., ... Georgakis, G. (2010). The characteristics and the energy behaviour of the residential building stock of Cyprus in view of Directive 2002/91/EC. *Energy and Buildings*, 42(11), 2083–2089. <https://doi.org/10.1016/j.enbuild.2010.06.018>
- Rao P. (2008). Infrared thermography and its app. In civil eng..pdf. *The Indian Concrete Journal*, 82(5), 41–50.
- RESNET. (2012). *Residential Energy Services Network, RESNET Interim Guideline for Thermographic Inspections of Buildings*.
- Rinaldi, R. (2012). Infrared devices: Short history and new trends. *Infrared Thermography Recent Advances and Future Trends, Bentham EBooks*, 29–59.
- Savaş, A. (In the process of publication). METU Faculty of Architecture Conservation Planning Report. METU Press.
- Sayın, M., & Tavukçuoğlu, A. (2015). *Binalarda ısı sorunlarının Kızıl Ötesi Isıl Görüntüleme ile incelenmesi: ODTÜ Kent örneği*. 253–262. Ankara: Mimarlar Odası.
- Sayın, M., & Tavukçuoğlu, A. (2016a). Cephelerin Isı Yalıtımlılık Durumlarının Isıl Görüntüleme İle Değerlendirilmesi. *Yalıtım Dergisi*, (152), 46–54.
- Sayın, M., & Tavukçuoğlu, A. (2016b). *Dış Duvarlarda Kızıl Ötesi Isıl Görüntüleme ile Isıl Verimlilik Analizi*. 253–262. İstanbul: Yapı Derneği.
- Sayın, M., & Tavukçuoğlu, A. (2017). *Quantitative Assessment of Thermal Transmittance in Building Walls by In-Situ Infrared Thermography*. 202–215. İstanbul: ICBEST.
- Seeley, T. T., Abramson, P. R., Perry, L. B., Rothblatt, A. B., & Seeley, D. M. (1980). Thermographic measurement of sexual arousal: A methodological note. *Archives of Sexual Behavior*, 9(2), 77–85.

- Sonntag, R. E., Borgnakke, C., & Van Wylen, G. J. (2005). *Fundamentals of thermodynamics*. Wiley.
- Stainton, W. (1980). Interpretation of Building Thermograms. In D. McElroy & R. Tye (Eds.), *Thermal Insulation Performance* (pp. 163-163–18).
<https://doi.org/10.1520/STP29272S>
- Stainton W. D. (1980). Interpration of building thermograms. *ThermalInsulation Performance. ASTM STP 718, D. L. McElroy and R. P. Tye, Eds., American Society for 'T'csting and Materials*, 163–180.
- Stewart, M., Webster, J. R., Verkerk, G. A., Schaefer, A. L., Colyn, J. J., & Stafford, K. J. (2007). Non-invasive measurement of stress in dairy cows using infrared thermography. *Physiology & Behavior*, 92(3), 520–525.
<https://doi.org/10.1016/j.physbeh.2007.04.034>
- Tanyer, A. M., Tavukcuoglu, A., & Bekboliev, M. (2018). Assessing the airtightness performance of container houses in relation to its effect on energy efficiency. *Building and Environment*, 134, 59–73.
<https://doi.org/10.1016/j.buildenv.2018.02.026>
- Tattersall, G. J. (2016). Infrared thermography: A non-invasive window into thermal physiology. *Comparative Biochemistry and Physiology Part A: Molecular & Integrative Physiology*, 202, 78–98. <https://doi.org/10.1016/j.cbpa.2016.02.022>
- Tavukçuoğlu, A., Akevren, S., & Grinzato, E. (2010). In situ examination of structural cracks at historic masonry structures by quantitative infrared thermography and ultrasonic testing. *Journal of Modern Optics*, 57(18), 1779–1789. <https://doi.org/10.1080/09500340.2010.484553>
- Tavukçuoğlu, A., Caner-Saltık, E.N., Akoğlu, K.G., Işıkoğlu, M., & Caner, E. (2011). *In-Situ Examination of Nemrut Dağ Sandstone and Limestone Statues by NDT Methods*. 204–213.

- Tavukçuoğlu, A., Düzgüneş, A., Caner-Saltık, E. N., & Demirci, Ş. (2005). Use of IR thermography for the assessment of surface-water drainage problems in a historical building, Ağzıkarahan (Aksaray), Turkey. *NDT & E International*, 38(5), 402–410. <https://doi.org/10.1016/j.ndteint.2004.11.003>
- Tavukçuoğlu, A., & Grinzato, E. (2006). Determination of critical moisture content in porous materials by IR thermography. *Quantitative InfraRed Thermography Journal*, 3(2), 231–245. <https://doi.org/10.3166/qirt.3.231-245>
- Tejedor, B., Casals, M., Gangoellis, M., & Roca, X. (2017). Quantitative internal infrared thermography for determining in-situ thermal behaviour of façades. *Energy and Buildings*, 151, 187–197. <https://doi.org/10.1016/j.enbuild.2017.06.040>
- Titman, D. J. (2001). Applications of thermography in non-destructive testing of structures. *NDT & E International*, 34(2), 149–154.
- TS 825. (2013). *Thermal insulation requirements for buildings*. Turkish Standards Institute, Ankara Turkey.
- TS EN ISO 6946. (2007). *Building components and building elements—Thermal resistance and thermal transmittance—Calculation method*.
- TS EN ISO 9869. (2004). *Thermal insulation, building elements in-situ measurement of thermal resistance and thermal transmittance*.
- TS EN ISO 13790. (2013). *Energy performance of buildings—Calculation of energy use for space heating and cooling*. Ankara. 146.
- Tuğla, R., & Tavukçuoğlu, A. (2016). Tuğla duvarlarda ısı sorununun kızıl ötesi ısı görüntüleme ile belirlenmesi. 3. *Ulusal Yapı Kongresi ve Sergisi*, 14.
- Tugla, R., Tavukçuoğlu, A., & Arslan, A. (2013). *Examination of thermal properties and failures of brick walls by the use of infrared thermography and hot box*

method. 180–199. Ankara: RenewBuild2013–1st Int. Conf. & Exhibition on “Application of efficient & renewable energy technologies in low cost buildings and construction.

Verbeke, S., & Audenaert, A. (2018). Thermal inertia in buildings: A review of impacts across climate and building use. *Renewable and Sustainable Energy Reviews*, 82, 2300–2318. <https://doi.org/10.1016/j.rser.2017.08.083>

Zalewski, L., Lassue, S., Rousse, D., & Boukhalfa, K. (2010). Experimental and numerical characterization of thermal bridges in prefabricated building walls. *Energy Conversion and Management*, 51(12), 2869–2877. <https://doi.org/10.1016/j.enconman.2010.06.026>

APPENDICES

A. Specifications of the IR Cameras used for in-situ thermal imaging

| | FLIR E60 | TESTO 875-1i |
|--------------------------------|----------------|------------------------|
| Thermal sensitivity | <50mK | <50mK |
| Spectral range (Wave length) = | 7,5-13 μ m | 8-14 μ m |
| Field of view (FOV) = | 25-19° | 32-23° |
| IR resolution = | 320 x 240 | 160 x 120 |
| Temperature range | -20 to +120 | -30 to +100 (\pm 2) |
| Accuracy | \pm 2 | \pm 2 |

B. Specifications of the software's used for IR analysis


| | Flir Tools + | Testo IRTSoft 4.4 |
|------------------------------------|--------------|-------------------|
| Compatibility | FLIR Cameras | Testo Cameras |
| INPUTS | | |
| Emissivity of the target surface | 0,01-1 | 0,01-1 |
| Ambient temperature | ✓ | ✓ |
| Reflected temperature | ✓ | ✓ |
| Relative Humidity | ✓ | ✓ |
| Distance between target and sensor | ✓ | X |
| Palette alternatives | ✓ | ✓ |
| OUTPUTS | | |
| Histogram temperature dist. | X | ✓ |
| Profiled temp. dist. | ✓ | ✓ |
| Real image | ✓ | ✓ |
| Overlay of real and thermal images | Automatic | Manual |
| Export to CSV | ✓ | ✓ |

C. Saturation pressure of water-vapour at various temperatures

| temperature (°C) | saturation pressure (Pa) | temperature (°C) | saturation pressure (Pa) |
|---------------------|-----------------------------|---------------------|-----------------------------|
| -7 | 342 | 4 | 820 |
| -6 | 374 | 5 | 872 |
| -5 | 406 | 6 | 943 |
| -4 | 438 | 7 | 1014 |
| -3 | 481 | 8 | 1086 |
| -2 | 525 | 9 | 1157 |
| -1 | 568 | 10 | 1228 |
| 0 | 611 | 11 | 1323 |
| 1 | 663 | 12 | 1419 |
| 2 | 715 | 13 | 1514 |
| 3 | 768 | 14 | 1610 |

D. Sample energy performance certificate (EPCs)

Energy Performance Certificate (EPC)



17 Any Street, District, Any Town, B5 5XX


Dwelling type: Detached house **Reference number:** 0919-9628-8430-2785-5996
Date of assessment: 15 August 2011 **Type of assessment:** RdSAP, existing dwelling
Date of certificate: 13 March 2012 **Total floor area:** 165 m²

Use this document to:

- Compare current ratings of properties to see which properties are more energy efficient
- Find out how you can save energy and money by installing improvement measures

| | |
|---|---------------|
| Estimated energy costs of dwelling for 3 years | £5,367 |
| Over 3 years you could save | £2,865 |

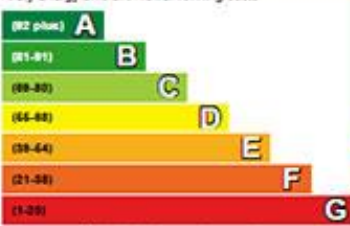
Estimated energy costs of this home

| | Current costs | Potential costs | Potential future savings |
|----------------|---------------------|---------------------|--|
| Lighting | £375 over 3 years | £207 over 3 years |  |
| Heating | £4,443 over 3 years | £2,073 over 3 years | |
| Hot water | £549 over 3 years | £222 over 3 years | |
| Totals: | £5,367 | £2,502 | |

These figures show how much the average household would spend in this property for heating, lighting and hot water. This excludes energy use for running appliances like TVs, computers and cookers, and any electricity generated by microgeneration.

Energy Efficiency Rating

Very energy efficient - lower running costs



Not energy efficient - higher running costs

| Current | Potential |
|---------|-----------|
| 49 | 76 |

The graph shows the current energy efficiency of your home.

The higher the rating the lower your fuel bills are likely to be.

The potential rating shows the effect of undertaking the recommendations on page 3.

The average energy efficiency rating for a dwelling in England and Wales is band D (rating 60).

Top actions you can take to save money and make your home more efficient

| Recommended measures | Indicative cost | Typical savings over 3 years | Available with Green Deal |
|--------------------------------------|-----------------|------------------------------|---------------------------|
| 1 Increase loft insulation to 270 mm | £100 - £350 | £141 | ✓ |
| 2 Cavity wall insulation | £500 - £1,500 | £537 | ✓ |
| 3 Draught proofing | £80 - £120 | £78 | ✓ |

See page 3 for a full list of recommendations for this property.

To find out more about the recommended measures and other actions you could take today to save money, visit www.direct.gov.uk/savingenergy or call 0300 123 1234 (standard national rate). When the Green Deal launches, it may allow you to make your home warmer and cheaper to run at no up-front cost.

Page 1 of 4

E. U Value Comparison Table

| wall type | thermal imaging season | sample no | thermal image no | method-1 | | | | | | | | | | | | method-2 | | | | | | | | | | | | method-3 | | percentage deviation | | | | |
|---------------------------------------|------------------------|-----------|------------------|---|--|------|---|--|------|---|--|--------|------------------|---|--|-----------|---|--|---------|---|--|-----|---|--|---------|--|--|--|---|----------------------|--|--|--|--|
| | | | | reference | | | average | | | SD | | | defect | | | reference | | | average | | | SD | | | defect | | | U _{calc} Wm ² K ⁻¹ | percentage deviation (U _{INSTU} / U _{CALC}) | | | | | |
| | | | | U _{INSTU-1} Wm ² K ⁻¹ | average Wm ² K ⁻¹ | SD | U _{INSTU-1} Wm ² K ⁻¹ | average Wm ² K ⁻¹ | SD | U _{INSTU-1} Wm ² K ⁻¹ | average Wm ² K ⁻¹ | SD | thermal image no | U _{INSTU-2} Wm ² K ⁻¹ | average Wm ² K ⁻¹ | SD | U _{INSTU-2} Wm ² K ⁻¹ | average Wm ² K ⁻¹ | SD | U _{INSTU-2} Wm ² K ⁻¹ | average Wm ² K ⁻¹ | SD | U _{INSTU-2} Wm ² K ⁻¹ | average Wm ² K ⁻¹ | SD | | | | | | | | | |
| W1 Insulated cavity wall | winter 2015 | 1 | IV 73 | 0.94 | 0.85 +0.11 | | 1.27 | 1.12 +0.20 | | 1.91 | 1.67 +0.26 | | IV 114 | 0.48 | 0.62 +0.15 | | 0.64 | 0.73 +0.15 | | 0.80 | 0.85 +0.14 | | 0.5 | 70.25% | 24.75% | | | | | | | | | |
| | | 2 | IV 74 | 0.89 | 0.83 +0.11 | | 1.27 | | | 1.94 | | | IV 112 | 0.72 | 0.56 +0.10 | | 0.82 | | | 0.95 | 0.87 +0.13 | | | | | | | | | | | | | |
| | | 3 | IV 76 | 0.67 | | | 0.83 | | | 1.58 | | | IV 113 | 0.54 | | | 0.64 | | | 0.75 | | | | | | | | | | | | | | |
| | | 4 | IV 78 | 0.78 | | | 0.94 | | | 1.38 | | | IV 115 | 0.64 | | | 0.77 | | | 0.86 | | | | | | | | | | | | | | |
| | | 5 | IV 82 | 0.86 | | | 1.08 | | | 1.44 | | | IV 116 | 0.44 | | | 0.52 | | | 0.67 | | | | | | | | | | | | | | |
| | | 6 | IV 85 | 0.94 | | | 1.27 | | | 1.91 | | | IV 119 | 0.86 | | | 0.96 | | | 1.13 | | | | | | | | | | | | | | |
| | | 7 | IV 86 | 1.00 | | | 1.36 | | | 1.86 | | | IV 120 | 0.54 | | | 0.62 | | | 0.75 | | | | | | | | | | | | | | |
| | | 8 | IV 94 | 0.73 | | | 0.92 | | | 1.36 | | | IV 120 | 0.77 | | | 0.86 | | | 0.86 | | | | | | | | | | | | | | |
| W2 Externally-insulated shear wall | winter 2015 | 1 | IV 73 | 0.81 | 0.58 +0.16 | 1.00 | 0.74 +0.24 | | 1.38 | 1.20 +0.25 | | IV 111 | 0.56 | 0.59 +0.12 | | 0.82 | 0.76 +0.14 | | 1.10 | | | 0.6 | -2.71% | -1.04% | | | | | | | | | | |
| | | 2 | IV 74 | 0.75 | 0.54 +0.12 | | 1.03 | | | 1.47 | 1.27 +0.15 | | IV 113 | 0.48 | 0.59 +0.08 | | 0.59 | | | 0.69 | | | | | | | | | | | | | | |
| | | 3 | IV 76 | 0.51 | | | 0.59 | | | 1.25 | | | IV 114 | 0.40 | | | 0.59 | | | 0.90 | | | | | | | | | | | | | | |
| | | 4 | IV 78 | 0.48 | | | 0.54 | | | 1.14 | | | IV 115 | 0.79 | | | 0.95 | | | 1.08 | 0.97 +0.19 | | | | | | | | | | | | | |
| | | 5 | IV 82 | 0.43 | | | 0.51 | | | 1.03 | | | IV 116 | 0.59 | | | 0.67 | | | 0.79 | | | | | | | | | | | | | | |
| | | 6 | IV 85 | 0.56 | | | 0.81 | | | 1.27 | | | IV 117 | 0.69 | | | 0.89 | | | 1.16 | | | | | | | | | | | | | | |
| | | 7 | IV 86 | 0.73 | | | 0.97 | | | 1.36 | | | IV 118 | 0.57 | | | 0.72 | | | 0.84 | | | | | | | | | | | | | | |
| | | 8 | IV 94 | 0.40 | | | 0.48 | | | 0.70 | | | IV 120 | 0.67 | | | 0.82 | | | 1.18 | | | | | | | | | | | | | | |
| W3 Externally-insulated shear wall | winter 2015 | 1 | IV 132 | 0.85 | 1.29 +0.34 | | 0.99 | 1.54 +0.40 | | 1.38 | 1.74 +0.38 | | IV 198 | 1.40 | 0.96 +0.29 | | 1.52 | 1.09 +0.33 | | 1.68 | 1.28 +0.35 | | 0.75 | 72.12% | 27.48% | | | | | | | | | |
| | | 2 | IV 127 | 0.80 | 1.14 +0.25 | | 0.91 | | | 1.01 | 1.85 +0.26 | | IV 199 | 1.00 | 0.96 +0.19 | | 1.11 | | | 1.27 | 1.34 +0.32 | | | | | | | | | | | | | |
| | | 3 | IV 134 | 1.22 | | | 1.62 | | | 1.89 | | | IV 214 | 0.79 | | | 0.87 | | | 1.08 | | | | | | | | | | | | | | |
| | | 4 | IV 135 | 1.33 | | | 1.73 | | | 1.92 | | | IV 214 | 0.76 | | | 0.85 | | | 0.94 | | | | | | | | | | | | | | |
| | | 5 | IV 136 | 1.30 | | | 1.46 | | | 1.62 | | | IV 212 | 0.85 | | | 0.96 | | | 1.21 | | | | | | | | | | | | | | |
| | | 6 | IV 137 | 1.36 | | | 1.76 | | | 1.92 | | | IV 222 | 0.50 | | | 0.61 | | | 0.83 | | | | | | | | | | | | | | |
| | | 7 | IV 136 | 1.70 | | | 1.95 | | | 2.11 | | | IV 232 | 1.14 | | | 1.27 | | | 1.40 | | | | | | | | | | | | | | |
| | | 8 | IV 137 | 1.76 | | | 1.92 | | | 2.08 | | | IV 238 | 1.21 | | | 1.52 | | | 1.83 | | | | | | | | | | | | | | |
| W4 Externally-insulated AAC wall | winter 2015 | 1 | IV 132 | 0.75 | 0.78 +0.19 | | 0.93 | 0.96 +0.15 | | 1.12 | 1.21 +0.14 | | IV 198 | 0.57 | 0.67 +0.34 | | 0.68 | 0.81 +0.39 | | 0.94 | 1.07 +0.39 | | 0.39 | 99.83% | 72.69% | | | | | | | | | |
| | | 2 | IV 127 | 0.52 | 0.77 +0.12 | | 0.62 | | | 0.91 | | | IV 203 | 1.06 | 0.80 +0.28 | | 1.29 | 1.04 +0.27 | | 1.54 | 1.22 +0.33 | | | | | | | | | | | | | |
| | | 3 | IV 134 | 0.65 | | | 0.96 | | | 1.33 | | | IV 204 | 1.11 | | | 1.21 | | | 1.46 | | | | | | | | | | | | | | |
| | | 4 | IV 135 | 0.67 | | | 0.99 | | | 1.22 | | | IV 207 | 0.96 | | | 1.21 | | | 1.48 | | | | | | | | | | | | | | |
| | | 5 | IV 136 | 0.72 | | | 0.99 | | | 1.20 | | | IV 212 | 0.43 | | | 0.50 | | | 0.68 | | | | | | | | | | | | | | |
| | | 6 | IV 136 | 0.91 | | | 1.06 | | | 1.28 | | | IV 222 | 0.23 | | | 0.34 | | | 0.59 | | | | | | | | | | | | | | |
| | | 7 | IV 137 | 1.09 | | | 1.14 | | | 1.28 | | | IV 232 | 0.33 | | | 0.38 | | | 0.72 | | | | | | | | | | | | | | |
| | | 8 | IV 148 | 0.93 | | | 0.96 | | | 1.33 | | | IV 238 | 0.70 | | | 0.83 | | | 1.19 | | | | | | | | | | | | | | |
| W5 Non-insulated shear wall | winter 2013 | 1 | IR 5473 | 2.92 | 2.53 +0.26 | | 3.22 | 2.80 +0.34 | | 3.50 | 3.23 +0.22 | | NA | | | | | | | | | | 3.46 | -26.85% | NA | | | | | | | | | |
| | | 2 | IR 5474 | 2.56 | 2.69 +0.16 | | 2.97 | 3.02 +0.16 | | 3.48 | 3.32 +0.17 | | | | | | | | | | | | | | | | | | | | | | | |
| | | 3 | IR 5475 | 2.53 | | | 2.86 | | | 3.17 | | | | | | | | | | | | | | | | | | | | | | | | |
| | | 4 | IR 5476 | 2.34 | | | 2.51 | | | 2.97 | | | | | | | | | | | | | | | | | | | | | | | | |
| | | 5 | IR 5477 | 2.78 | | | 3.17 | | | 3.42 | | | | | | | | | | | | | | | | | | | | | | | | |
| | | 6 | IR 5479 | 2.23 | | | 2.40 | | | 3.11 | | | | | | | | | | | | | | | | | | | | | | | | |
| | | 7 | IR 5480 | 2.21 | | | 2.37 | | | 2.95 | | | | | | | | | | | | | | | | | | | | | | | | |
| | | 8 | IR 5484 | 2.67 | | | 2.89 | | | 3.25 | | | | | | | | | | | | | | | | | | | | | | | | |
| W6 Non-insulated shear wall | winter 2016 | 1 | IV 587 | 1.98 | 1.95 +0.13 | | 2.19 | 2.16 +0.16 | | 2.86 | 2.51 +0.24 | | IV 572 | 1.94 | 1.75 +0.21 | | 2.09 | 1.93 +0.19 | | 2.31 | 2.14 +0.17 | | -47.20% | -52.59% | | | | | | | | | | |
| | | 2 | IV 588 | 2.11 | 2.05 +0.05 | | 2.37 | 2.26 +0.07 | | 2.63 | 2.67 +0.11 | | IV 576 | 1.98 | 1.82 +0.13 | | 2.13 | 1.98 +0.14 | | 2.35 | 2.21 +0.17 | | | | | | | | | | | | | |
| | | 3 | IV 589 | 2.02 | | | 2.28 | | | 2.59 | | | IV 577 | 1.90 | 1.88 +0.12 | | 2.05 | 2.05 +0.12 | | 2.24 | 2.26 +0.15 | | | | | | | | | | | | | |
| | | 4 | IV 590 | 2.06 | | | 2.19 | | | 2.63 | | | IV 579 | 1.75 | | | 1.98 | | | 2.20 | | | | | | | | | | | | | | |
| | | 5 | IV 590 | 1.84 | | | 2.06 | | | 2.24 | | | IV 580 | 1.33 | | | 1.60 | | | 1.94 | | | | | | | | | | | | | | |
| | | 6 | IV 591 | 2.06 | | | 2.28 | | | 2.63 | | | IV 581 | 1.64 | | | 1.75 | | | 1.90 | | | | | | | | | | | | | | |
| | | 7 | IV 591 | 1.76 | | | 1.93 | | | 2.11 | | | IV 582 | 1.67 | | | 1.83 | | | 1.98 | | | | | | | | | | | | | | |
| | | 8 | IV 592 | 1.80 | | | 1.98 | | | 2.41 | | | IV 584 | 1.83 | | | 2.01 | | | 2.20 | | | | | | | | | | | | | | |
| W6 Non-insulated shear wall | winter 2017 | 1 | IR 311 | 1.85 | 2.06 +0.48 | | 2.35 | 2.69 +0.60 | | 3.29 | 3.45 +0.60 | | IR 329 | 1.97 | 1.86 +0.14 | | 2.21 | 2.09 +0.19 | | 2.77 | 2.44 +0.22 | | 3.70 | -44.29% | -49.66% | | | | | | | | | |
| | | 2 | IR 313 | 1.85 | 2.02 +0.16 | | 2.49 | 2.42 +0.13 | | 3.65 | 3.09 +0.37 | | IR 379 | 1.63 | 1.92 +0.14 | | 1.76 | 2.10 +0.13 | | 2.22 | 2.32 +0.21 | | | | | | | | | | | | | |
| | | 3 | IR 315 | 2.06 | | | 2.56 | | | 3.29 | | | IR 349 | 1.82 | | | 2.13 | | | 2.45 | | | | | | | | | | | | | | |
| | | 4 | IR 317 | 2.06 | | | 2.42 | | | 3.14 | | | IR 351 | 2.03 | | | 2.39 | | | 2.75 | | | | | | | | | | | | | | |
| | | 5 | IR 341 | 1.56 | | | 1.92 | | | 2.78 | | | IR 373 | 1.74 | | | 2.03 | | | 2.27 | | | | | | | | | | | | | | |
| | | 6 | IR 343 | 1.63 | | | 2.64 | | | 3.65 | | | IR 375 | 1.70 | | | 1.89 | | | 2.20 | | | | | | | | | | | | | | |
| | | 7 | IR 363 | 3.29 | | | 4.02 | | | 4.76 | | | IR 453 | 1.97 | | | 2.24 | | | 2.50 | | | | | | | | | | | | | | |
| | | 8 | IR 381 | 1.99 | | | 2.28 | | | 2.64 | | | IR 455 | 1.98 | | | 2.25 | | | 2.57 | | | | | | | | | | | | | | |
| | | 9 | IR 401 | 2.32 | | | 2.92 | | | 3.43 | | | IR 465 | 1.81 | | | 1.99 | | | 2.18 | | | | | | | | | | | | | | |
| | | 10 | IR 403 | 2.02 | | | 3.33 | | | 3.84 | | | IR 469 | 1.99 | | | 2.04 | | | 2.46 | | | | | | | | | | | | | | |
| W6 Non-insulated shear wall | summer 2017 | 1 | IR 181 | 2.29 | 2.28 +0.13 | | 3.09 | 2.87 +0.32 | | 3.45 | 3.19 +0.37 | | IR 143 | 2.16 | 1.80 +0.19 | | 2.41 | | | 2.91 | | | -38.35% | -51.42% | | | | | | | | | | |
| | | 2 | IR 181 | 2.51 | 2.23 +0.09 | | 3.23 | 2.58 +0.06 | | 3.67 | 2.85 +0.09 | | IR 144 | 1.85 | 1.87 +0.19 | | 2.19 | | | 2.70 | | | | | | | | | | | | | | |
| | | 3 | IR 182 | 2.22 | | | 2.51 | | | 2.73 | | | IR 145 | 1.68 | | | 1.79 | | | 2.02 | | | | | | | | | | | | | | |
| | | 4 | IR 182 | 2.29 | | | 2.58 | | | 2.87 | | | IR 145 | 1.62 | | | 1.79 | 2.00 +0.25 | | 1.96 | 2.32 +0.39 | | | | | | | | | | | | | |
| | | 5 | IR 183 | 2.36 | | | 2.65 | | | 2.95 | | | IR 146 | 1.74 | | | 1.91 | | | 2.19 | | | | | | | | | | | | | | |
| | | 6 | IR 183 | 2.07 | | | 2.58 | | | 2.87 | | | IR 146 | 1.74 | | | 1.91 | | | 2.13 | | | | | | | | | | | | | | |
| | | 7 | IR 184 | 2.29 | | | 3.31 | | | 3.60 | | | | | | | | | | | | | | | | | | | | | | | | |
| | | 8 | IR 184 | 2.22 | | | 3.02 | | | 3.38 | | | | | | | | | | | | | | | | | | | | | | | | |